AD-A118 363 EIC LABS INC NEWTON MA F/6 10/3
INVESTIGATION OF LITHIUM SULFUR DIOXIDE (LI/SO2) BATTERY SAFETY--ETC(U)
APR 82 K M ABRAHAM, M W RUPICH, L PITTS N60921-81-C-0084
UNCLASSIFIED C-656 NSWC-TR-82-148 NL

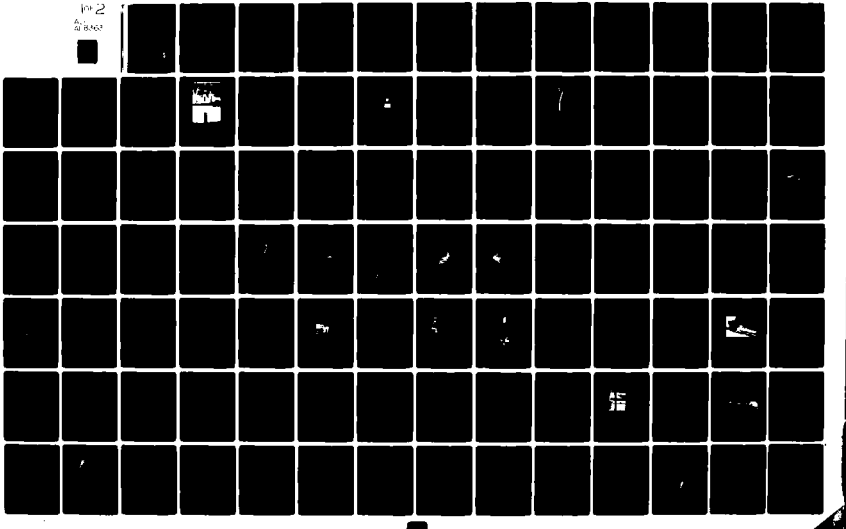

(12)

INVESTIGATION OF LITHIUM SULFUR DIOXIDE (Li/SO_2) BATTERY SAFETY HAZARDS - CHEMICAL STUDIES

Final Report for the Period December 24, 1980 - December 23, 1981

Contract No. N60921-81-C-0084

Prepared by

K. M. Abraham
M. W. Rupich
L. Pitts

EIC Laboratories, Inc.
67 Chapel Street
Newton, Massachusetts 02158

Prepared for
NAVAL SURFACE WEAPONS CENTER
Silver Spring-White Oak
Maryland 20910

April 1982

SECURITY CLASSIFICATION OF THIS PAGE (When Data Entered)

REPORT DOCUMENTATION PAGE

READ INSTRUCTIONS BEFORE COMPLETING FORM

1. REPORT NUMBER: NSWC TR 82-148	2. GOVT ACCESSION NO.: AD-A118363
3. RECIPIENT'S CATALOG NUMBER:	
4. TITLE (and Subtitle): Investigation of Lithium Sulfur Dioxide (Li/SO_2) Battery Safety Hazards - Chemical Studies	5. TYPE OF REPORT & PERIOD COVERED: Final Report 24 Dec. 1980-23 Dec. 1981
	6. PERFORMING ORG. REPORT NUMBER: C-656
7. AUTHOR(s): K. M. Abraham, M. W. Rupich and L. Pitts	8. CONTRACT OR GRANT NUMBER(s): N60921-81-C-0084
9. PERFORMING ORGANIZATION NAME AND ADDRESS: EIC Laboratories, Inc. 67 Chapel Street Newton, Massachusetts 02158	10. PROGRAM ELEMENT, PROJECT, TASK AREA & WORK UNIT NUMBERS:
11. CONTROLLING OFFICE NAME AND ADDRESS: Naval Surface Weapons Center Silver Spring-White Oak, Maryland 20910	12. REPORT DATE: April 1982
	13. NUMBER OF PAGES: 89
14. MONITORING AGENCY NAME & ADDRESS (if different from Controlling Office)	15. SECURITY CLASS. (of this report):
	15a. DECLASSIFICATION/DOWNGRADING SCHEDULE:

16. DISTRIBUTION STATEMENT (of this Report)

Approved for public release. Distribution unlimited.

17. DISTRIBUTION STATEMENT (of the abstract entered in Block 20, if different from Report)

18. SUPPLEMENTARY NOTES

19. KEY WORDS (Continue on reverse side if necessary and identify by block number)

Li/SO_2 cells, discharge, reaction stoichiometry, $Li_2S_2O_4$, forced over-discharge, safety hazards

20. ABSTRACT (Continue on reverse side if necessary and identify by block number)

The chemistry associated with the discharge and forced overdischarge of the Li/SO_2 cell was investigated in detail. A procedure for the quantitative determination of $Li_2S_2O_4$ in discharged Li/SO_2 cells is described. The amount of $Li_2S_2O_4$ found in cells discharged to potentials down to zero volt was in very good agreement with the discharge stoichiometry, $2Li + 2SO_2 \rightarrow Li_2S_2O_4$. The $Li_2S_2O_4$ formed in the carbon cathode was also characterized by infrared, ESCA, and X-ray analyses. A number of organic com-

DD FORM 1 JAN 73 1473 EDITION OF 1 NOV 65 IS OBSOLETE

UNCLASSIFIED

SECURITY CLASSIFICATION OF THIS PAGE (When Data Entered)

pounds including CH_4 and 3,5-diamino-2,4-hexenenitrile have been identified in forced overdischarged cells. Products identified in cells which vented during forced overdischarge include: CO_2, CS_2, COS, H_2S, CH_4, C_2H_4, C_2H_2, Li_2S, and Li_2SO_3.

The performance of two types of commercial C-size Li/SO_2 cells (Type X and Type Z) was evaluated under abusive use conditions.

The forced overdischarge behavior of the two types of cells was markedly different. The Type Z cell displayed hazardous behavior when forced overdischarged at rates ≥900 mA. The Type X cell, on the other hand, exhibited excellent abuse resistance to forced overdischarge at currents up to 1290 mA.

The forced overdischarge of both types of cells at -25°C was found to be a particularly hazardous operational mode. The Type Z cell was found to vent when forced overdischarged with a current of ≥150 mA. The Type X cells did not vent under similar conditions, but Li was found to plate onto the cathode. The plated Li is extremely reactive and is likely involved in exothermic reactions which produce similar reaction products as do the vented Type Z cells.

The resistance of the commercial cells to charging was also investigated briefly. Neither type of cell displayed unsafe behavior when charged after a partial discharge or a forced overdischarge.

PREFACE

A part of the experimental work in this project involves the testing of commercial Li/SO_2 cells. The objective of the program is to investigate the safety hazards of the Li/SO_2 system in general and not of any particular brand of commercial cell. No conclusions are presented or intended in regard to the performance of a given commercial cell.

In the present study, cells were subjected to abusive tests in order to provoke hazardous events under well defined conditions for systematic investigation. Therefore, the present data may be showing a higher frequency of hazards than would be encountered in the actual use of the cells.

This work was supported by the Electrochemical Technology Block Program-NSWC.

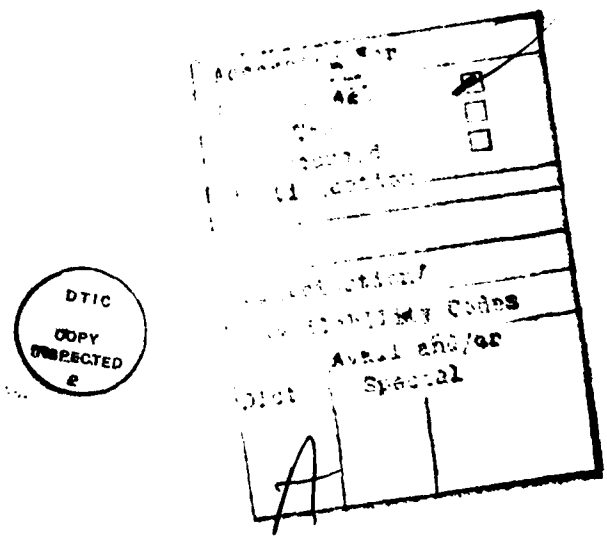

TABLE OF CONTENTS

TABLE OF CONTENTS
(continued)

LIST OF ILLUSTRATIONS

LIST OF ILLUSTRATIONS
(continued)

LIST OF ILLUSTRATIONS
(continued)

LIST OF ILLUSTRATIONS
(continued)

LIST OF TABLES

1.0 INTRODUCTION

The $Li/LiBr,CH_3CN/SO_2$ battery is one of the most advanced high-energy density battery systems available today. Several manufacturers currently produce Li/SO_2 cells in large volumes for military, industrial, and commercial applications. The outstanding features of the Li/SO_2 system which make it attractive to users include its high specific energy, high volumetric energy density, long shelf life, extremely stable voltage, and outstanding low temperature performance (1-10). However, the same active cell materials which provide for these desirable properties can also make the cell unsafe under certain operating conditions. As the use of the Li/SO_2 system increases, concern over its safety also grows.

Despite earlier claims that commercial Li/SO_2 cells are sufficiently abuse resistant for specific applications (5,11,12), there has been an increasing number of reports (13) of hazardous behavior exhibited by the cell under both test and actual use conditions. Clearly, the present Li/SO_2 cell has not been perfected to the point of being safe under all use conditions.

During the first phase of this program, we conducted a literature and user survey of the safety related problems of Li/SO_2 cells. The detailed results of this survey have been published previously (13). The study identified three conditions under which use of the Li/SO_2 system is particularly hazardous:

(i) Forced overdischarge of Li/SO_2 cells. This situation, experienced by a weak cell in a series-connected battery, is the most frequent cause of cell or battery venting or explosion.

(ii) Increased vulnerability of partially discharged and stored Li/SO_2 cells and batteries to subsequent abuse; e.g., shorts, high current pulses, overdischarge or incineration. This is a particularly hazardous condition in practical situations.

(iii) Low temperature discharge, particularly when a cell is driven into voltage reversal and subsequently warmed up to room temperature.

The second part of this program involved an experimental investigation of the safety hazards of the Li/SO_2 system, particularly those associated with forced overdischarge. A major objective of this study was the thorough characterization of the cell chemistry occurring during the normal discharge, as well as the chemistry associated with hazardous use conditions. The experimental techniques and results are presented in this report.

2.0 EXPERIMENTAL PROCEDURES

2.1 Testing and Analysis of Li/SO_2 Cells

The electrochemical testing, opening of unvented cells, and collection of gaseous products were carried out in a specially designed, hermetically sealed test chamber illustrated in Fig. 1. The chamber was designed to contain all compounds released from cells which vented during testing or from cells deliberately opened for analysis. An Ar or He atmosphere was maintained in the container during testing.

When placed in the test chamber, the cell was in contact with only a Teflon block on the bottom surface of the chamber and a narrow Teflon ring around 3/4 of the circumference of the cell. The safety vents were unimpeded with both type cells tested.

Cells were galvanostatically discharged using a constant current power supply with a maximum voltage of 12V. The wall temperature of the cells was measured with a copper-constantan thermocouple mechanically attached to the outside of the cell wall and calibrated against an Omega electronic ice point reference. The cell potential and temperature were measured continuously during discharge.

During the low temperature experiments, the test chamber containing the cell was placed in a Tenney environmental chamber maintained at $-25^{o}C$. All cells were allowed to equilibrate at $-25^{o}C$ for at least 12 hours before being discharged. After the discharge or forced overdischarge, the test chamber was removed from the environmental chamber and the cells were allowed to warm to room temperature (indicated by the thermocouple mounted on the cell wall). Except where noted, the cells were allowed to stand at room temperature for at least an additional three hours before being opened.

Analyses of the cells and their contents were carried out as follows. The gases were released from the cell by piercing the end of the cell with the stainless steel plunger illustrated in Fig. 1. The plunger is moved up or down by screwing it through a series of air-tight threads in the cover of the test chamber. All volatile products released from the cell were completely retained within the test chamber.

The test chamber was equipped with two collection ports secured by valves. The gaseous compounds released into the test chamber were collected by one of two methods: i) the gases were directly transferred through one of the collection ports to evacuated gas IR cells, G. C. syringes, etc.

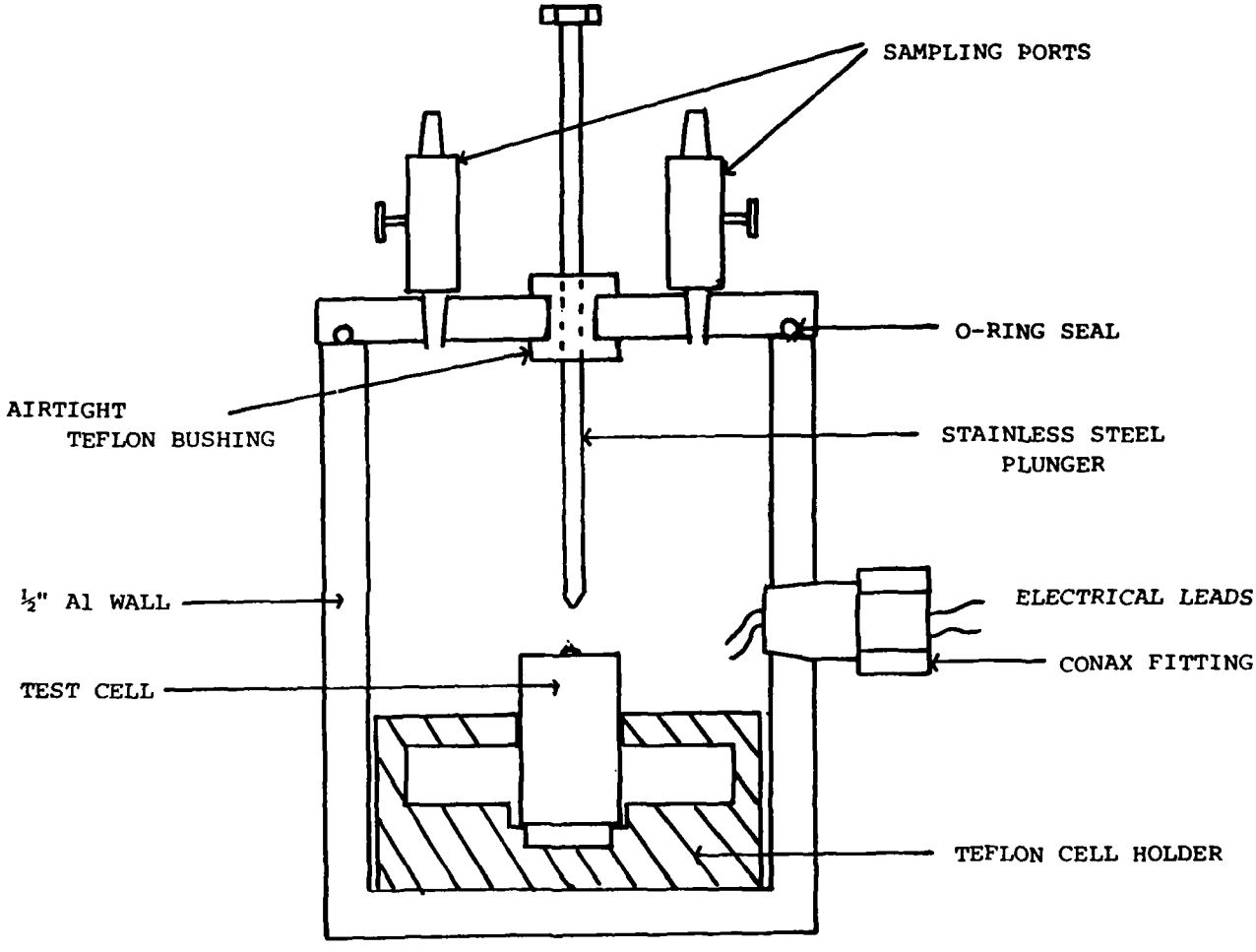

Fig. 1. Illustration of the test chamber used for the testing and opening of Li/SO_2 cells.

for analysis in the respective instruments, ii) the gases were collected in an evacuated collection/storage vial and saved. The collection/storage vials had sampling ports for subsequent analysis of the gases.

The less volatile components (such as CH_3CN) were collected from the cell after attaching the test chamber to a vacuum system.

A picture of the assembled test chamber and gas collection system is shown in Fig. 2. All analyses of the internal components of the cell were performed in an Ar filled glove box. Thus, throughout the entire analytical procedure, there was no atmospheric contamination. The internal cell components were removed by cutting the metal can in half, lengthwise, with a carbide grinding wheel.

Qualitative tests (14-16) were performed as follows: SO_3^{-2} was identified by reaction with sodium nitroprusside and/or by conversion to SO_2 by reaction with acid; $S_2O_4^{-2}$ was identified by reaction with Napthol Yellow-S; S^{-2} was identified by conversion of H_2S after treatment with acid and/or by reaction with sodium nitroprusside in alkaline solution; CN^- was identified by reaction with CuS; SO_4^{-2} was identified by reaction with Ba^{+2} and through elimination of other species; S was identified by melting point after extraction with CS_2.

2.2 Instrumental Analyses

Infrared spectra were recorded on a Beckman Acculab II spectrophotometer. Solid samples were pulverized to ensure their homogeneity then pressed into KBr discs. Volatile species were analyzed with a Beckman Universal Gas cell with KBr windows. X-ray diffraction data were obtained by the Debye-Scherrer method with CuK_α radiation. All X-ray samples were ground into a fine powder and sealed in quartz capillaries under an Ar atmosphere.

ESCA measurements of finely ground, discharged cathodes were made at Surface Science Laboratories, Inc., Palo Alto, CA. The samples were handled under Ar. The binding energies were referenced to hydrocarbon C(1s) at 284.6 eV. Surface elemental compositions were based on a Na_2SO_4 reference. Mass spectra data were obtained with a Nuclide 1290G mass spectrophotometer at Biomeasure, Inc., Hopkinton, MA. Gas chromotographic analyses were performed on a Varian 920 Gas Chromotograph equipped with a thermal conductivity detector and either a 4 ft Spherocarb (Analabs) or a 4 ft Chromosorb 104 (Analabs) resin in a stainless steel column at temperatures between 25-150°C. The assignment of peak identities was based on comparison to the retention times of standard samples.

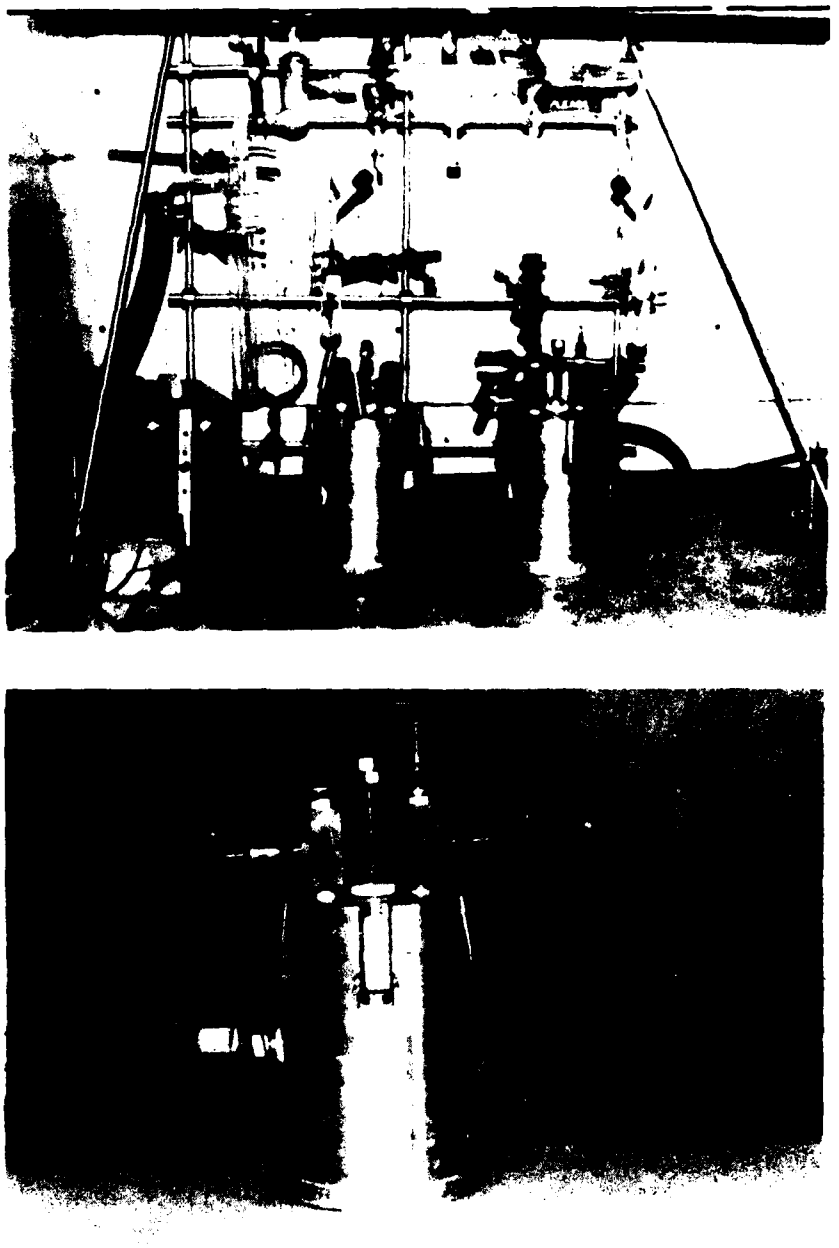

Fig. 2. Pictures of the assembled Li/SO_2 test chamber and of the gas collection system.

3.0 CHARACTERISTICS OF THE COMMERCIAL Li/SO_2 CELLS

The evaluation of the safety hazards of Li/SO_2 cells was performed with commercial C-size cells purchased from two different manufacturers. The cells are designated Type X and Type Z in this report.

The Type X cell has a rated capacity of 3.0 Ah at a discharge current of 100 mA at 25°C. The capacity of the Type Z cell is listed at 3.3 Ah at a discharge current of 135 mA.

The analysis and description of fresh Type X and Type Z cells are summarized in Table 1.

There are a number of significant differences between the cell designs which are discussed below.

The major difference is in the cathode design. Figure 3 shows a picture of the inner section of the cathodes from the two types of cells.

The cathode of the Type X cell has a geometric area of ~178 cm^2 and was constructed with carbon pasted onto both sides of an Al grid. As seen in Fig. 3, the Al grid is attached to an Al tab at the inner end of the wrapped cathode (i.e., the center of the cell) which in turn is connected to the positive lead in the center of the cover assembly.

The cathode of the Type Z cell has a geometric area of 125 cm^2 and has carbon pasted onto only one side of an Al grid. The Al grid is attached to an Al tab in the center of the cell as in the Type X cell.

Both types of cells employ a polypropylene separator. However, they apparently have different pore sizes. The material in Type Z cell is apparently more open (larger pore size) than that in Type X cell.

The Li anode in the Type X cell has essentially the same width as the cathode. It is attached to the inner wall of the can apparently by physical contact only.

The Li anode in the Type Z cell is 0.7 cm wider than the cathode. The electrodes are positioned such that the Li overlaps both edges of the cathode. The outer end of the wrapped Li is attached to a copper tab which in turn is attached to the negative lead. Post-mortem analysis of Type Z cells showed that after a discharge to 2.0V, the excess Li along the edges of the electrode package is essentially unused, insuring that the Li throughout the length of the electrode remains electrochemically accessible.

TABLE 1

DESIGN PARAMETERS[a] OF TYPE X AND TYPE Z Li/SO_2 CELLS

	Li	Cathode	SO_2	CH_3CN	Separator	Can
Type X	1.25 gm (4.8 Ah) 26.0 x 3.6 cm	4.8 gm[b] 25.5 x 3.5 x 0.09 cm	~9.6 gm (4 Ah)	~2.3 gm	Polypropylene	Ni-plated steel with vent on bottom
Type Z	1.73 gm (6.68 Ah) 26.0 x 3.2 cm	3.0 gm[b] 25.0 x 2.5 x 0.075 cm	~8.8 gm (3.7 Ah)	~1.5 gm	Polypropylene	Ni-plated steel with vent on side.

[a]The values reflect the analysis of one cell of each type.

[b]Includes weight of Al grid.

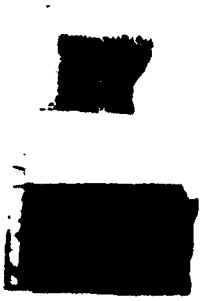

Fig. 3. Photograph of the inner section of the cathodes from the Type Z (upper) and Type X (lower) cells.

In contrast, after a discharge to 2.0V the Li remaining in the Type X cell is very thin throughout the entire length of the electrode, making it likely that most of the Li is electrochemically inaccessible during overdischarge.

The differences in the cell designs suggest that in actual use the Type X cell is anode limited, while the Type Z cell is cathode limited. Without a reference electrode in the cell this cannot be verified; however, the discharge characteristics of the cells seem to support this.

Typical voltage profiles of the discharge and forced overdischarge of Type Z and Type X cells are shown in Figs. 4 and 5, respectively. The potential profile of the Type Z cell during forced overdischarge is characterized by small negative voltages (< -500 mV) which do not show substantial changes during continued overdischarge. This behavior is consistent with an end of cell-life caused by cathode limitations.

The forced overdischarge of the Type X cell is characterized by a deep reversal of the cell voltage. After a short period in deep reversal, the cell voltage generally returns to less negative values, but consistently displays large, rapid voltage fluctuations throughout the forced overdischarge. This type of behavior is most likely to occur because of disconnection or depletion of the Li at the end of useful cell life.

It should be emphasized that even though the two types of cells are apparently of different designs, the same forced overdischarge products have been identified from both (see later).

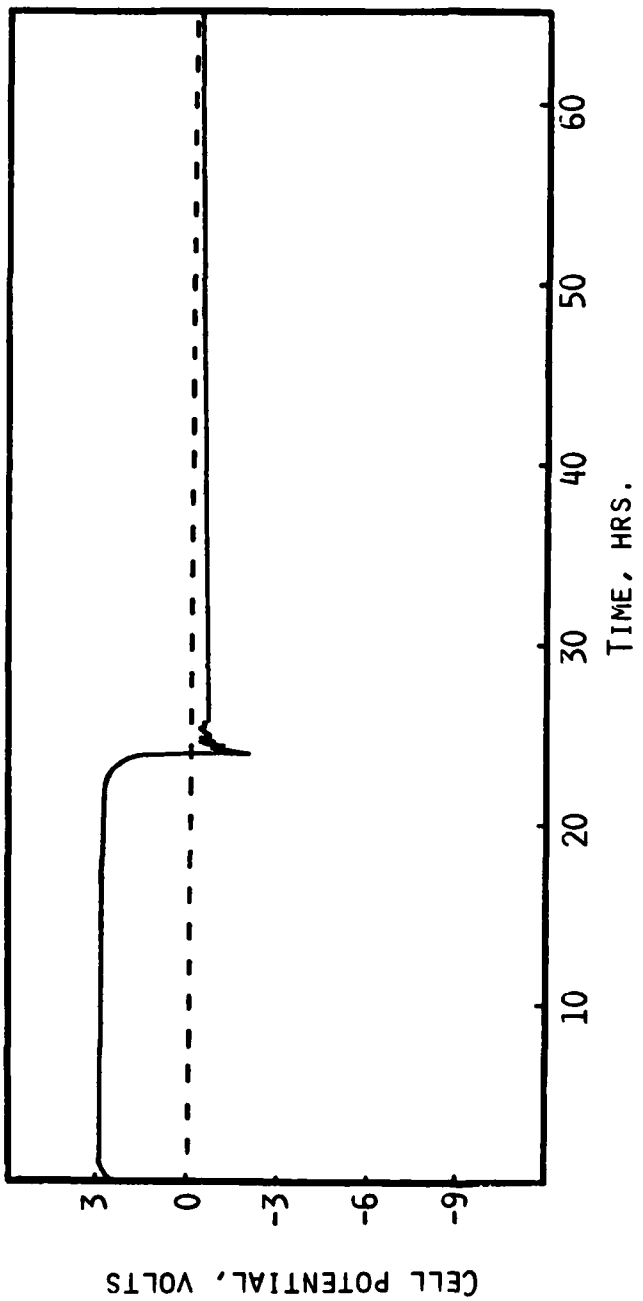

Fig. 4. The discharge and forced overdischarge of a Type z Li/SO_2 cell at 150 mA (~1.20 mA/cm^2).

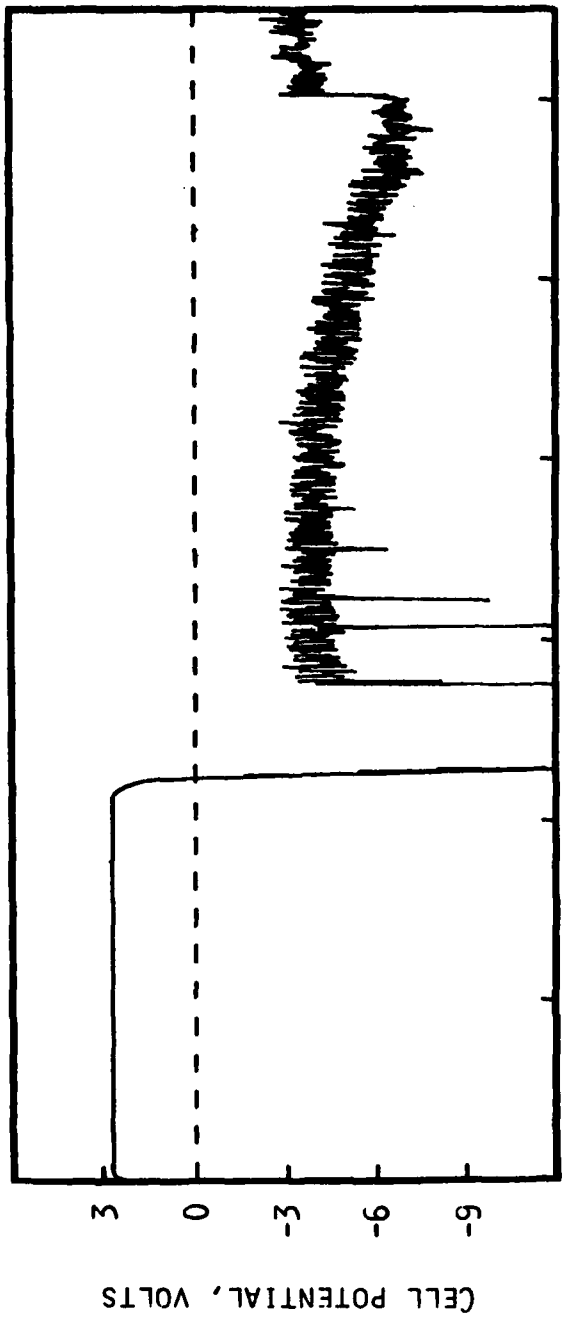

Fig. 5. The discharge and forced overdischarge of a Type X Li/SO_2 cell at 150 mA (~0.85 mA/cm^2).

4.0 INVESTIGATION OF THE DISCHARGE REACTION IN Li/SO_2 CELLS

A series of commercial Li/SO_2 cells were discharged, either galvanostatically or resistively, to cell potentials down to 0V at 25°C. At the end of the discharges the cells were opened and analyzed. The conditions of the discharges are listed in Table 2.

4.1 Quantitative Analysis and Characterization of the Li/SO_2 Cell Discharge Product

4.1.1 Quantitative Analysis of $Li_2S_2O_4$ in Carbon Cathodes

The discharge reaction of the Li/SO_2 cell results in the formation of an insoluble product in the carbon cathode. The formation of the product renders the initially flexible carbon cathode very stiff and brittle. Chemical spot tests with Napthol Yellow-S confirmed that discharged cathodes contained $Li_2S_2O_4$. $Li_2S_2O_4$ was not detected in any other part of the cell.

Quantitative determination of the $Li_2S_2O_4$ in the cathodes of eight cells was carried out using the following procedure: The cathode was carefully removed from the cell inside a glove box, washed with acetonitrile to remove LiBr, and dried under vacuum. The entire cathode was then added to a deaerated ammoniacal silver nitrate solution (1N $AgNO_3$ in 9N NH_4OH). The $AgNO_3$ was in a 50% to 100% excess over that required for the reaction of Eq. 1, based on the electrochemical capacity (to 2.0V) of each cell.

$$2Ag^+ + S_2O_4^{-2} \rightarrow 2Ag_{(s)} + 2SO_{2(g)} \qquad (1)$$

The mixture was maintained under an Ar atmosphere and stirred for at least five hours. The mixture was then filtered and the solids repeatedly washed with 6N NH_4OH until free of excess Ag^+. The remaining solids (Ag^o, C, Al, Teflon) were added to an excess of HNO_3 (based on the amount of Ag^o formed in Eq. 1) and stirred overnight to dissolve the elemental silver. The mixture was then filtered and the remaining solids repeatedly washed in 6N HNO_3 until free of silver. The filtrates were combined and diluted to a convenient (typically 500 ml) volume with distilled water.

Aliquots (5-25 ml) of the Ag^+ solution were neutralized with 6N NaOH, then adjusted to a pH of 4-5 with 3N NHO_3. The solutions were then boiled for five minutes to remove nitrogen oxides. After cooling to room temperature, the Ag^+ was determined by titration with a standard (0.1N) KSCN solution using a ferric ammonium sulfate indicator.

TABLE 2

SUMMARY OF Li/SO_2 CELLS DISCHARGED DOWN TO 0.0V

Cell	Current (mA)	Capacity (mA) to 2.0V	Capacity (mA) to 0.0V
X-1	150	3400	-
X-2	160	3310	-
X-3	150	3310	-
X-4	150	3200	-
Z-1	150	3360	-
X-5	750	2280	-
X-16[a]	100	1500[a]	-
X-19	150	3450	3560
X-20	150	3300	3350
X-14	Resistive discharge across 10Ω	3140	3350
X-22	Resistive discharge across 10Ω	3300	-

[a]Cell was partially discharged.

Species which could be present in solution such as SO_3^{-2}, $S_2O_3^{-2}$, SO_4^{-2}, SCN^-, Br^-, Al^{+3} were found not to interfere with the determination.

Experiments showed that Li_2S does interfere with the analysis. However, chemical spot tests with Cu^{+2}, Ca^{+2} and Ag^+ along with X-ray data (see below) gave no evidence for the presence of Li_2S in the cathode.

The results of the dithionite analyses and the experimental discharge parameters of each of the eight cells are presented in Table 3.

Three of the cells, X-1, X-2, and Z-1 were galvanostatically discharged to a cell potential of 2.0V and one cell, X-19, to a cell potential of 0.0V at 150 mA.

The amount of $Li_2S_2O_4$ found in the cells is in good agreement with the measured electrochemical capacities. The small scatter in the data is reasonable considering the relatively tedious procedure required for quantitative removal of the cathode containing the $Li_2S_2O_4$ from commercial cells.

The amount of $Li_2S_2O_4$ found in cell X-16, which was partially discharged, is slightly high. However, it should be noted that the absolute error in the analysis (300-400 mg of $Li_2S_2O_4$) is similar to that obtained in the fully discharged cells.

The amount of $Li_2S_2O_4$ formed in cells X-17 and X-21, which were forced overdischarged, was approximately 10% greater than the electrochemical capacity to 0 volt. These results indicate that at least part of the charge passed during forced overdischarge results in the formation of $Li_2S_2O_4$ in the cathode. The data show that further reduction of $Li_2S_2O_4$ to other sulfuroxy species does not occur during forced overdischarge.

Cell X-25 was discharged for 1600 mAh at a current of 100 mA then recharged an equivalent amount. Analysis of the cathode found, within experimental error, no $Li_2S_2O_4$.

Thus, the analytical results in Table 3 establish that under the conditions investigated, $Li_2S_2O_4$ is the major and most likely the sole product formed on the cathode during discharge of Li/SO_2 cells down to 0V. Furthermore, the data verify that the stoichiometry of the discharge reaction is

$$2Li + 2SO_2 \rightarrow Li_2S_2O_4 \qquad (2)$$

The results from cell X-25 also verify that the cathodic reaction is reversible (see Section 7.0).

TABLE 3

DITHIONITE DETERMINATION IN COMMERCIAL C-SIZE Li/SO_2 CELLS DISCHARGED AT 25°C

Cell	Discharge Current (mA)	Electrochemical Capacity (mAh) to 2.0V	to 0.0V	Including Forced Overdischarge	$S_2O_4^{-2}$ Found (mAh)	% of Theoretical[a]
X-1	150	3400	-	-	3410	100.3
X-2	150	3310	-	-	3430	103.6
Z-1	150	3360	-	-	3250	96.7
Z-19	150	3450	3560	-	3650	102.5
X-16[b]	100	1500[b]	-	-	1650	110.0
X-17[c]	150	3420	3450	9750	3790	109.8
X-21[c]	150	3480	3500	3930	4000	114.3
X-25[d]	100	-	-	-	-	-

[a]Based on the total measured electrochemical capacity above 0.0V.

[b]Cell was partially discharged.

[c]Cell was forced overdischarged.

[d]Cell was discharged 1600 mAh then recharged 1600 mAh.

4.1.2 ESCA Analysis of $Li_2S_2O_4$

Cell X-14 was discharged across a 10Ω resistor until the voltage fell to 0 volt. The capacity of the cell was 3350 mAh. The discharge curve is shown in Fig. 6.

The ESCA spectrum of the cathode is shown in Fig. 7. A high resolution scan of sulfur, showing the S(2p) binding energy, is given in Fig. 8.

The binding energy of dithionite S is not available in the literature. Therefore, a sample of $Na_2S_2O_4$ (Fisher Scientific) was used as a standard.

The binding energies of the cathode containing the discharge product and $Na_2S_2O_4$ are given in Table 4. The peak at 166.3 eV in both the $Li_2S_2O_4$ and $Na_2S_2O_4$ corresponds to the binding energy of S(2p) in $S_2O_4^{-2}$. An analysis of the binding energies of S(2p) versus the charge on S shows that the value of 166.3 eV lies where expected for S with a formal charge of +3.

The high resolution scan for S shows an additional peak at 170.4 eV in both the cathode and $Na_2S_2O_4$ samples. The peak accounts for ~14% of the surface S in the cathode sample.

Cell X-22 was also discharged across a 10Ω resistor but only to 2.0V. The cell yielded a capacity of 3300 mAh. An ESCA analysis of the surface sulfur was identical to that of the previous cell, showing two peaks for S at 166.3 and 170.4 eV. A time dependent study showed that the intensity of the 170.4 eV peak increased relative to that of the 166.3 eV peak with increased exposure of the sample to the atmosphere. Thus the peak at 170.4 eV can be attributed to the slight decomposition of the surface dithionite due to exposure to the atmosphere during sample preparation and not to other discharge products.

There is no evidence for the presence of any other sulfur species such as $S_2O_3^{-2}$ (160.9, 166.9 eV), SO_4^{-2} (168.0 eV), SO_3^{-2} (167.0 eV), S^{-2} (160.8 eV) or S^{O} (162.2 eV) in the cathode of cells discharged to 2.0 or 0.0V.

The surface elemental compositions of the cathode of cell X-14, based on a standard sample of Na_2SO_4, is listed in Table 5. Lacking the identity of the minor decomposition species (the 170.4 eV peak) a stoichiometric calculation of the amount of $S_2O_4^{-2}$ in the cathode is not possible. However, estimates show that $Li_2S_2O_4$ accounts for at least 90% of the surface sulfur.

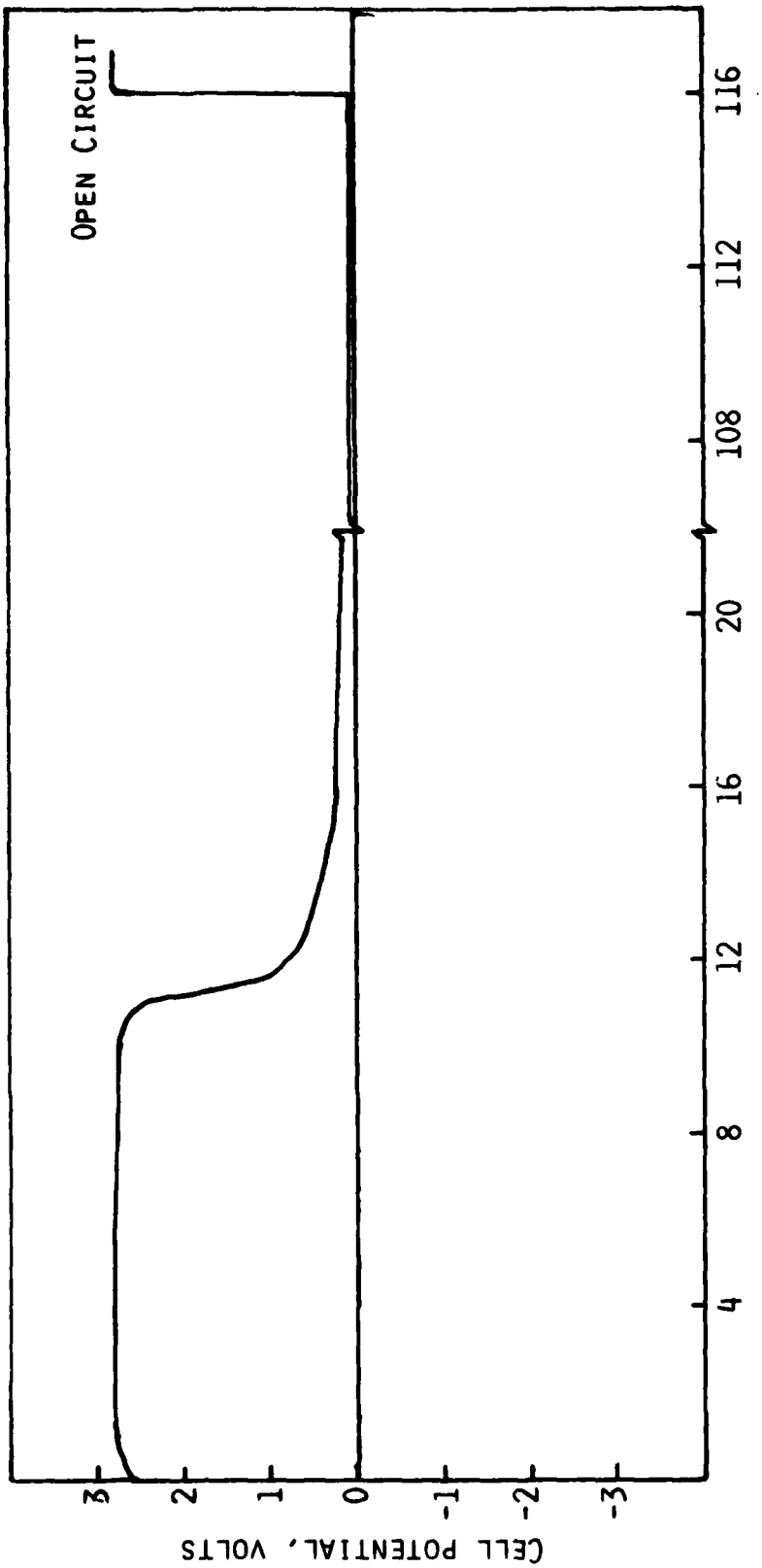

Fig. 6. Cell voltage of Li/SO_2 cell X-14 during discharge across a 10Ω resistor.

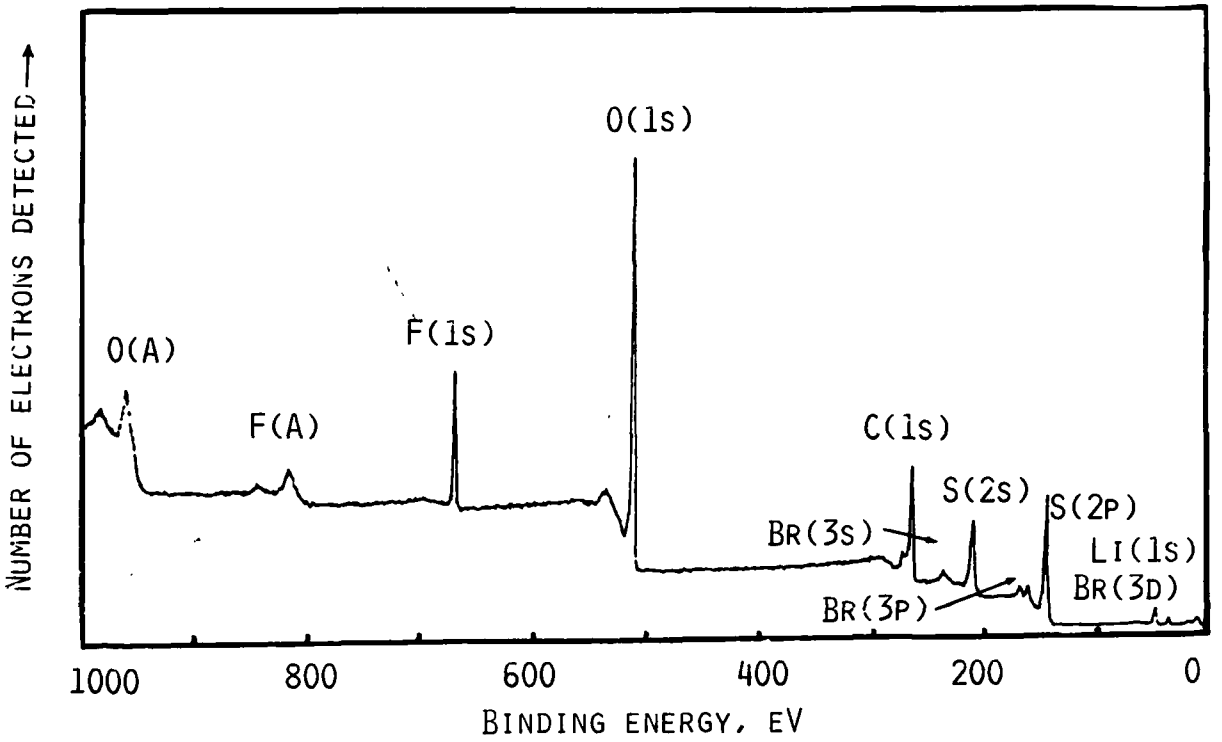

Fig. 7. ESCA spectrum of the cathode from cell X-14 after discharge to 0 volt

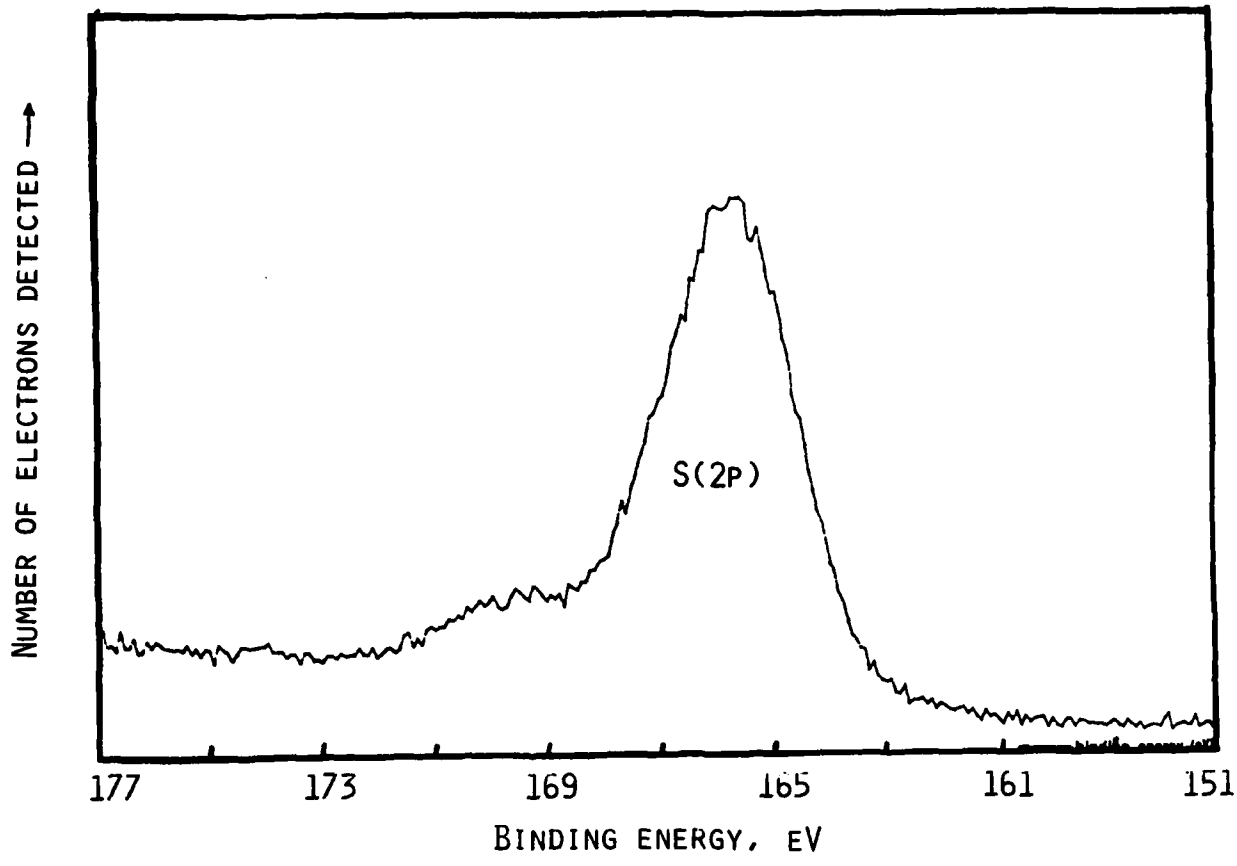

Fig. 8. High resolution ESCA scan of the surface S on the cathode from cell X-14.

TABLE 4

BINDING ENERGIES (eV) FROM HIGH-RESOLUTION SPECTRA

Samples	C (1s)	O (1s)	S (2p)	Li (1s)	F (1s)
Discharged Cathode of Cell X-14	284.6	531.7	166.3, 170.4	55.6	688.9
Sodium Dithionite	284.6	531.8	166.4, 170.4	-	-

TABLE 5

SURFACE ELEMENTAL COMPOSITIONS[a] OF THE DISCHARGED CATHODE FROM Li/SO_2 CELL X-14

C	O	S	Li	Br	F	O/S	Li/S[b]
32.0	29.0	14.0	17.0	1.5	6.7	2.1	1.1

[a]Expressed as atom percent for the detected species and based on a Na_2SO_4 standard.

[b]After subtracting the contribution of LiBr.

The ESCA scan in Fig. 5 also confirms the presence of all the other elements expected in the cathode. High resolution scans of C show ~2% in the form of a fluorocarbon - the Teflon binder.

4.1.3 Infrared Characterization of $Li_2S_2O_4$

The infrared spectrum of the $Li_2S_2O_4$ formed on the cathode of cell X-14, which was discharged to 2.0V, is shown in Fig. 9 along with the background spectrum of the Teflon bonded carbon cathode of an undischarged Type X cell (undischarged Type Z cathodes also displayed no IR absorption). The IR spectra of discharged Type Z cathodes were identical to that of the Type X.

The infrared spectra shown in Fig. 10 are from inner and outer sections of the cathode from cell X-1 (capacity 3400 mAh at 150 mA to 2.0V). The spectra are identical, showing that the same discharge product forms throughout the cathode.

The infrared spectrum of the discharge product was identical over all depths of discharge and under all discharge conditions investigated with both types of cells.

The IR spectrum of pure $Li_2S_2O_4$ has not been reported in the literature. Therefore, the IR spectrum of the $Li_2S_2O_4$, formed in the carbon cathode, was compared to that of $Na_2S_2O_4$.

The infrared absorption frequencies of the discharge product in the cathode matrix are listed in Table 6 along with those of a sample of $Na_2S_2O_4$ (Fisher Scientific Company). The spectrum of $Na_2S_2O_4$ is shown in Fig. 11.

There are several similarities between the spectra of the discharge product in the cathode and $Na_2S_2O_4$. Both spectra have a strong absorption at ~900 cm^{-1}. Also present in both compounds are two medium intensity absorptions at 520 and 420 cm^{-1} in $Na_2S_2O_4$ and 550 and 500 cm^{-1} in the discharged cathode.

The major difference between the two spectra is that the product in the cathode from the discharged cells exhibits two strong bands at 1028 and 1085 cm^{-1} while $Na_2S_2O_4$ has only one strong band at 1050 cm^{-1}. It should be noted that the frequency of this $Na_2S_2O_4$ band is midway between those observed in the discharged cathodes. Since the spectra were obtained on solid samples, the crystallographic effects on absorption frequencies can be significant between the Li and Na salts.

There was no evidence in any of the cathodes examined for the presence of other Li sulfuroxy compounds such as $Li_2S_2O_3$ (1120, 1000, 670 cm^{-1}), (970, 630, 395 cm^{-1}), or Li_2SO_4 (~1120, 645 cm^{-1}).

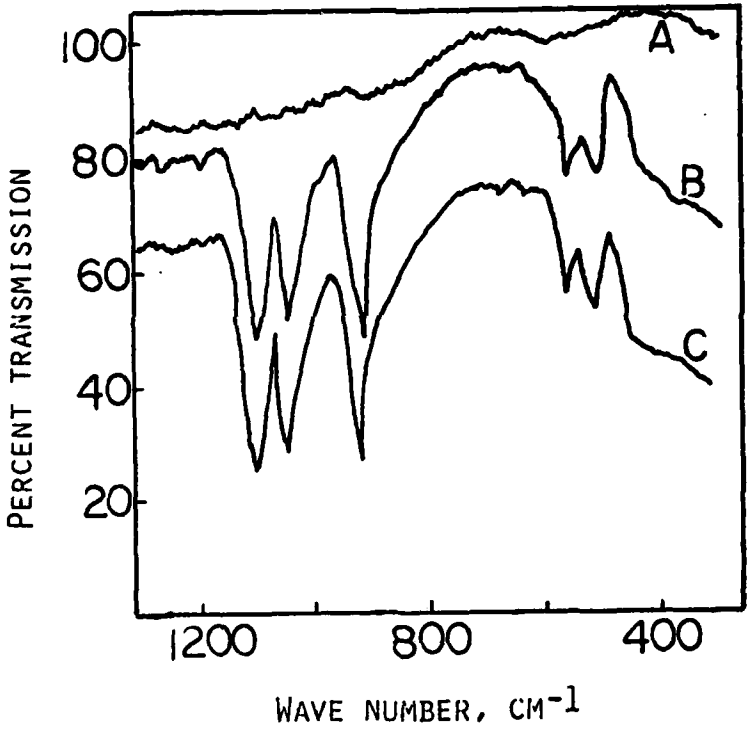

Fig. 9. Infrared spectra of $Li_2S_2O_4$ formed in the carbon cathode of a Li/SO_2 cell. Curve A: background spectrum of a fresh carbon cathode, Curve B: spectrum of a cathode after a discharge to 2.0V, and Curve C: spectrum of a cathode after a forced overdischarge.

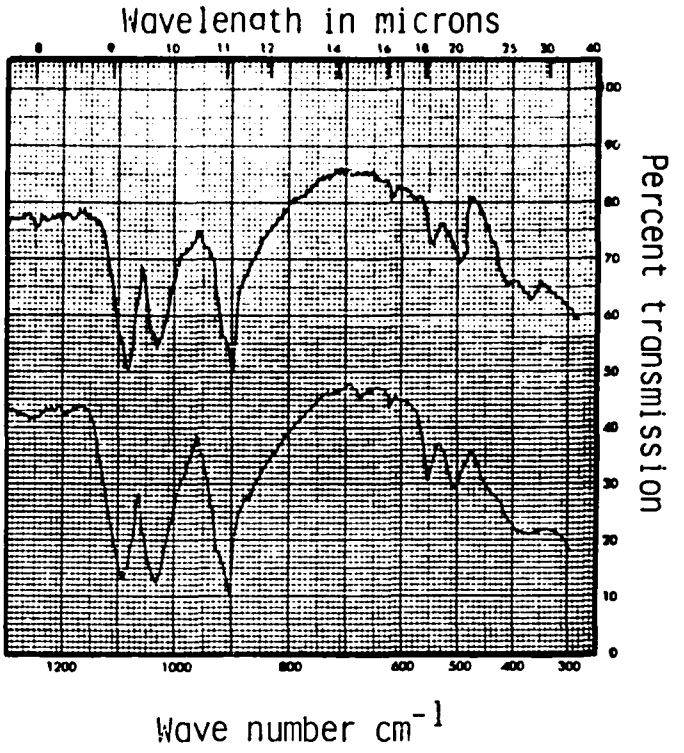

Fig. 10. IR spectra of an inner section (upper) and an outer section (lower) of the cathode from cell X-1 after discharge to 2.0V.

TABLE 6

MAJOR INFRARED FREQUENCIES OBSERVED IN DISCHARGED Li/SO_2 CATHODES AND $Na_2S_2O_4$ (Fisher)

Discharged Li/SO_2 Cathodes (cm^{-1})	$Na_2S_2O_4$ (cm^{-1})
500 (m)	420 (m)
550 (m)	520 (m)
902 (s)	551 (w)
1020 (s)	920 (s)
1085 (s)	1050 (s)

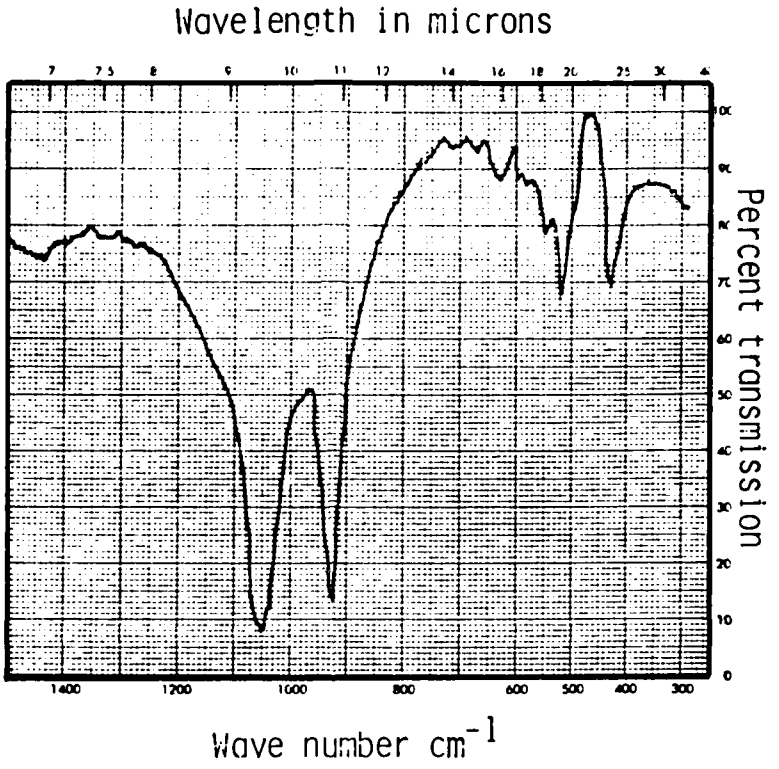

Fig. 11. IR spectrum of $Na_2S_2O_4$

The IR spectrum of the $Li_2S_2O_4$ on the cathode showed no change after storage for over two months in an Ar filled dry box at room temperature. However, significant changes occurred in the infrared spectrum of the $Li_2S_2O_4$ (in the cathode matrix) after exposure to the atmosphere for ~16 hours. This is seen in Fig. 12. This is consistent with the ESCA results which indicated that the $Li_2S_2O_4$ decomposes upon exposure to the atmosphere.

The thermal stability of the $Li_2S_2O_4$ (in the cathode matrix) was also briefly investigated. Up to ~170°C there is no change in the infrared spectrum of the $Li_2S_2O_4$ (again in the cathode matrix). Between 170-200°C the infrared spectrum shows a substantial change indicating the thermal decomposition of $Li_2S_2O_4$. This is depicted in Fig. 13 which shows the infrared spectra of two samples of $Li_2S_2O_4$ which were heated to 170°C and 200°C, under vacuum, for one hour. This observation substantiates previous thermal studies (17-19) which assigned an exothermic transition observed in cathodes from discharged cells at ~180°C to the decomposition of $Li_2S_2O_4$.

4.1.4 X-Ray Analyses of Discharged Cathodes

X-ray powder diffraction data were collected on the cathodes of cells X-14, X-22, X-2, and on a predominantly white material removed from the cathode of cell X-3 by shaking it in a small amount of CH_3CN. This whitish material gave a positive test for $S_2O_4^{-2}$ and had the infrared spectrum of $Li_2S_2O_4$.

The four powder patterns are tabulated in Table 7. The X-ray patterns of all four cathodes are essentially identical except for variations in the relative intensities of some lines. The data clearly show that the same product is present in all the cathodes. The powder pattern also contains lines corresponding to those of LiBr (3.18, 2.75, 1.94, 1.66, 1.54, 1.38, 1.26, 1.23, 1.12 and 1.06 Å). There is no evidence in the X-ray data for the presence of Li_2S, Li/Al alloy or Li/C intercalates (Li/C intercalates would probably not be detected even if present because of the amorphous nature of the carbon) in the cathodes of discharged cells.

4.2 Analyses of Volatile Species in Discharged Li/SO_2 Cells

The gases and volatile species present in discharged Li/SO_2 cells were qualitatively examined by infrared and/or gas chromatographic analyses. In all of the cells examined (except cells X-2 and Z-1) which were discharged to potentials down to 0.0V, SO_2 and CH_3CN were the only species detected. Analyses of cells X-2 and Z-1 revealed trace amounts of CH_4 in addition to SO_2 and CH_3CN.

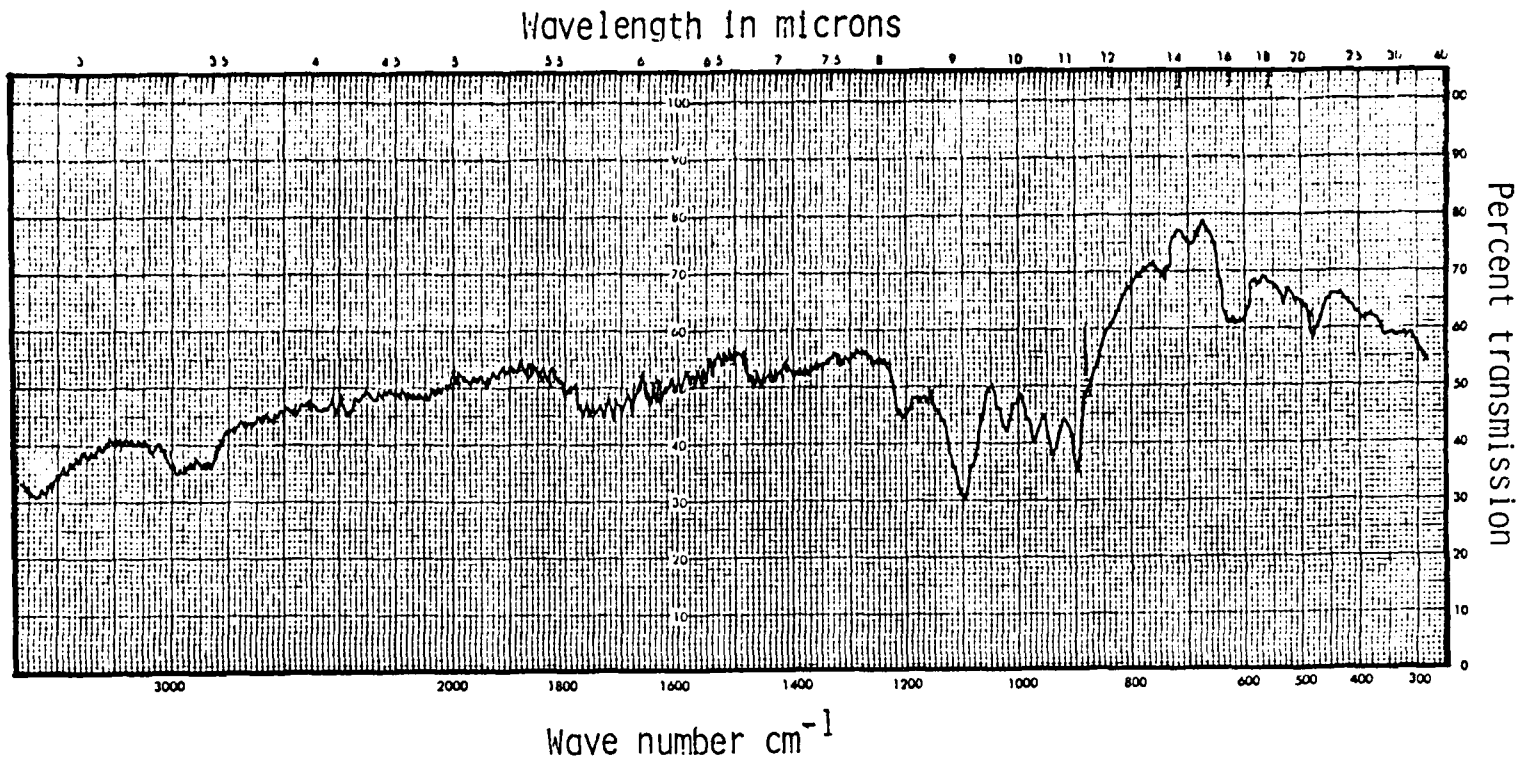

Fig. 12. IR spectrum of "$Li_2S_2O_4$" from a discharged Li/SO_2 cathode (cell X-3) after exposure to the atmosphere for 16 hours.

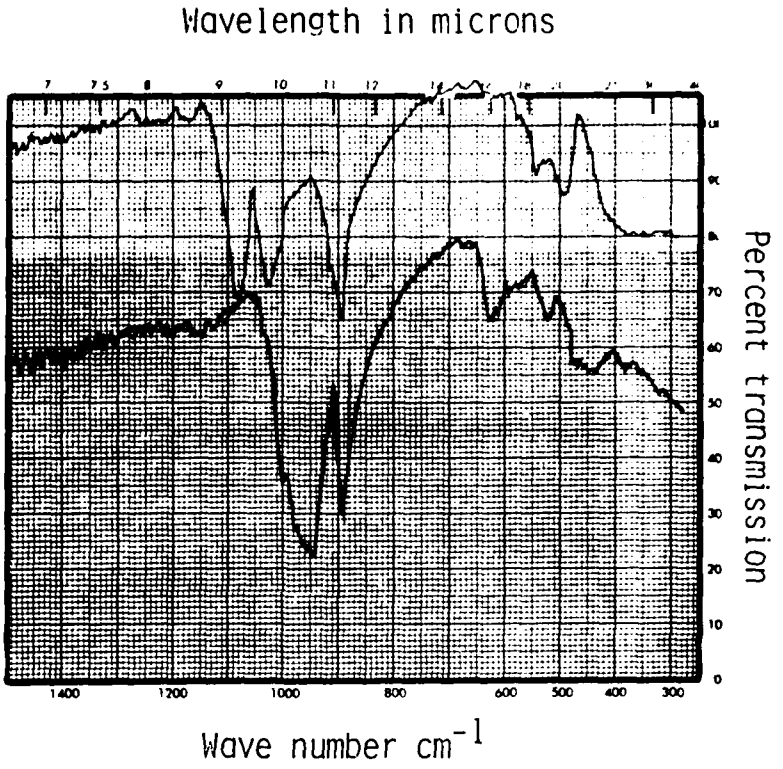

Fig. 13. IR spectra of "$Li_2S_2O_4$" from the cathode of a discharged Li/SO_2 cell showing the effect of temperature on its stability. Top spectrum was obtained after heating to 170°C and bottom spectrum after heating to 200°C.

TABLE 7

X-RAY[a] DIFFRACTION DATA OF CATHODES FROM Li/SO_2 CELLS

Cell X-14[b]		Cell X-22[c]			Cell X-2[d]		Cell X-3[e]	
d, Å	I/I_o	d, Å	I/I_o		d, Å	I/I_o	d, Å	I/I_o
5.10	< 5	5.09	10					
4.35	90	4.35	75		4.33	80	4.37	80
3.73	80	3.70	95		3.69	90	3.73	100
3.23	80	3.19	100	(broad)	3.22	80	3.20	80
2.96	50	2.95	60		2.93	40	2.94	40
		2.74	40					
2.67	100	2.66	100		2.66	100	2.70	100
2.53	70	2.53	80		2.52	70	2.54	80
2.43	5	2.44	5		2.43	5		
2.26	10	2.25	30		2.24	20	2.25	15
2.01	< 5							
1.92	15	1.93	50		1.92	15	1.93	15
1.80	10	1.79	< 5		1.79	5	1.78	< 5
1.75	10	1.75	< 5		1.75	5		
1.71	10	1.72	5		1.72	5	1.72	< 5
		1.65	15					
1.62	10	1.62	10		1.61	< 5	1.62	< 5
		1.58	10					
1.57	10	1.57	10		1.57	< 5	1.57	< 5
1.53	10	1.53	10				1.53	< 5
1.47	10	1.47	10		1.47	< 5	1.47	< 5
1.42	10	1.41	10				1.41	< 5
1.31	< 5							
1.30	< 5	1.29	5		1.29	< 5		
1.28	< 5	1.26	5					
		1.23	5					
1.19	< 5	1.19	5		1.19	< 5		
1.17	< 5	1.16	5		1.16	< 5		
1.14	< 5	1.14	5		1.14	< 5		
		1.06	5					
		0.93	5					
		0.92	5					

[a]Debye-Sherrer method, CuK_α radiation.

[b]Resistively discharged to 0.0V across 10Ω.

[c]Resistively discharged to 2.0V across 10Ω.

[d]Galvanostatically discharged at 160 mA to 2.0V.

[e]Galvanostatically discharged at 150 mA to 2.0V, white material separated.

4.3 Li Anodes in Discharged Cells

In each of the discharged cells examined, excess, unused Li was found throughout the length of the jelly roll electrode. The Li was thickest at the point where it was attached to the negative lead in both types of cells. In the Type X cell the Li was very thin throughout. There were numerous holes through the Li, especially near its edges. In the Type Z cells the edges of the Li strip anode were essentially unused while the mid portions were very thin.

4.4 Conclusions

The quantitative analysis of the $Li_2S_2O_4$ formed on the carbon cathode of the Li/SO_2 cell was accomplished by a procedure based on the reduction of Ag^+ by $S_2O_4^{-2}$. Quantitative analyses of discharged Li/SO_2 cells verified that $Li_2S_2O_4$ is the major and most likely the sole product formed on the cathode during discharges to 0.0V. The $Li_2S_2O_4$ was additionally characterized by infrared, X-ray, and ESCA analyses.

5.0 SAFETY HAZARDS DURING ROOM TEMPERATURE FORCED OVERDISCHARGE OF Li/SO_2 CELLS

The abuse resistance of both Type X and Type Z cells towards forced overdischarge at room temperature was evaluated. Type Z cells were tested at currents up to 1000 mA or a current density of 8 mA/cm^2. Type X cells were forced overdischarged at currents up to 1290 mA, which is equal to a current density of 7.2 mA/cm^2. The data show that there is a significant difference in the safety characteristics of the two types of cells during forced overdischarge.

Type Z cells were found to vent, often with flame, when forced overdischarged at currents of 900 mA or greater. At currents between 600-800 mA there was evidence of charring within the cell; however, the cells did not vent.

The Type X cells showed excellent abuse resistance. None of the cells tested vented at currents up to 1290 mA.

Table 8 summarizes the test conditions and the results of the cells tested in a forced overdischarge mode. The behavior and analyses of the cells are discussed below.

5.1 Forced Overdischarge Behavior of Type X Cells

Voltage and temperature profiles of the discharge and forced overdischarge of a number of Type X cells are given in Figs. 14-18.

In the forced overdischarge of Type X cells at $\leq$300 mA, the cell potential initially fell to very negative values. When measured, the potential was approximately -12V, the voltage of the power supply. In each case, the rapid drop in cell potential at the end of discharge and the deep reversal at the beginning of forced overdischarge were mirrored by an increase in the cell wall temperature. After this point, each cell displayed slightly different behavior. In most cells, the potential rose to less negative values in 2-4 hours, but in others it remained at -12V. However, in general, further forced overdischarge resulted in large fluctuations in the cell potential which were often accompanied by changes in the cell wall temperature.

At discharge rates of $\geq$1000 mA the behavior of the Type X cells was slightly different. The main difference is that the cells did not experience an immediate deep reversal upon forced overdischarge. This suggest that at high rates the cells become cathode limited. However, even under these conditions none of the cells tested vented.

TABLE 8

SUMMARY OF THE RESULTS OF FORCED OVERDISCHARGE STUDIES OF Li/SO_2 CELLS

Cell	Discharge Current (mA)	Forced-Overdischarge Current (mA)	Capacity (mAh) to 2.0V	Capacity (mAh) to 0.0V	Extent of Forced Overdischarge (mAh)	Results
Z-2	150	150	3540	3580	5600	Did not vent.
Z-3	1000	1000	1100	1735	2565	Vented with flame.
Z-4	1000	1000	1175	2000	3600	Vented.
Z-5	1000	1000	1610	2360	340	Vented.
Z-6	900	900	1530	2300	3370	Vented with flame.
Z-7	800	800	1240	1760	18,560	Did not vent, evidence of burning within cell.
Z-8	600	600	1560	2100	45,000	Did not vent.
Z-9	150	1000	3300	3300	93,000	Did not vent.
Z-10	300	750	2840	2900	157,900	Did not vent.
X-6	300	300	3140	3170	4970	Did not vent.
X-7	300	300	3360	3390	1840	Did not vent.
X-8	150	150	3490	3500	6320	Did not vent.
X-11	1000	1000	2700	3243	7760	Did not vent.
X-12	1000	1000	2620	3117	101,880	Did not vent.
X-13	1290	1290	1700	2525	13,600	Did not vent.
X-17	150	150	3420	3450	9750	Did not vent.
X-21	150	150	3480	3495	3936	Did not vent.

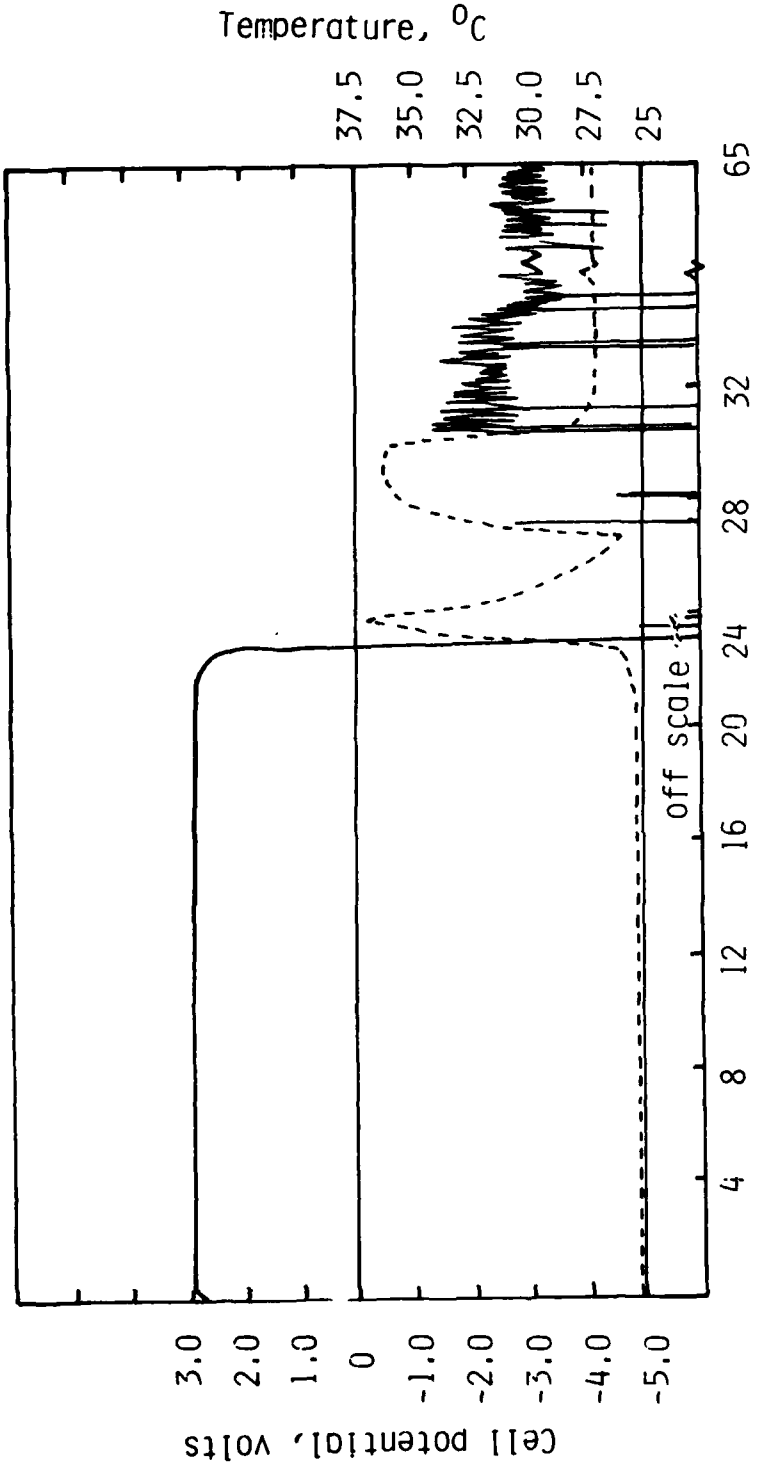

Fig. 14. Voltage (———) and temperature (- - - - - -) profiles of the discharge and forced overdischarge of Li/SO_2 cell X-8 at 150 mA.

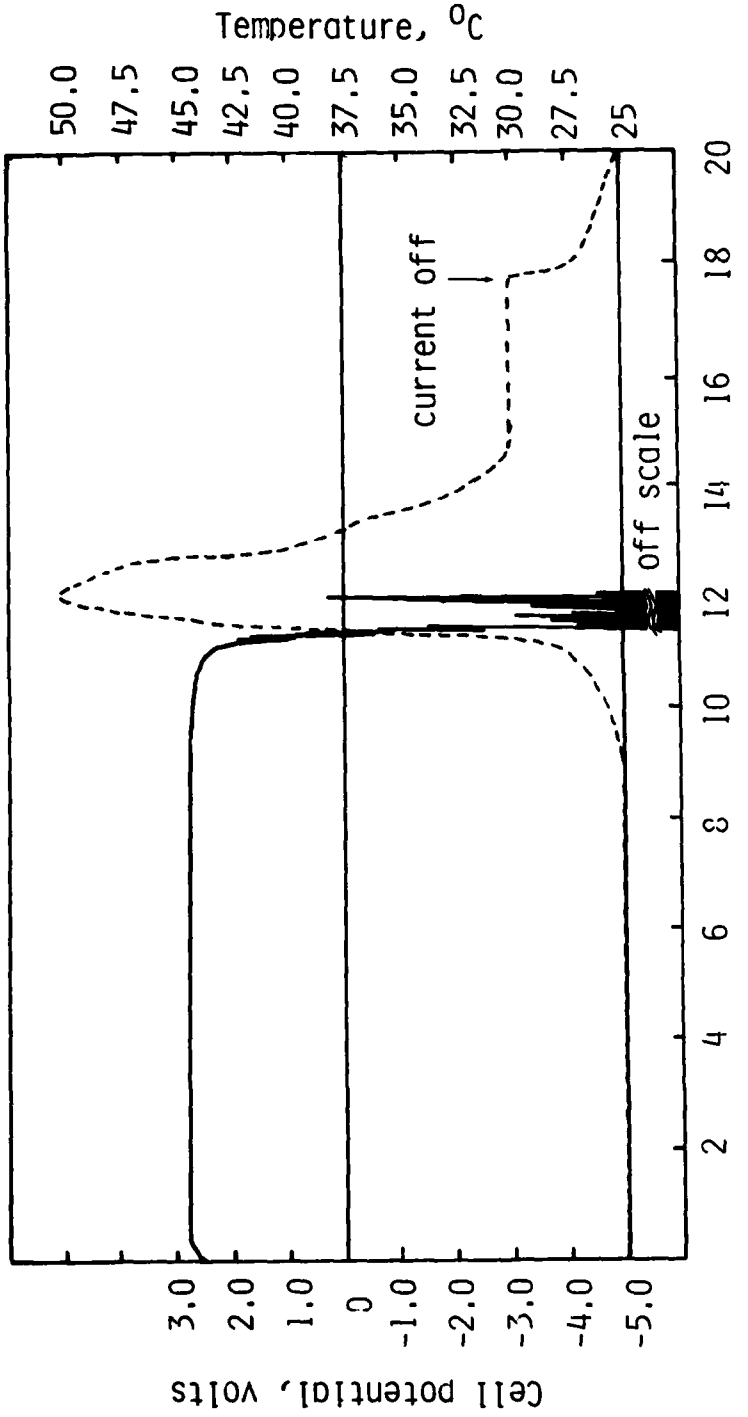

Fig. 15. Voltage (———) and temperature (- - - - - -) profiles of the discharge and forced overdischarge of Li/SO_2 cell X-7 at 300 mA.

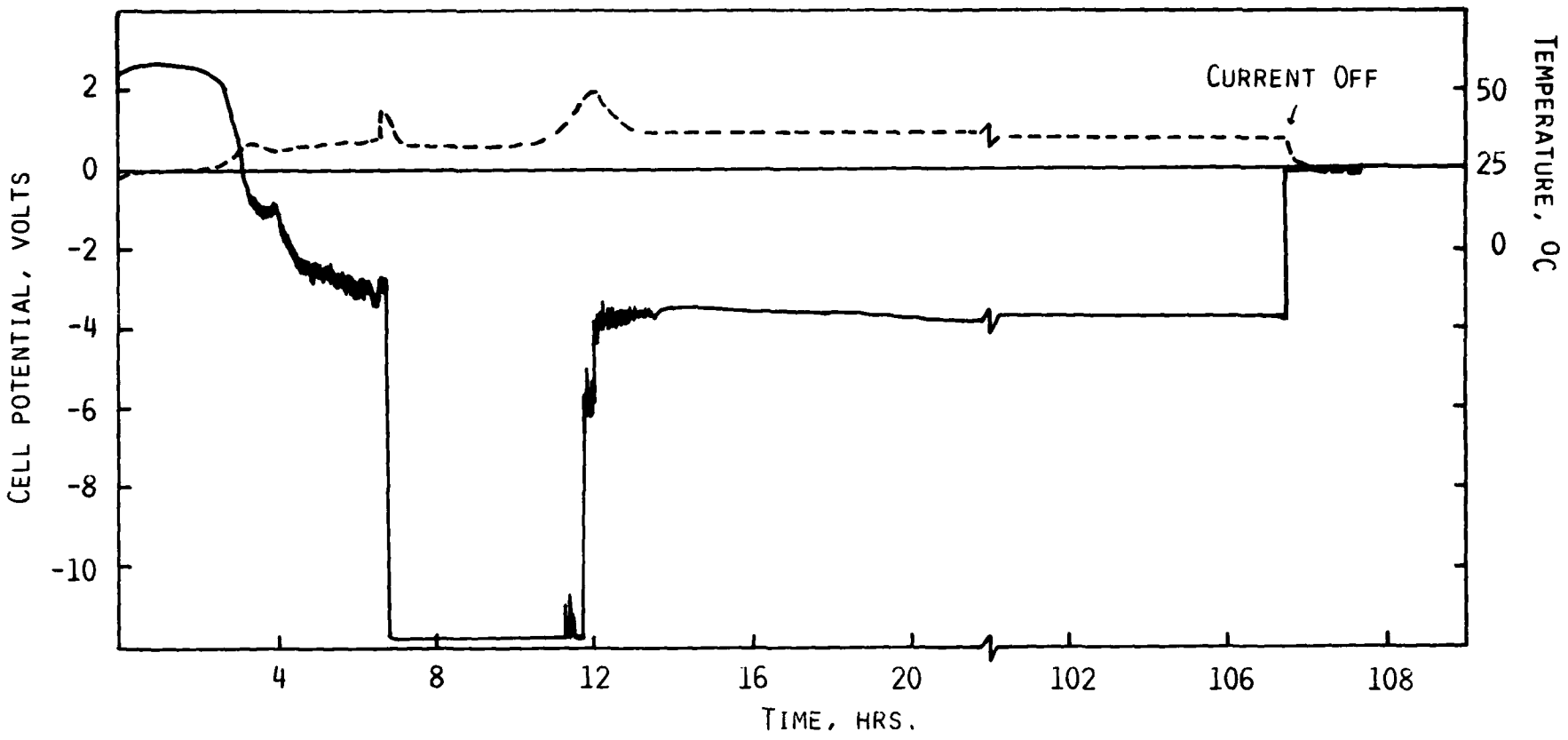

Fig. 16. Voltage (___) and temperature (---) profiles of the discharge and forced overdischarge of Li/SO_2 cell X-12 at 1000 mA.

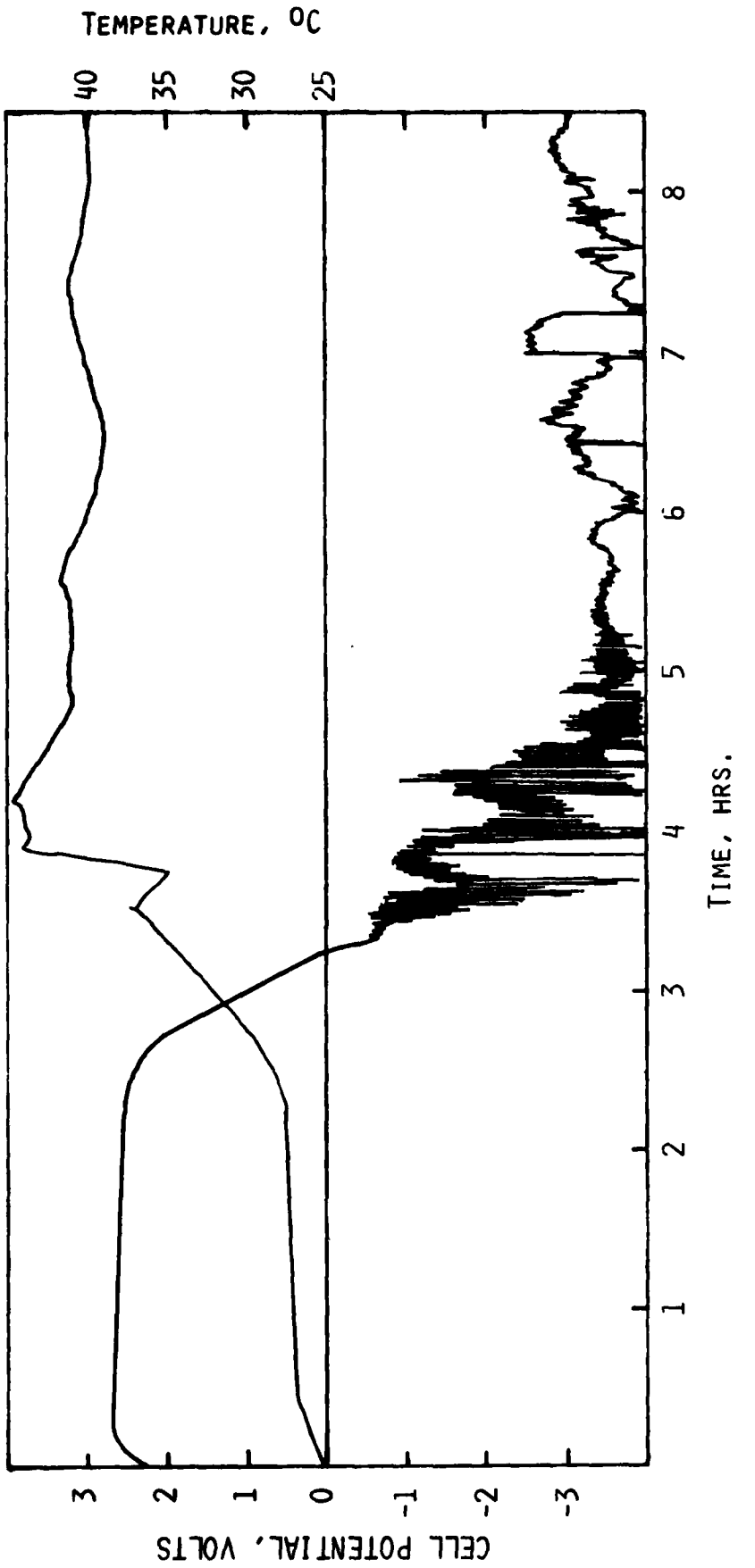

Fig. 17. Voltage (——) and temperature (---) profiles of the discharge and forced overdischarge of Li/SO_2 cell X-11 at 1000 mA.

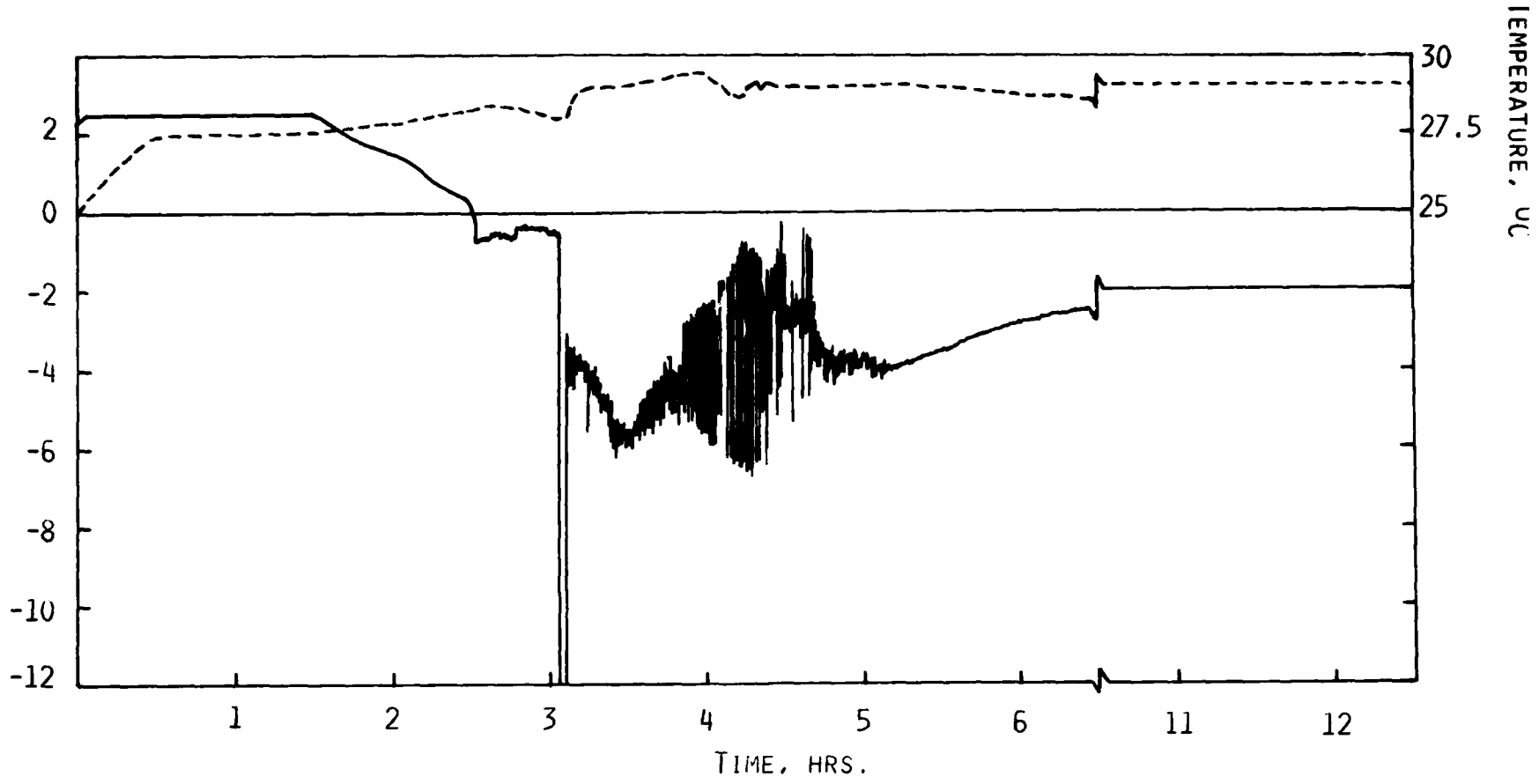

Fig. 18. Voltage (——) and temperature (---) profiles of the discharge and forced overdischarge of cell X-13 at 1290 mA.

5.2 Forced Overdischarge Behavior of Type Z Cells

The behavior of the Type Z cell on forced overdischarge at ≤300 mA was quite different as seen in Fig. 19. Once the cell potential reached 2.0V the cell rapidly went into shallow reversal. The accompanying temperature increase was less than in the Type X cells. After this point the cell potential gradually increased, levelling off usually between 0 and 0.5V, while the temperature slowly declined to room temperature. It should also be noted that the large voltage fluctuation observed with the Type X cells are not present with the Type Z cell.

At discharge rates ≥600 mA the discharge and forced overdischarge behavior was different. Figures 20-25 show the voltage and wall temperature profiles of cells forced overdischarged at rates of 600, 800, 900 and 1000 mA. In contrast to the Type X cells, the useful capacity of the Type Z cells decreased markedly with increasing discharge rates, as seen in Table 8. All the Type Z cells discharged at high rates displayed a sloping potential between 2.0 and 0 volts and each had a significant capacity near 0 volt. With continued forced overdischarge all the cells experienced large increases in the reversal potentials. All Type Z cells discharged at rates of ≥900 mA vented during forced overdischarge.

5.3 Post Test Analyses of Forced Overdischarged Cells

5.3.1 Type X and Type Z Cells Forced Overdischarged at Rates of ≤300 mA

Four Li/SO_2 cells (X-6, X-7, X-8 and Z-2) which were forced overdischarged at low rates (i.e., ≤300 mA) were opened and the products analyzed. All of the cells were opened within one day after the forced overdischarge was terminated except cell X-6 which was stored at room temperature for 18 days following the forced overdischarge.

Figure 26 shows the infrared spectrum of the gases released into the test chamber from cell X-7 when its top was pierced. The infrared spectrum shows the presence of SO_2 -- only its most intense peak at 1361 cm^{-1} is observed. The presence of CH_4 is also confirmed by the two sharp absorptions at 3020 and 1310 cm^{-1}. The infrared spectrum also shows the presence of another component(s) with a strong absorption at 1740 cm^{-1}, a triplet centered at 1220 cm^{-1} and a weak absorption at ~2950 cm^{-1}.

A GC analysis of the gaseous mixture showed only SO_2 and CH_4. The identity of the third component observed in the infrared spectrum is not certain. The absorption at 1740 cm^{-1} is characteristic of the C=O stretch of an aldehyde or ketone, the weak peaks at ~2950 cm^{-1} are in the C-H region of an aldehyde, and the triplet at 1220 cm^{-1} is in the region of the C-O stretch of dimerized or trimerized aldehydes. Based on the infrared data, particularly the strong absorption at 1740 cm^{-1}, this third component appears to be a volatile aldehyde.

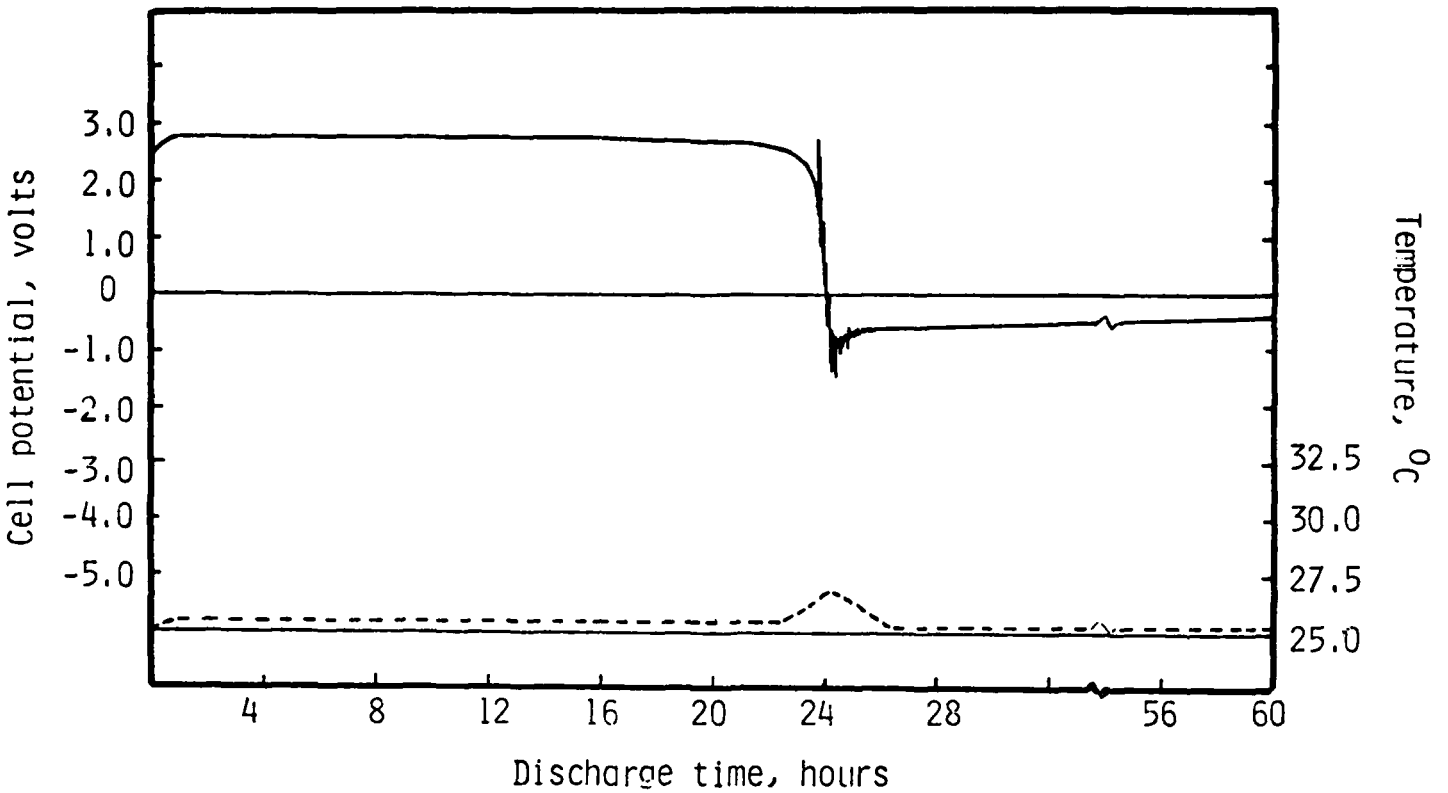

Fig. 19. Voltage (————) and temperature (-------) profiles of the discharge and forced overdischarge of Li/SO_2 cell Z-2 at 150 mA.

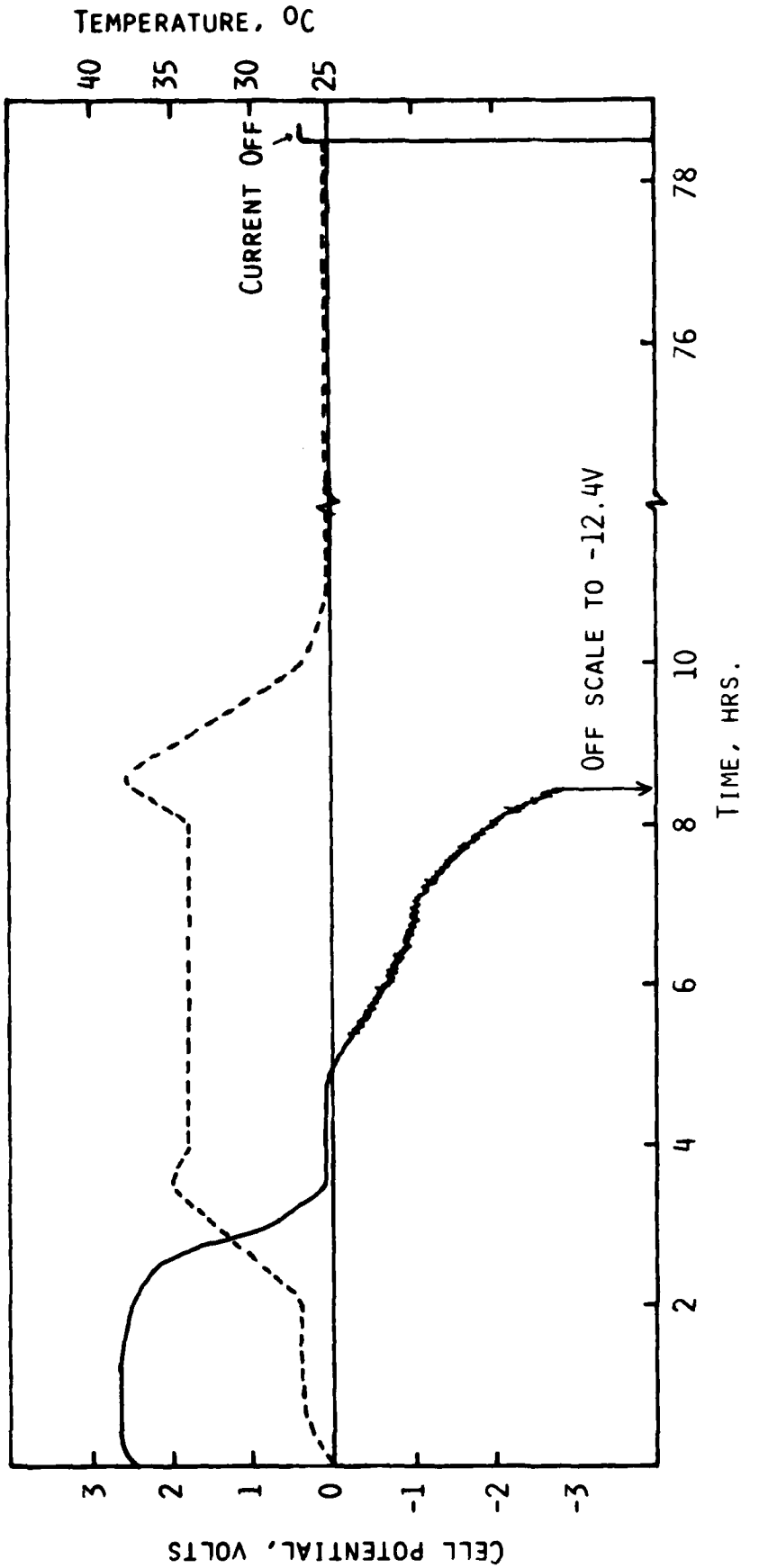

Fig. 20. Voltage (——) and temperature (---) profiles of the discharge and forced overdischarge of Li/SO_2 cell 2-8 at 600 mA.

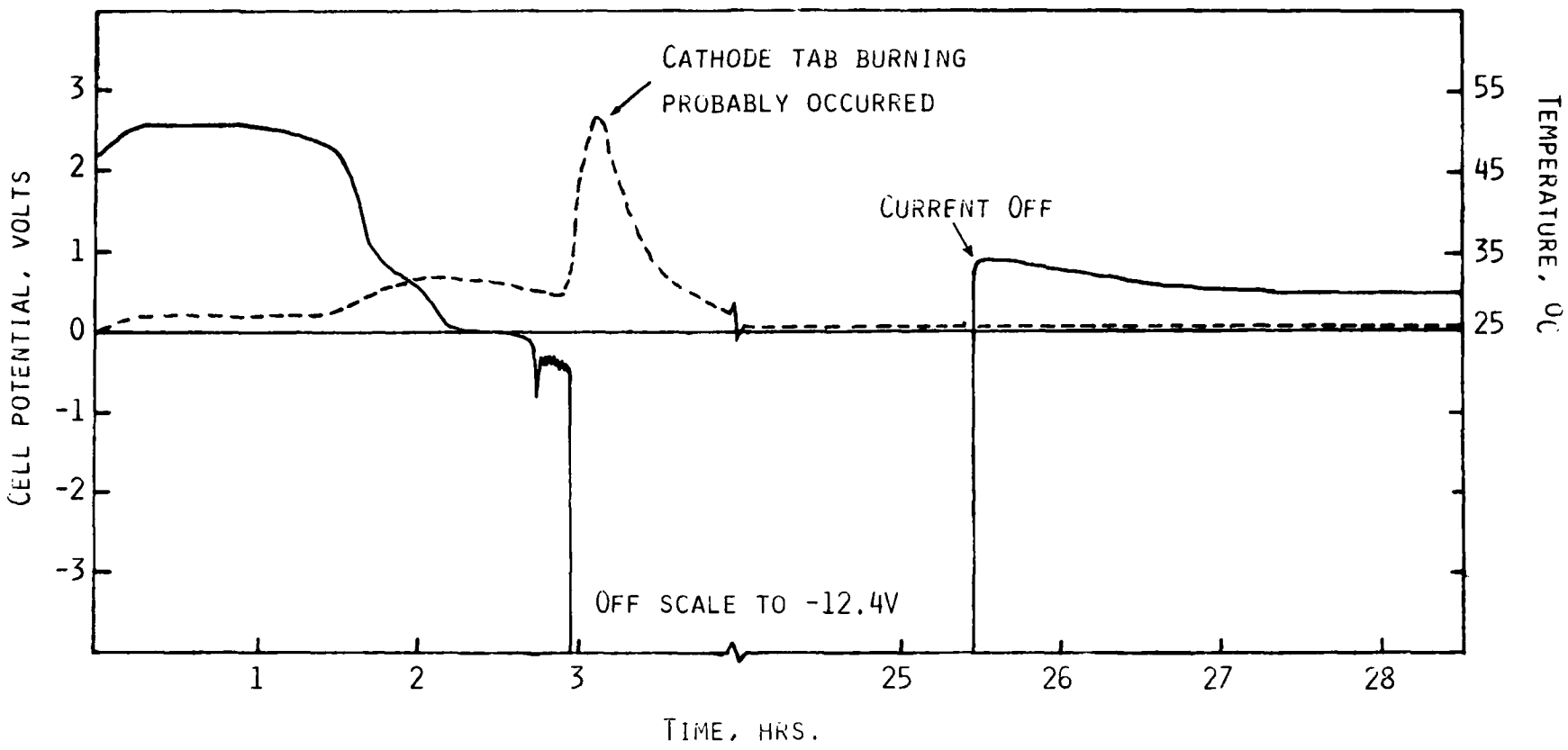

Fig. 21. Voltage (——) and temperature (---) profiles of the discharge and forced overdischarge of Li/SO_2 cell Z-7 at 800 mA.

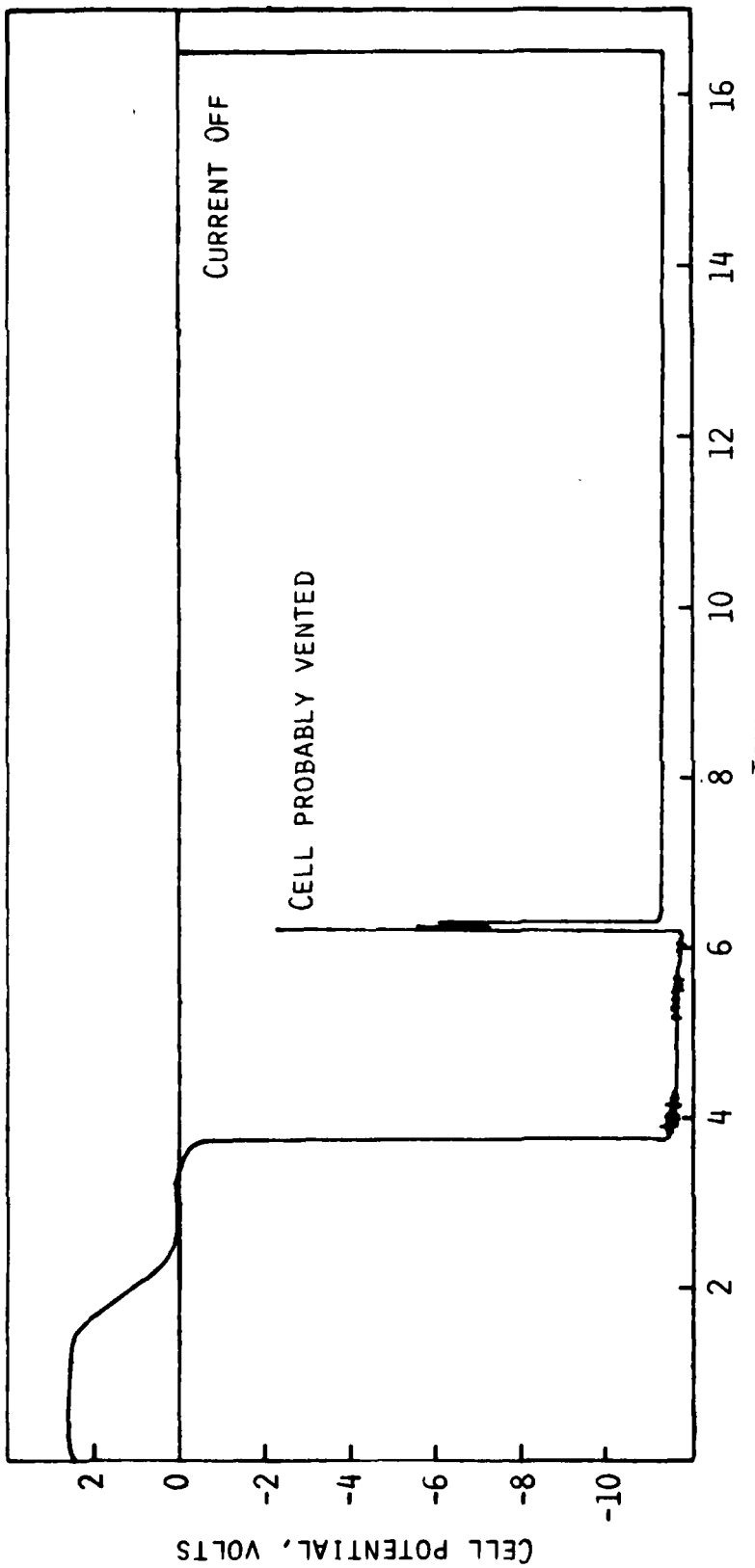

Fig. 22. Voltage profile of the discharge and forced overdischarge of Li/SO_2 cell Z-6 at 900 mA.

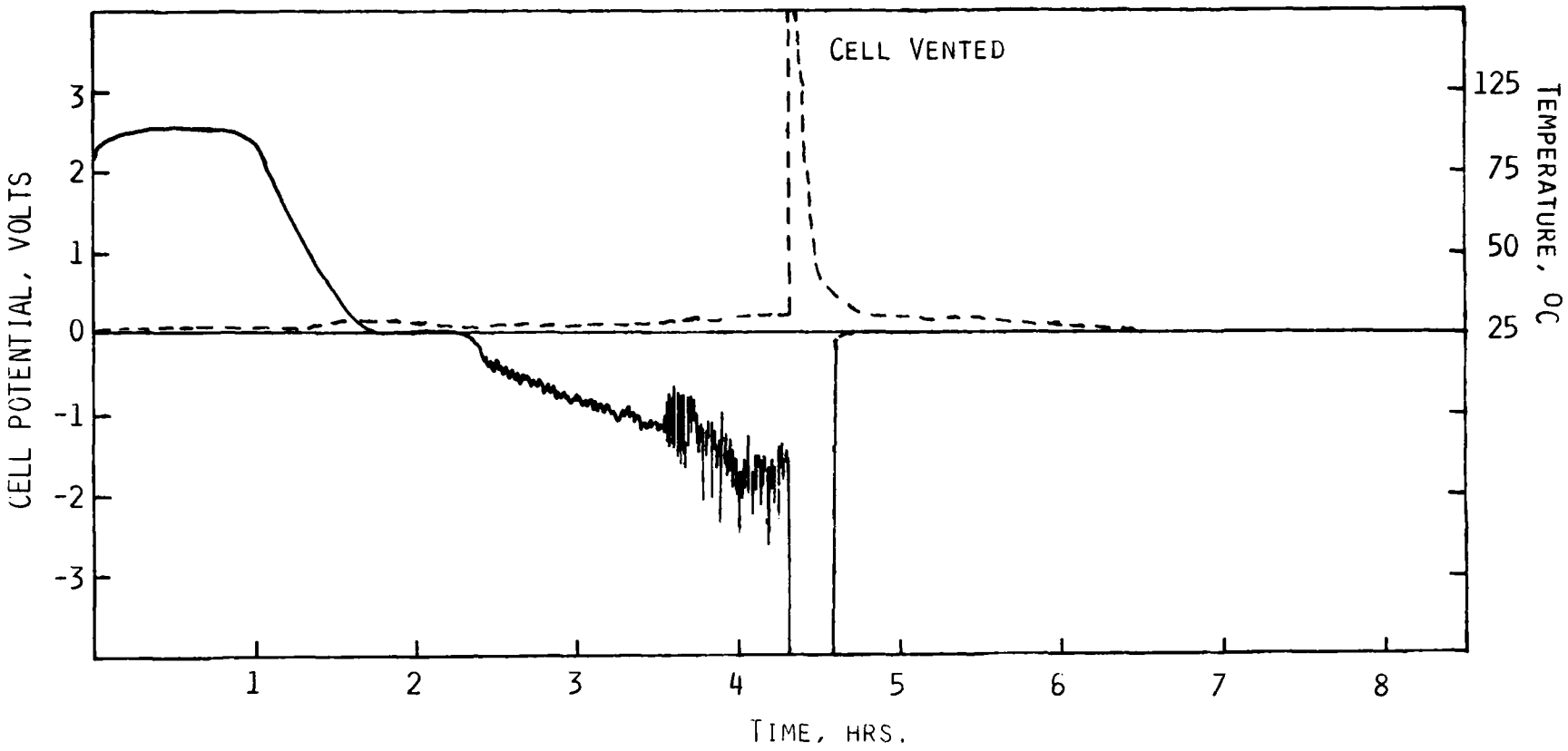

Fig. 23. Voltage (___) and temperature (---) profiles of the discharge and forced overdischarge of Li/SO_2 cell Z-3 at 1000 mA.

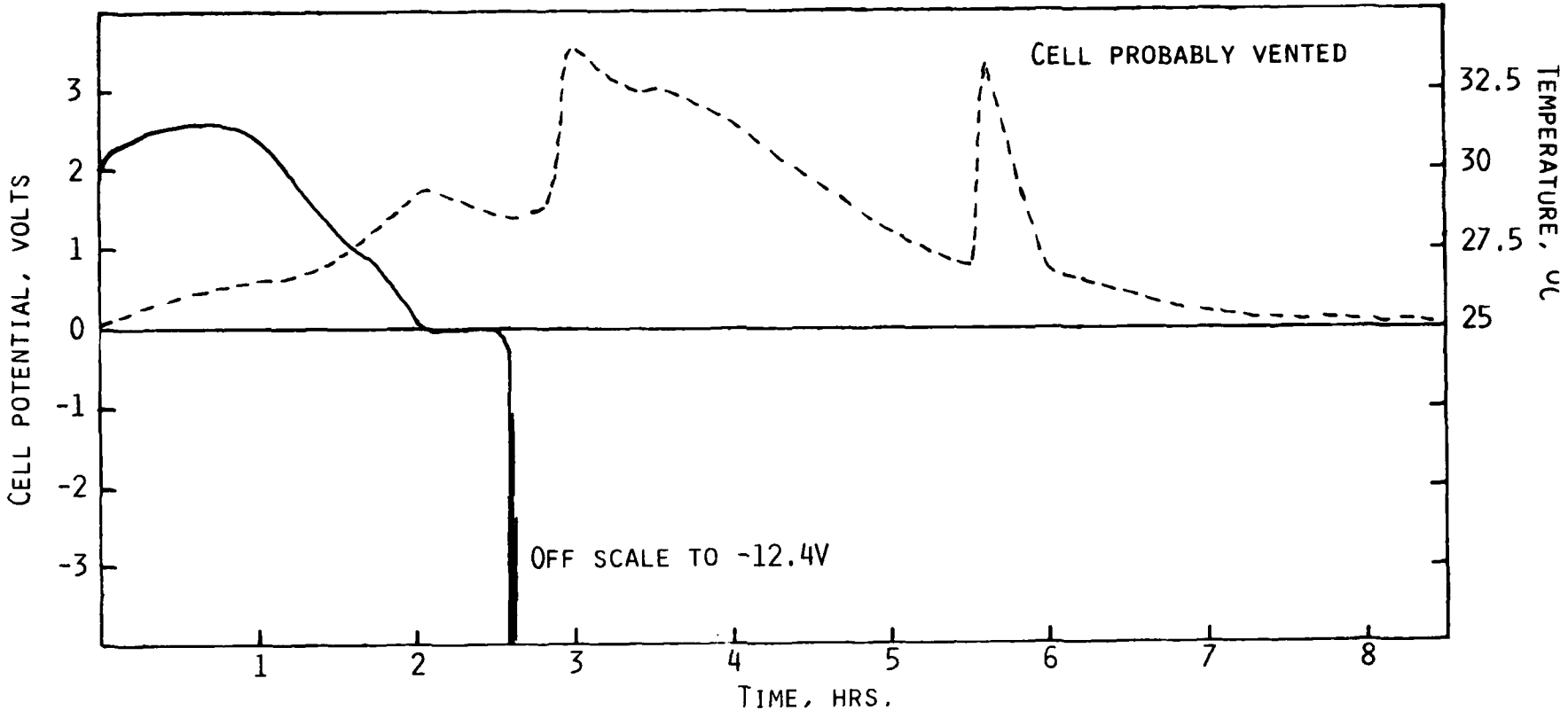

Fig. 24. Voltage (___) and temperature (---) profiles of the discharge and forced overdischarge of Li/SO_2 cell Z-4 at 1000 mA.

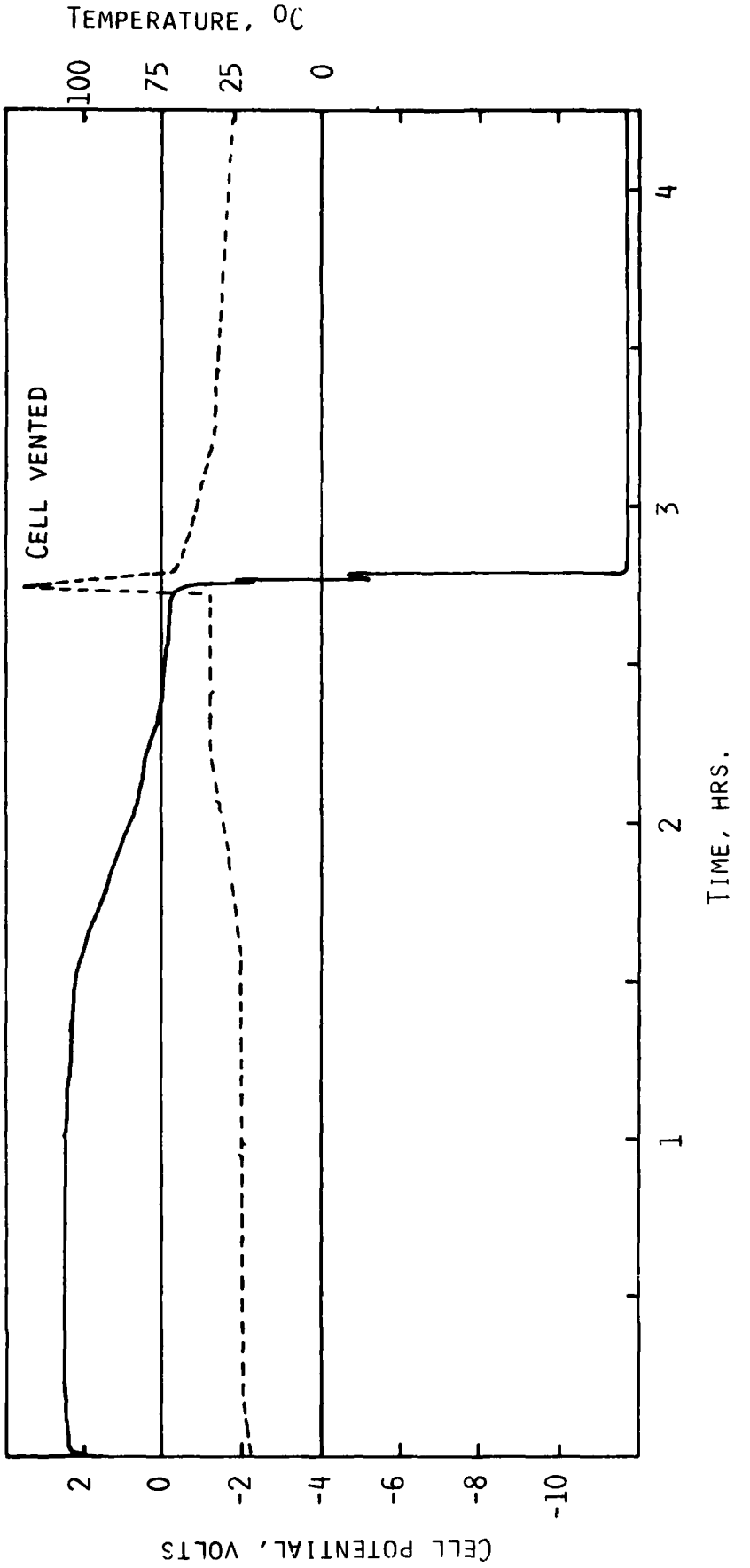

Fig. 25. Voltage (——) and temperature (---) profiles of the discharge and forced overdischarge of Li/SO_2 cell Z-5 at 1000 mA.

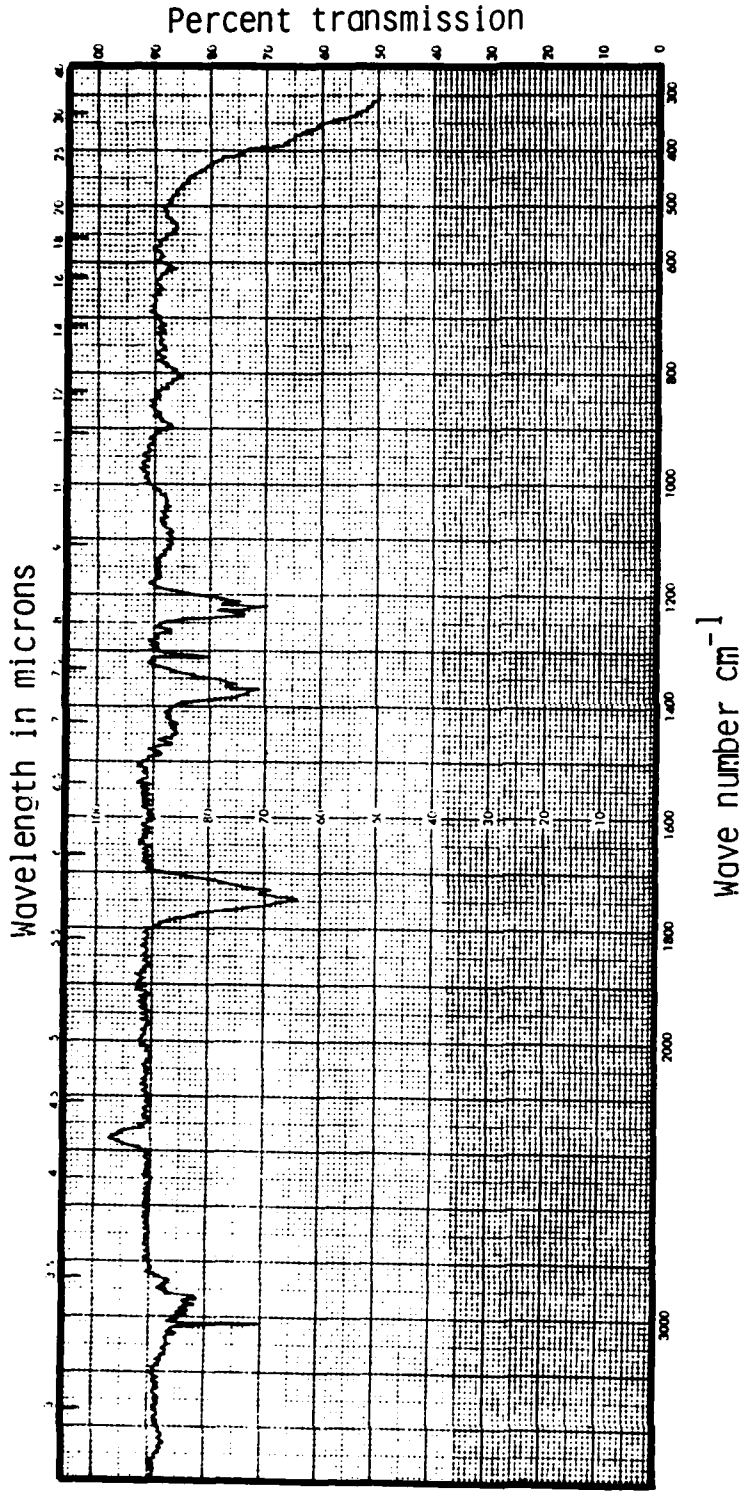

Fig. 26. IR spectrum of the gases from Li/SO_2 cell X-7 after reversal.

The remainder of the cell was disassembled in a dry box. A small amount of Li was found on the cell wall where the Li anode was originally attached. A yellow-brown material was located throughout the rest of the anode compartment. Approximately 500 mg of the material was removed from the cell. A more detailed analysis of this material is presented later.

The infrared spectrum of the cathode from cell X-7 is shown in Fig. 27. The infrared spectrum of this cathode, even after the cell was forced overdischarged into voltage reversal, is identical to that of $Li_2S_2O_4$. This shows that during the forced overdischarge of a Li/SO_2 cell no other, at least infrared detectable, species are formed on the carbon cathode. There is also no evidence for the further reduction of the $Li_2S_2O_4$ formed during discharge.

Cell X-8 was opened immediately after the current was turned off. The gases released from the cell into the test chamber were identified by IR and GC analyses as SO_2 and the "aldehyde" identified in the previous cell. No CH_4 was detected in the gases released from the cell. The analysis of the remainder of the cell was the same as that of cell X-7.

Cell Z-2 was analyzed immediately after being forced overdischarged at 150 mA for 160% of its capacity to 2.0V. CH_4 and a small amount of SO_2 were the only gases identified in the cell. A yellow-brown material was also found in the anode compartment of cell Z-2 and identified as the same product as found in cells X-7 and X-8. The infrared spectrum of the cathode showed only $Li_2S_2O_4$.

Cell X-6 was stored for 18 days before it was opened and analyzed. SO_2 was the only gas identified. The infrared spectrum of the cathode again showed only $Li_2S_2O_4$. Unlike the three previous cells no yellow-brown product was found in the anode compartment. Acetonitrile was found in all the cells.

5.3.2 Type X Cells Forced Overdischarged at High Rates

Three Type X cells, X-11, X-12 and X-13, were opened and examined after being forced overdischarged at rates of 1000 and 1290 mA as indicated in Table 8.

SO_2 and CH_4 were the only gases detected in the cells. Examination of the inside of the cells showed very little Li left in the anode compartment. In each cell there was also the brown crystal typically found in the anode of forced overdischarge cells.

Infrared analyses of the cathodes showed only the presence of $Li_2S_2O_4$. The Al cathode support was very brittle around the outside of the jelly roll. The Al grid also was covered with a brown compound in a few areas, however, it had formed in amounts too small to identify.

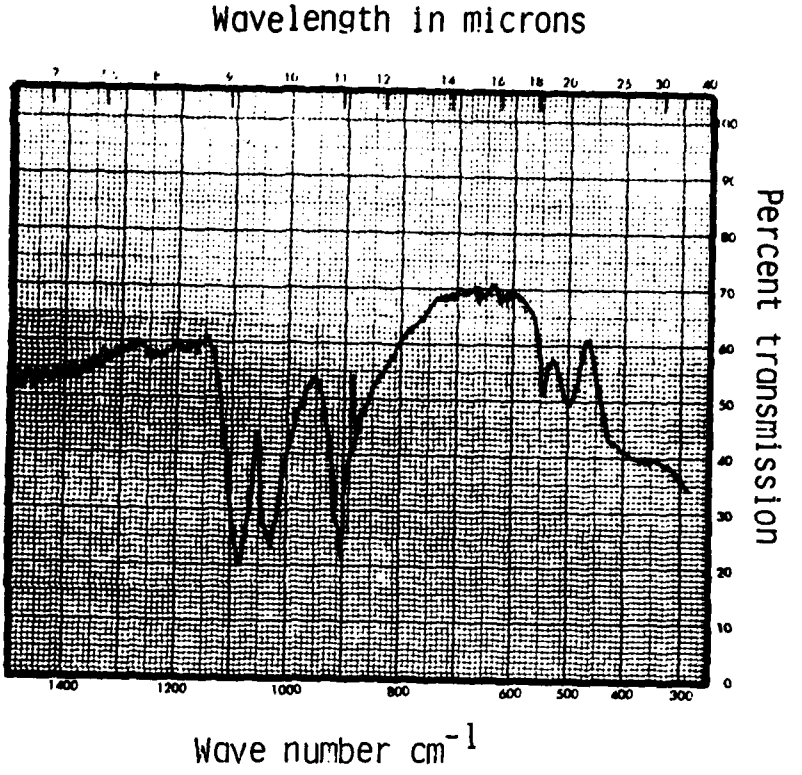

Fig. 27. IR spectrum of the cathode of Li/SO_2 cell X-7 after forced overdischarge.

The separator showed an orange discoloration around the outer wind of the jelly roll electrode. Attempts to obtain spectral data on the orange material were unsuccessful.

5.3.3 Type Z Cells Forced Overdischarged at High Rates

The high rate overdischarge of the Type Z cells was found to reproducibly result in cell venting, in some cases with flame. These cells were examined in greater detail.

Three cells Z-3, Z-4 and Z-5 were forced overdischarged with a current of 1000 mA and Z-6 at 900 mA. All four cells vented; however, only cells Z-3 and Z-6 vented with flame.

The gases released from cell Z-3 were collected within 10 minutes after the venting. The IR spectrum of the gaseous mixture is shown in Fig. 28. Infrared and gas chromatographic analyses identified the gases as a mixture of CO_2, SO_2, CH_4, COS, CS_2, C_2H_4, C_2H_2 and H_2S (identified by GC only). The entire outside of the cell was completely charred. A picture of the cell after removal from the test chamber is shown in Fig. 29. The Teflon cell holder in the test chamber was melted indicating the intense heat generated when the cell vented. A yellowish-brown material was expelled during venting. Its infrared spectrum is shown in Fig. 30. Spot tests confirmed the presence of sulfur, S^{-2}, SO_3^{-2}, and organic compounds. The inside of the cell was fused into a solid mass as seen in Fig. 29. Thus the cathode could not be unrolled. There was no evidence of the separator or any Li left in the fused cathode. The Al tab which connects the cathode to the positive lead was completely burned away. Decomposition of the $Li_2S_2O_4$ on the cathode was apparent by its infrared spectrum, shown in Fig. 31, and chemical spot test. The analysis of cell Z-6 showed identical results.

The gaseous mixture from cell Z-4 was identified as containing the same species as found in cell Z-3. However, the relative amounts of CO_2, CH_4, H_2S, C_2H_2, C_2H_4, CS_2 and COS were different from those in cell Z-3. Examination of the interior of the cell showed that the separator was charred and fused to the cathode along the top edge of the jelly roll. In the core of the cell the excess separator was completely fused and again the Al tab connecting the cathode to the positive lead was completely burned away. The remainder of the cell showed no visible evidence of damage. An infrared spectrum of the cathode did not show any evidence for the decomposition of $Li_2S_2O_4$. Examination of cell Z-4 showed that the most intense heating occurred in the center of the cell where the Al tab connects the cathode to the positive lead.

Cell Z-5 was discharged in an inverted position and the exterior wrappings were removed before testing. Analyses showed identical results to those of cell Z-4. The Al tab on the end of the cathode was again

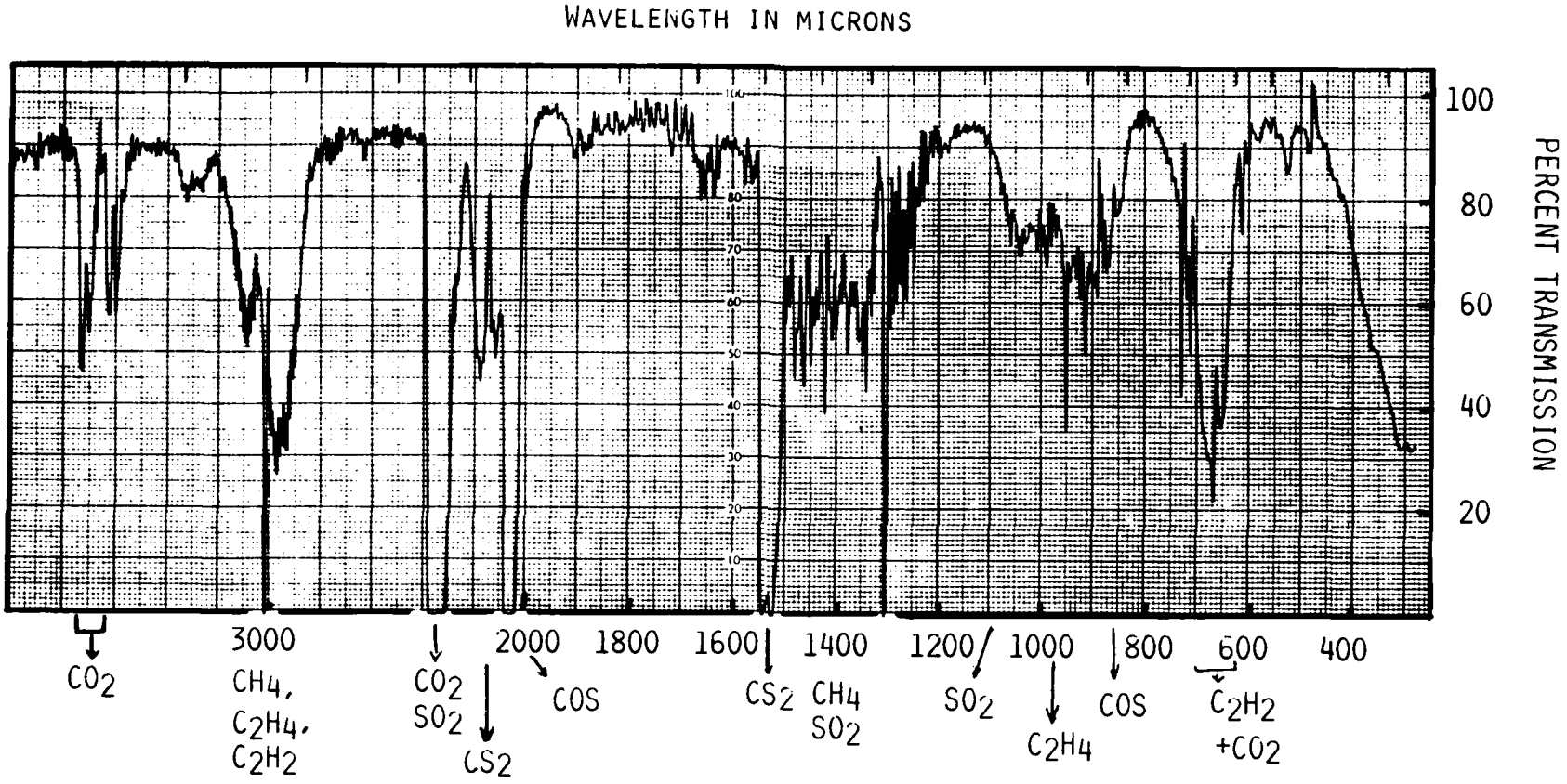

Fig. 28. Infrared spectrum of the gases released from Li/SO_2 cell Z-3 after venting during a 1000 mA discharge.

Fig. 29. Top photograph shows the condition of the outside of Li/SO_2 cell Z-3 after venting with flame. Bottom photograph shows the completely burned interior of the same cell.

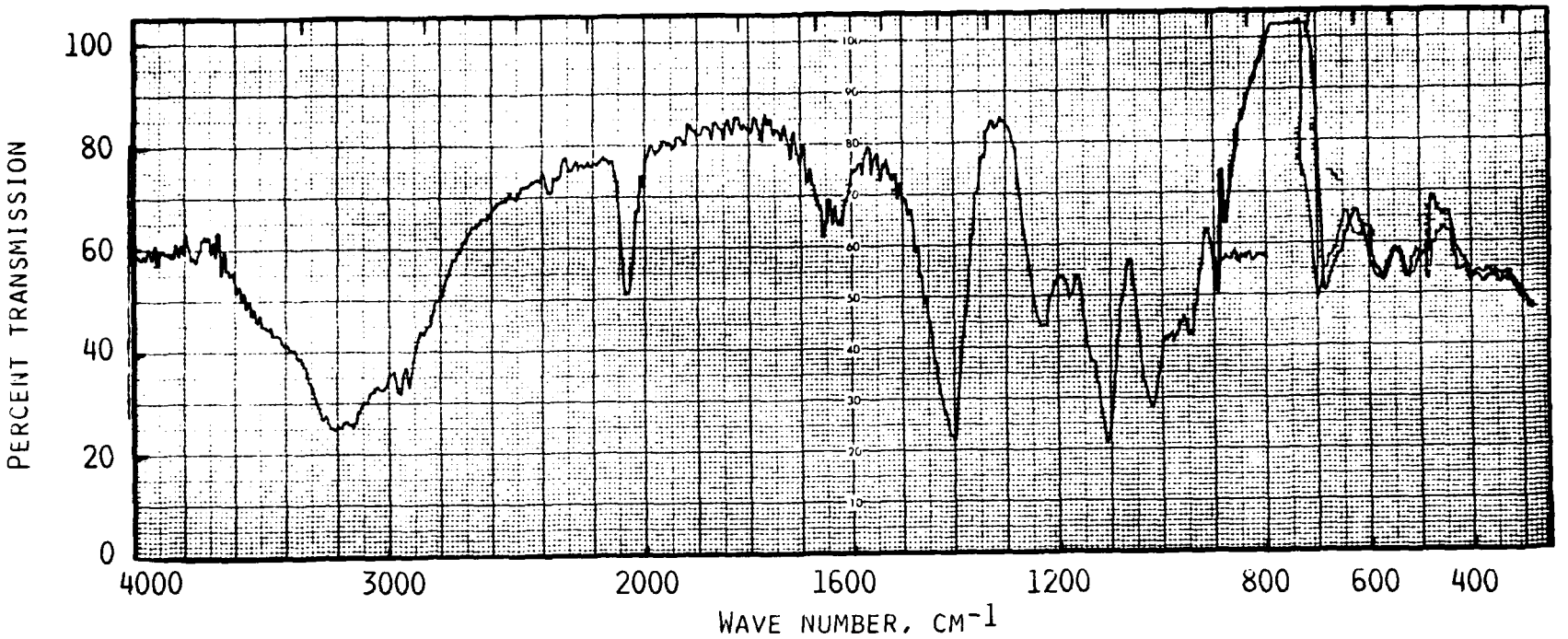

Fig. 30. Infrared spectrum of the solid material expelled from cell Z-3 during venting.

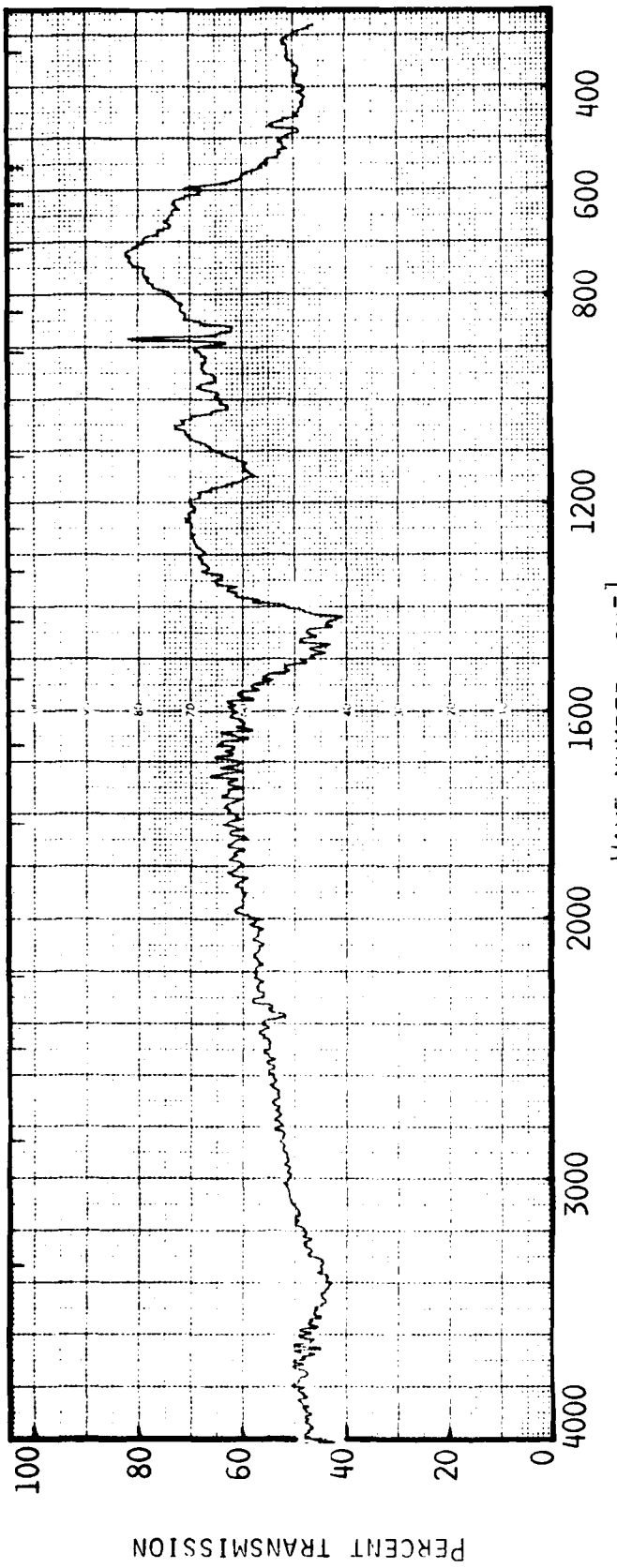

Fig. 31. Infrared spectrum of the cathode of Li/SO_2 cell 2-3 after venting.

burned away and the separator along the top of the jelly roll was fused to the cathode.

The gaseous products found in cell Z-5 were the same as in cells Z-3 and Z-4. This indicates that the gases are formed from reactions within the cell and not from the burning of the exterior wrappings.

The fact that the area surrounding the cathode tab in the top center of the cell sustained the most intense heat in all cells, even though they had been mounted in opposite orientations, shows that the process leading to the venting is not a vapor phase reaction.

Cells Z-7 and Z-8 were forced overdischarged at 800 and 600 mA, respectively. The voltage profiles of the cells are shown in Figs. 20 and 21 and the capacities are listed in Table 8. Neither cell vented. However, post test examination revealed the cathode had become disconnected in both cells.

CH_4 and SO_2 were detected in cell Z-7 while only CH_4 was found in cell Z-8.

A picture of the disassembled cell Z-7 is shown in Fig. 32. Examination of the cell showed that the Al tab on the cathode was burned off near the positive lead connector. The separator in the immediate area around the burned tab was also charred as seen in the picture. There were no other visible damages. The excess Li remained intact through the length of the anode compartment.

The X-ray diffraction pattern of the inner section of the cathode from cell Z-8 is tabulated in Table 9. The X-ray pattern contains lines which can be assigned to Li/Al alloy of the composition LiAl along with the lines of $Li_2S_2O_4$, LiBr and Al. If the entire Al grid was converted to LiAl, the w/o of LiAl would account for ~7% of the total weight of the discharged cathode. In the cathode of cell Z-8, whose X-ray pattern shows the presence of unalloyed Al, the actual amount of LiAl is much less. Thus any diffraction lines of LiAl are expected to be weak, as is found in Table 9. There is no evidence in the X-ray data for the presence of unalloyed Li (2.48 Å) or any other products such as Li/C intercalates, Li_2S, etc. which could form during forced overdischarge.

Cells Z-9 and Z-10 (Table 8) were discharged to 0 volt at low rates (i.e., 150 and 300 mA, respectively) then forced overdischarged at 1000 and 750 mA, respectively. When the current was increased the potential of both cells immediately fell to -12V and remained there. Neither cell vented. Post test examination of the cells showed that the cathode remained connected in both cells. However, the Al cathode grid in cell Z-9 appeared to have fallen apart over the inner section of the cathode as was seen in cell Z-8.

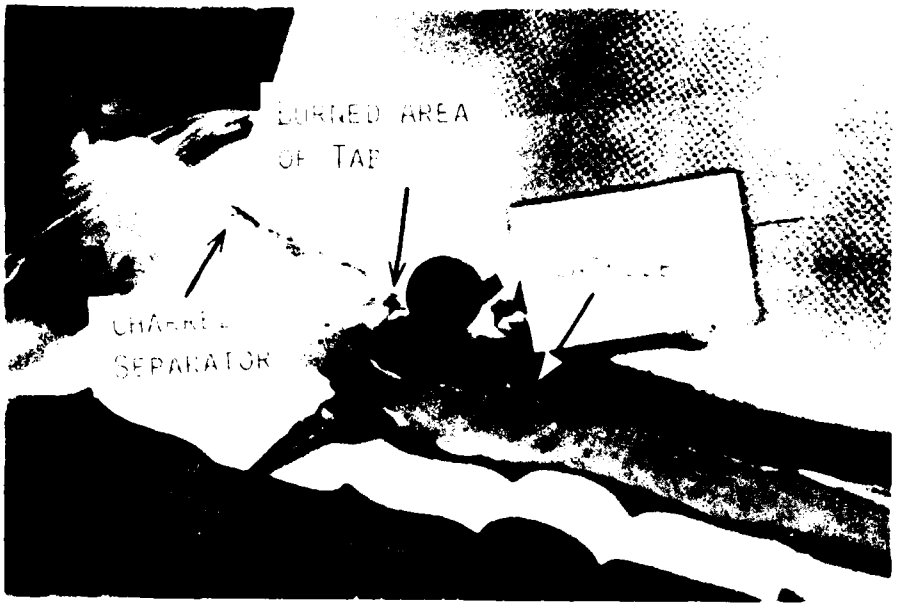

Fig. 32. Photograph of Li/SO_2 cell X-7 showing the burned Al tab and separator in the top interior of the cell. The cell did not vent.

TABLE 9

X-RAY[a] DIFFRACTION DATA OF THE CATHODE OF CELL Z-8

Cell Z-8		LiAl		Al	
d, Å	I/I_o	d, Å	I/I_o	d, Å	I/I_o
5.09	5				
4.37	40				
3.70	90	3.65	75		
3.22	80				
2.96	30				
2.73	10				
2.66	100				
2.53	30				
2.43	5				
2.34	35			2.34	100
2.24	30	2.26	100		
2.02	20			2.02	100
1.92	25	1.92	75		
1.79	5				
1.70	5				
1.65	10				
1.62	10				
1.59	10	1.58	60		
1.57	10				
1.53	10				
1.46	10	1.46	60	1.47	22
1.43	15				
1.41	10				
1.29	15	1.30	100		
1.28					
1.26	5				
1.22	15	1.22	75	1.22	24
1.17	5				
1.14	< 5				
1.12	5	1.12	75		
1.08	5	1.07	75		
1.06	5	1.01	85		
0.93	5	0.92	50		
0.91	5	0.89	75		
0.85	5	0.85	125		
0.83	5	0.83	100		
		0.80	60		

[a]Debye-Sherrer method, CuK_α radiation.

[b]Cell was discharged and forced overdischarged at 600 mA.

5.4 Analysis of the Products Formed at the Anode During Reversal

In both the Type X and Type Z which did not vent when forced over-discharged (except X-6), a few hundred milligrams of a yellow-brown material was found throughout the anode compartment. Little or no Li remained in the anode compartments. The infrared spectra of the material from each cell were identical. The infrared spectrum of the material, shown in Fig. 33, indicates the presence of N-H groups (3000-3500 cm^{-1}), -C=N in a conjugated, unsaturated system (2200-2250 cm^{-1}), C=C bonds (1620-1680 cm^{-1}) and S-O bonds (900-1000 cm^{-1}).

The material used in the following analysis was obtained from cell X-8. An elemental analysis (Galbraith Labs, Knoxville, TN) gave the following composition: C, 38.22%; N, 16.63%; H, 4.33%; S, 9.10%; Br, 4.52%; and Li, 9.30%. The remainder of the sample is presumably oxygen which by difference is 29.90%.

The material was separated into three components by sublimation. The first sublimate, which was the major component, was obtained as a white solid, I. A second higher boiling component, II, was obtained as a brown oil in very small amounts. The third component was a brown solid residue which did not sublime even at 200°C. The infrared spectrum of I is shown in Fig. 33.

The mass spectrum of I, shown in Fig. 34, gives a molecular weight of 123. The combined infrared and mass spectral data identify I as 3,5-diamino-2,4-hexenenitrile, $CH_3-\underset{\underset{NH_2}{|}}{C}=CH-\underset{\underset{NH_2}{|}}{C}=CH-C\equiv N$. This is consistent with the fragmentation pattern tabulated in Table 10. It is likely that I also contains some diacetonitrile, $CH_3-\underset{\underset{NH_2}{|}}{C}=CH-CN$, III, (MW 82). The infrared spectra of these two compounds are indistinguishable.

Solid probe mass spectral data of the original material from the anode of cell X-8 show that there are three components which can be at least partially separated below 250°C. A solid residue still remained after heating the sample to 250°C in the mass spectrophotometer. The presence of I is clearly seen in the mass spectrograph of the original material shown in Fig. 35.

The other species seen in the mass spectrum of the original material were not identified. However, one component appears to have a molecular weight of 207. The infrared spectrum shows no carbonyl groups and the elemental analysis shows a C/N ratio of 2. Thus it appears that these other species are probably longer polymers of CH_3CN, possibly containing sulfur.

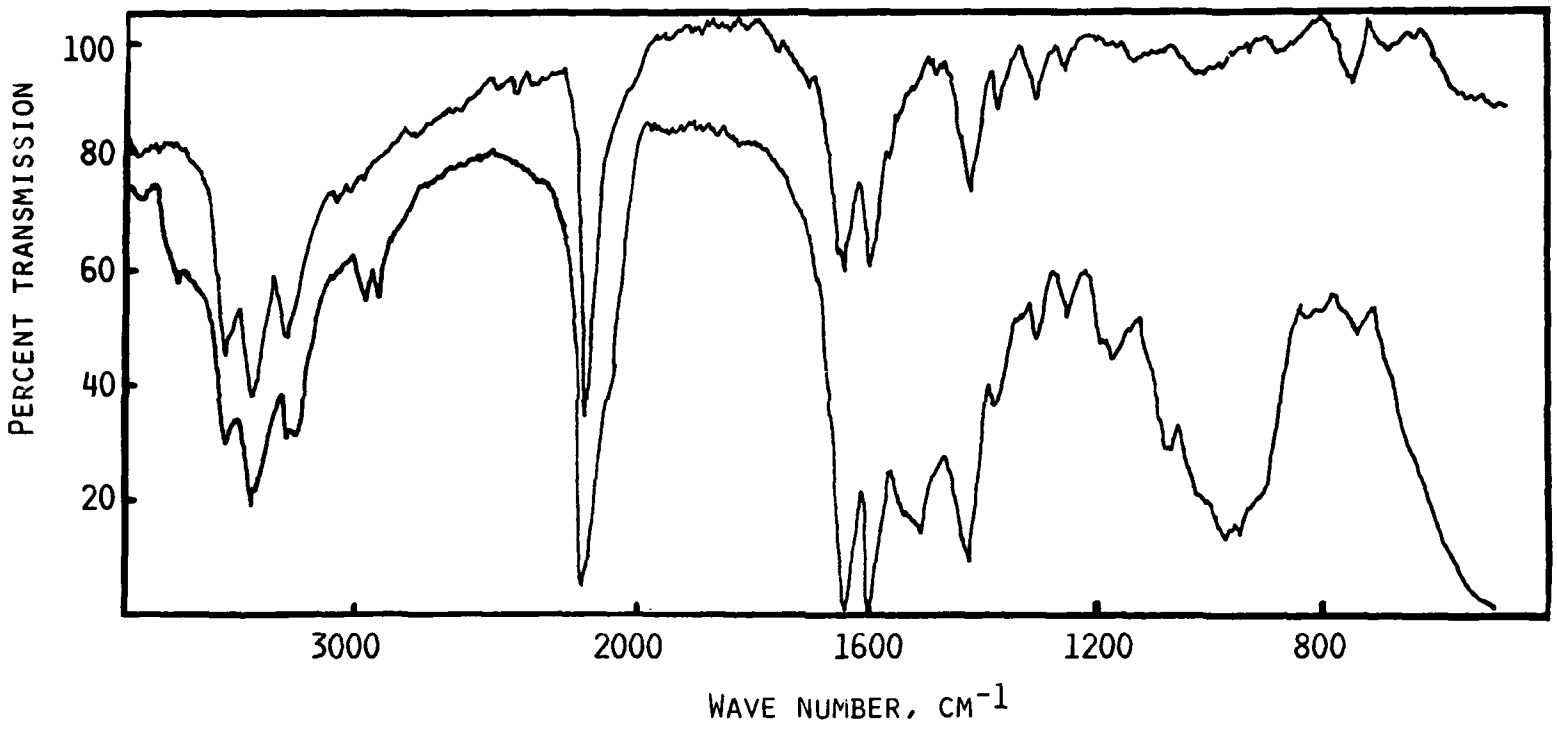

Fig. 33. Infrared spectra of the product formed in the anode compartment of a Li/SO_2 cell during forced overdischarge (lower curve) and a 3,5-diamino-2,4-hexene-nitrile (upper curve) after sublimation from the anode product.

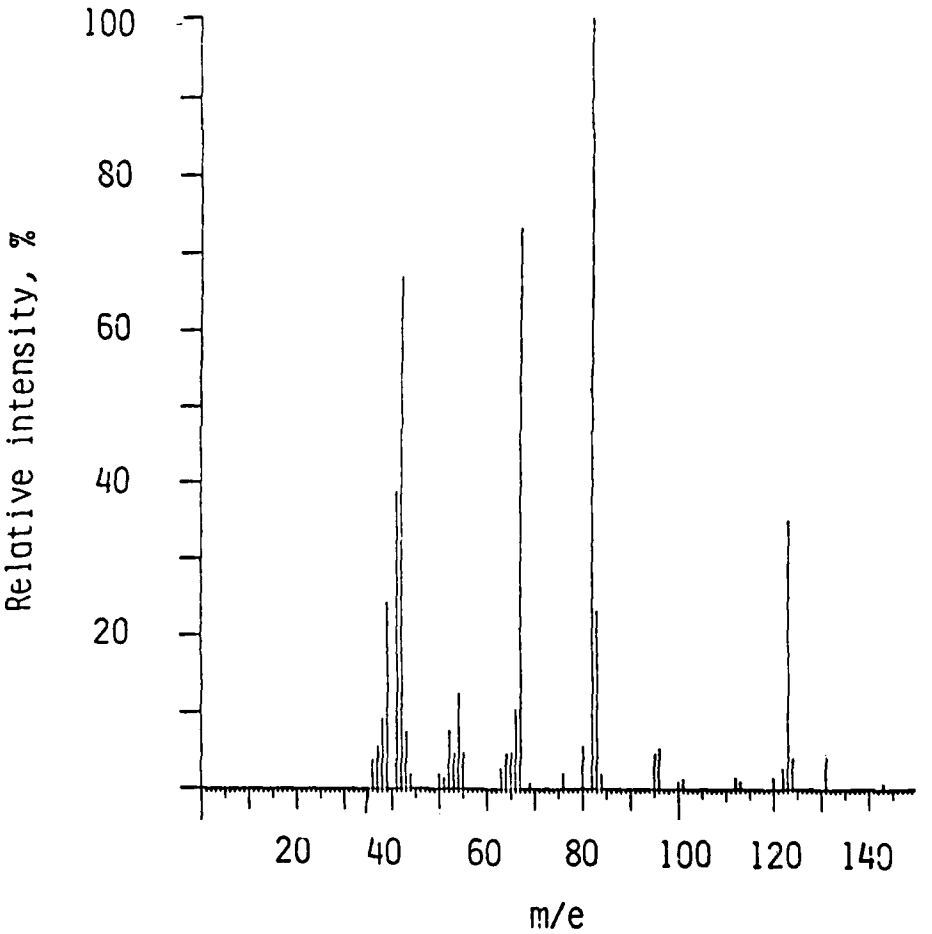

Fig. 34. Mass spectrum of 3,5-diamino-2,4-hexenenitrile, I.

TABLE 10

MASS SPECTRAL DATA OF I

M/e	Assignment (all positive ions)
123	$CH_3C(NH_2)=CH-C(NH_2)=CH-CN$
96	$CH_3C(NH_2)=CH-C(NH_2)-CH$
82	$H_2N-C=CH-C(NH_2)-CH$
67	$NH_2-C=CH-CN$
54	$HC-C(NH_2)=CH$
42	CH_3CNH
41	CH_3CN
39	C_3H_3 or CHCN

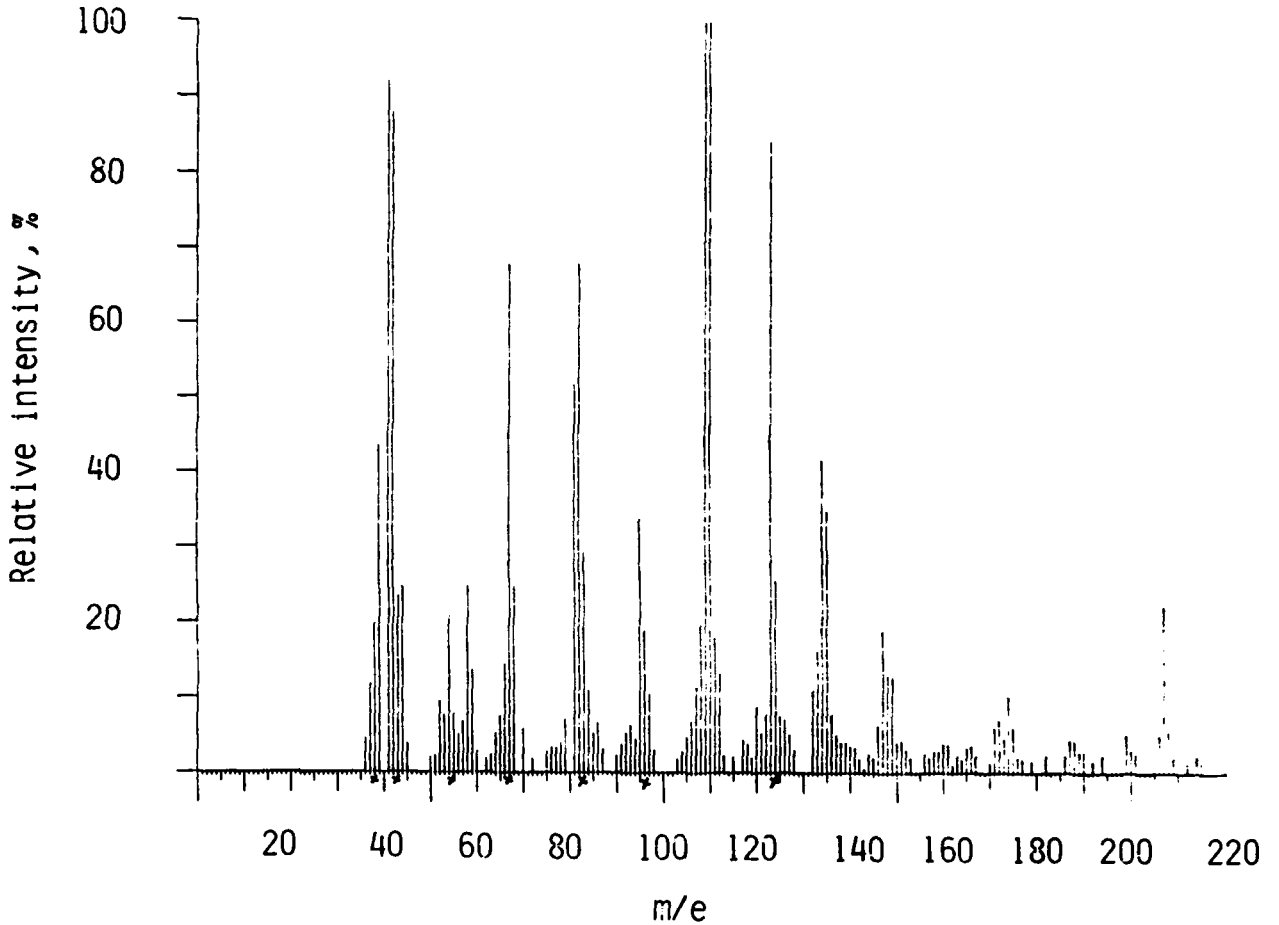

Fig. 35. Mass spectrum of the product isolated in the anode of cell X-8 after a discharge into reversal. * indicates peaks from I.

Infrared and qualitative data indicate that the sulfuroxy species present in the original anode product are a mixture of $Li_2S_2O_4$ and Li_2SO_3.

It is unlikely that the formation of the anode products is electrochemical in nature since the potentials of the anodes in the Type X and Type Z cells differ substantially during forced overdischarge. Experiments with a series of cells (X-18, X-19, X-20, and X-21) showed that the formation of the anode products requires a few hours of forced overdischarge (at 150 mA) and was not the result of a temperature increase at the end of discharge. Thus the products most probably result from chemical reactions between Li and acetonitrile.

Lithium and acetonitrile apparently do not react in the presence of a sufficient concentration of SO_2 because of the formation of a passivating film, presumably of $Li_2S_2O_4$, on the Li surface (20). However, during forced overdischarge the SO_2 concentration could decrease to a level where Li and acetonitrile react. Possible mechanisms for the formation of I, III and CH_4 are:

$$CH_3CN + 2Li \rightarrow CH_3^- + CN^- + 2Li^+ \quad (3)$$

$$CH_3^- + CH_3CN \rightarrow CH_4 + {}^-CH_2CN \quad (4)$$

$$CH_3C{\equiv}N + {}^-CH_2CN \rightarrow CH_3-\underset{\underset{N}{\|}}{C}-CH_2CN \quad (5)$$

$$CH_3-\underset{\underset{N}{\|}}{C}-CH_2CN + CH_3CN \rightarrow {}^-CH_2CN + CH_3-\underset{\underset{NH}{\|}}{C}-CH_2CN \quad (6)$$

$$CH_3-\underset{\underset{NH\ H}{\|}}{C}-CH-CN \rightarrow CH_3-\underset{\underset{NH_2}{|}}{C}=CH-CN \quad (7)$$

III

$$CH_3-\underset{\underset{NH_2}{|}}{C}=CH-CN + {}^-CH_2CN \rightarrow\rightarrow CH_3-\underset{\underset{NH_2}{|}}{C}=CH-\underset{\underset{NH_2}{|}}{C}=CH-CN \quad (8)$$

I

The formation of Li_2SO_3 in the anode compartment probably resulted from the reaction between SO_2 and organic Li compounds, e.g., $LiCH_2CN$. Supporting this, we have found that reactions between $n\text{-}C_4H_9Li$ and SO_2 result mainly in Li_2SO_3.

Other organic compounds such as 4-amino-2,6-dimethylpyrimidine (MW 123) acetoacetonitrile, 6-phenyl-2-pyridone, etc. have reportedly been identified in cells after forced overdischarge (21). We found no evidence for such species in the cells we examined. While it is possible that com-

pounds such as 4-amino-2,6-dimethylpyrimidine could form in the cell with reactions similar to those of Eqs. 3-8 (22-24), it is equally likely that some of the compounds could have formed during isolation procedures. For instance, acetoacetonitrile which was identified after extraction into a $CHCl_3$ layer from an HCl solution (21) probably resulted from the hydrolysis of I or III.

In Section 5.3.1 it was noted that a compound believed to be an aldehyde was found in two cells after forced overdischarge. This compound probably resulted from the hydrolysis of I or III, possibly from trace amounts of H_2O in the two cells.

The formation of methane and other organic compounds has previously been explained by the reaction between Li (or LiAl) and acetonitrile. However, it has been assumed that the reaction occurred on the cathode where Li deposited during forced overdischarge (21). Although we found evidence for Li/Al alloy we have no evidence in the cathodes of forced overdischarged cells for unalloyed Li or any reaction products such as those found on the anode.

5.5 Comparison of the Behavior of Type X and Type Z Cells during Forced Overdischarge

The results of the room temperature forced overdischarge studies show that the forced overdischarge of Type Z cells presents considerable safety hazards at currents >600 mA. In actual use, it is likely that a few cells would display unsafe behavior even at lower currents; however, this would have to be verified with extensive testing of a large number of cells. The Type X Li/SO_2 cells appear to have a much greater resistance to forced overdischarge abuse.

A major difference in the behavior of the Type X and Type Z cells is the amount of capacity each cell yields above 0 volts.

At low discharge rates, the Type Z cell yields a slightly greater capacity to 2.0V than the Type X cell. Both types of cells yield little capacity between 2 and 0 volts at low discharge rates. At higher discharge rates (>300 mA) there are substantial differences in the capacities of the two types of cells. The difference in capacities are seen in Table 8 which list the capacities to 2.0V and 0.0V for cells discharged at high rates. For instance at 1000 mA the capacity of the Type Z cell is ~1200 mAh to 2.0V and ~2000 mAh to 0.0V, while the capacity of the Type X cell is 2650 mAh and 3200 mAh to 2.0V and 0.0V, respectively. At high discharge rates both types of cells yield a considerable capacity between 2 and 0 volts. However, this capacity is generally greater in the Type Z cell. Whether the high rate discharge capacity between 2-0 volts results in discharge products besides $Li_2S_2O_4$ is not certain and needs additional study. No evidence has been found to date for the formation of any products besides $Li_2S_2O_4$ and LiAl in the cathode. Probably, the low voltage discharge represents Li/Al alloy formation.

The important point is that even at high currents the capacity to 0.0V of the Type X cell is nearly equal to the capacity obtained at lower rates. In contrast, the capacity of the Type Z cell is approximately 60% (in the 1000 mA case) of the low rate capacity. This results in the presence of a large excess of unreacted Li and SO_2 remaining in the Type Z cell when it goes into reversal during forced overdischarge.

The importance of excess, unreacted Li and SO_2 is apparent in the experiments with cells Z-9 and Z-10. The cells, discharged at low rates, had much less excess Li and SO_2 when forced into reversal. The cells displayed no adverse behavior even though they were forced overdischarged at high rates.

All of the cells which vented contained CO_2, COS, CS_2, H_2S, S, C_2H_2, and C_2H_4 along with CH_4 and SO_2. All of the species except C_2H_4 and C_2H_2 are known to result from the reaction of SO_2 and CH_4 (25). The distribution of products depends on the reaction conditions (temperature, pressure, catalyst, etc.) The C_2H_2 and C_2H_4 probably result from the high temperature reaction of Li and CH_3CN via the formation of $CH_3^{\cdot}$.

The above products were not identified in any cells which did not vent. Thus it appears that one of the high energy reactions which leads to excessive pressure buildup and subsequent cell venting is that between SO_2 and CH_4. However, this reaction is not spontaneous and needs a high energy source of initiation.

A hypothesis for the initiation of the hazardous reactions during forced overdischarge is as follows. During a high rate discharge the carbon electrode in the cathode limited Type Z cell is rather inefficiently utilized, resulting in unused Li and SO_2 in the cell. The resistivity of the cathode near the Al tab increases (possibly due to LiAl formation). The excessive heat, due to the increased resistance, initiates a violent reaction between excess Li (or Li/Al) and CH_3CN and/or between SO_2 and CH_4. The formation of the large amounts of gaseous products along with the corresponding increase in temperature results in excessive pressure. The cell vents.

6.0 LOW TEMPERATURE FORCED OVERDISCHARGE EXPERIMENTS OF Li/SO_2 CELLS

Our survey of the safety of Li/SO_2 cells indicated that low temperature forced overdischarge of Li/SO_2 could be particularly hazardous. Our investigation of the low temperature behavior of Li/SO_2 cells confirmed this. The results, discussed below indicate that forced overdischarging of Li/SO_2 cells at low temperature can present a serious hazard even at low currents.

Table 11 summarizes the results of forced overdischarge experiments at $-25^{o}C$.

One Type X cell, X-23, was forced overdischarged at 300 mA. The voltage and temperature profiles are shown in Fig. 36. The cell capacity above zero volts was 2700 mAh. The cell voltage remained at ~ -1V for three hours. Then it began to rapidly fluctuate between -4V and -12.0V. During the forced overdischarge there were a number of small temperature increases. At about the 73rd hour, a large, sharp temperature increase occurred and the cell potential rose to just under 0 volts.

The cell did not vent. The cell was warmed to room temperature before being opened. The infrared spectrum of the gases collected from the cell after it was opened is shown in Fig. 37. Analyses of the gas mixture showed the presence of SO_2, CH_4, COS, CS_2, H_2S and a small amount of CO_2. Interestingly enough, no C_2H_4 or C_2H_2 was present.

Examination of the cell showed a series of areas where the separator was burned away. This can be seen in Fig. 38 which shows a picture of the separator and disassembled cell.

Infrared analyses of the cathode revealed that the $Li_2S_2O_4$ on the cathode had decomposed at those areas which were adjacent to the spots where the separator burned. The IR spectrum in Fig. 39 is identical to that obtained after heating a cathode sample to $>170^{o}C$. All the burned areas were located in the outer two wraps of the cathode.

Large areas of the remainder of the cathode were covered with plated Li. These areas were very reactive. Scraping the cathode with a metal spatula resulted in small, localized explosions accompanied by an orange flame.

It was also noted that none of the brown material was present in the anode compartment.

Cell X-24 was discharged and forced overdischarged under identical conditions and did not vent. Analysis of the gases in the cell showed only SO_2. While the cathode was being removed from the can (under an Ar atmosphere) it violently decomposed. The decomposition resulted in a burst of

TABLE 11

SUMMARY OF THE RESULTS OF FORCED OVERDISCHARGE STUDIES OF Li/SO_2 CELLS AT -25°C

Cell	Discharge Current (mA)	Forced-Overdischarge Current (mA)	Capacity (mAh) to 2.0V	Capacity (mAh) to 0.0V	Extent of Forced Overdischarge (mAh)	Results
X-23	300	300	1200	2700	19,200	Li plated on cathode; areas of cathode and separator burned.
X-24	300	300	1410	2700	11,850	Cathode decomposed during removal from cell.
Z-11	300	300	780	1500	3000	Vented with flame.
Z-12	150	150	1200	2100	1500	Vented with flame.
Z-13	100	100	1420	2400	3700	Did not vent.
Z-14	100	100	1150	2000	2400	Did not vent.

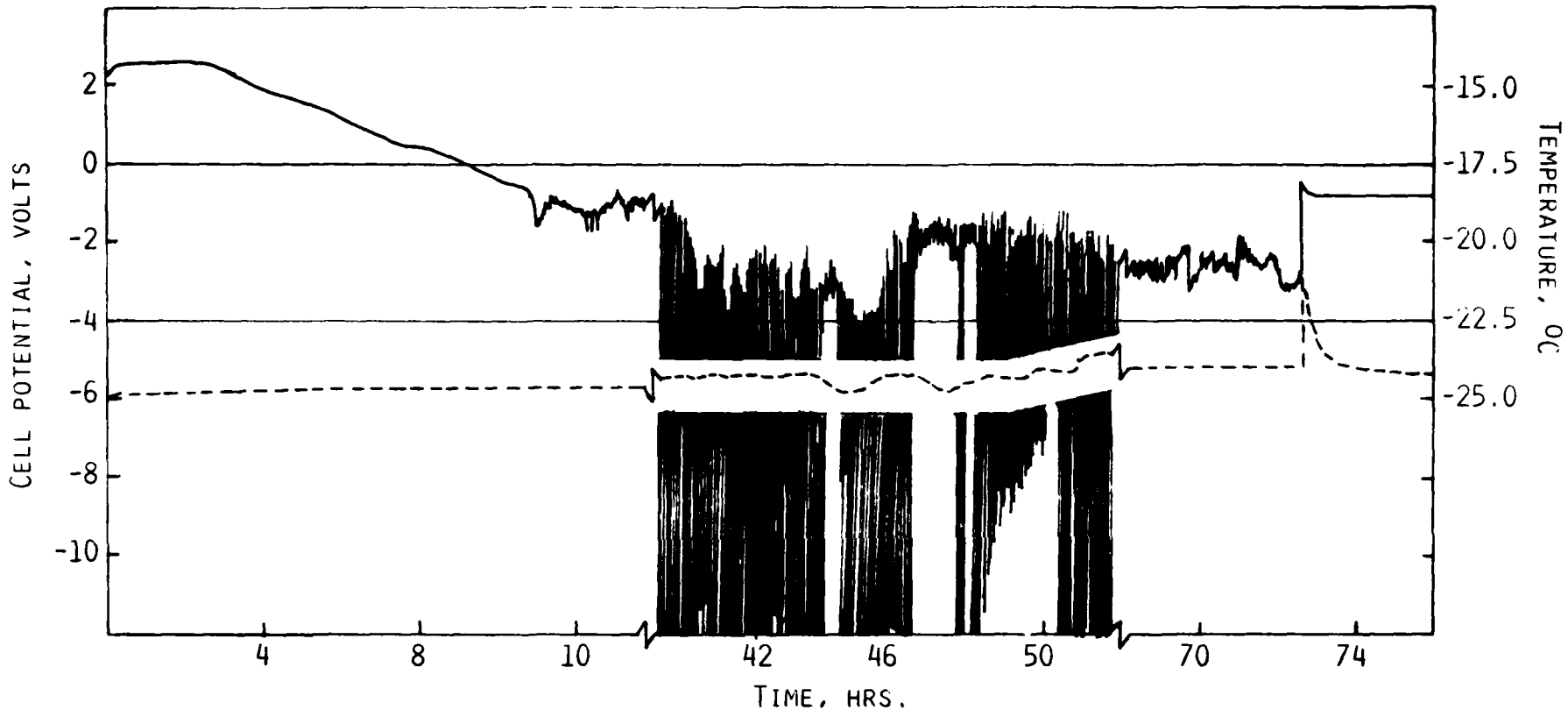

Fig. 36. Voltage (____) and temperature (---) profiles of the low temperature (-25°C) discharge and forced overdischarge of cell X-23 at 300 mA.

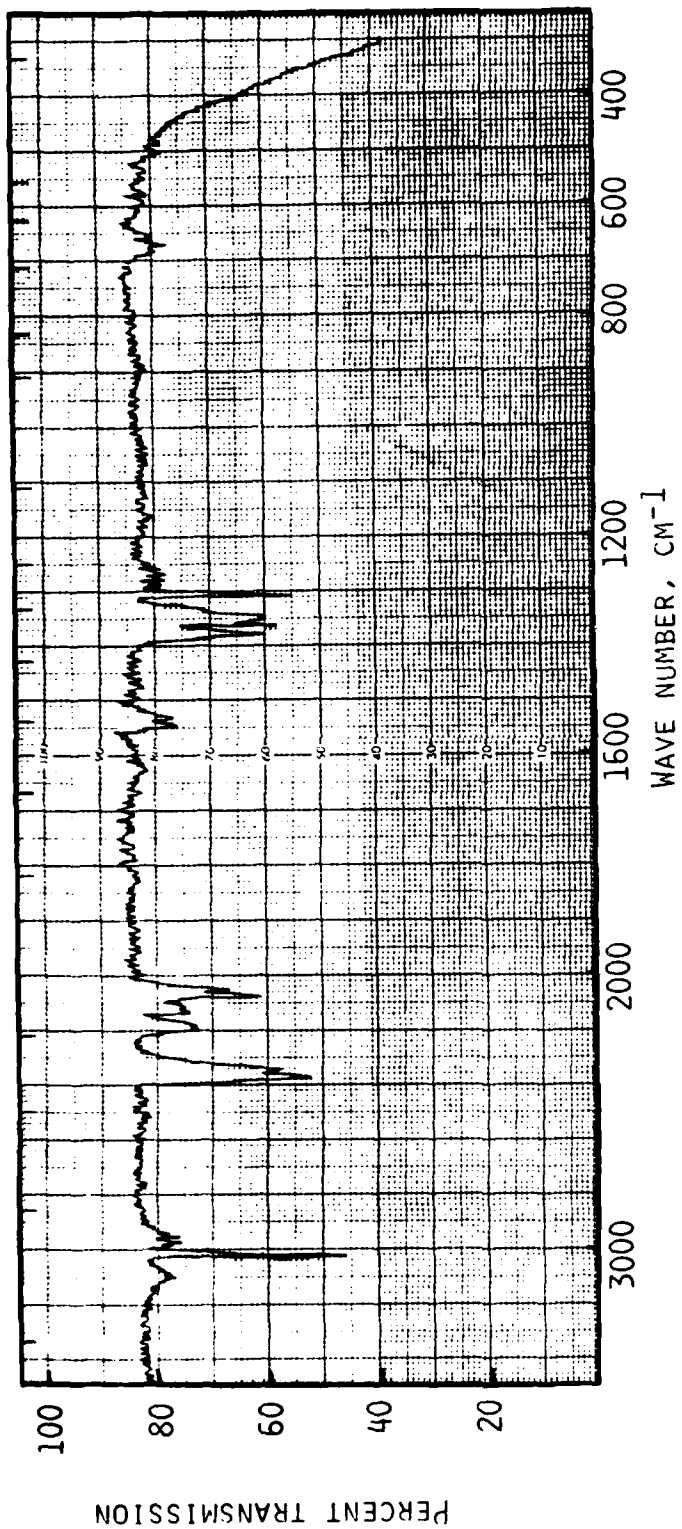

Fig. 37. Infrared spectrum of the gases formed in Li/SO_2 cell X-23 during a forced overdischarge at -25°C and a current of 300 mA.

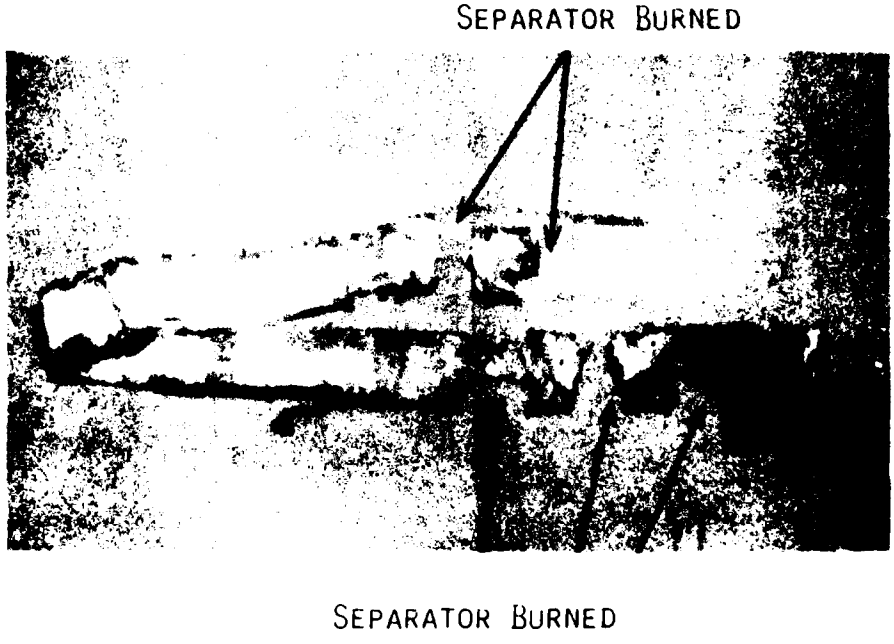

Fig. 38. Photograph shows the separator from cell X-23 after a forced overdischarge at -25°C. Note the burned areas which occurred near the outside of the wound electrode.

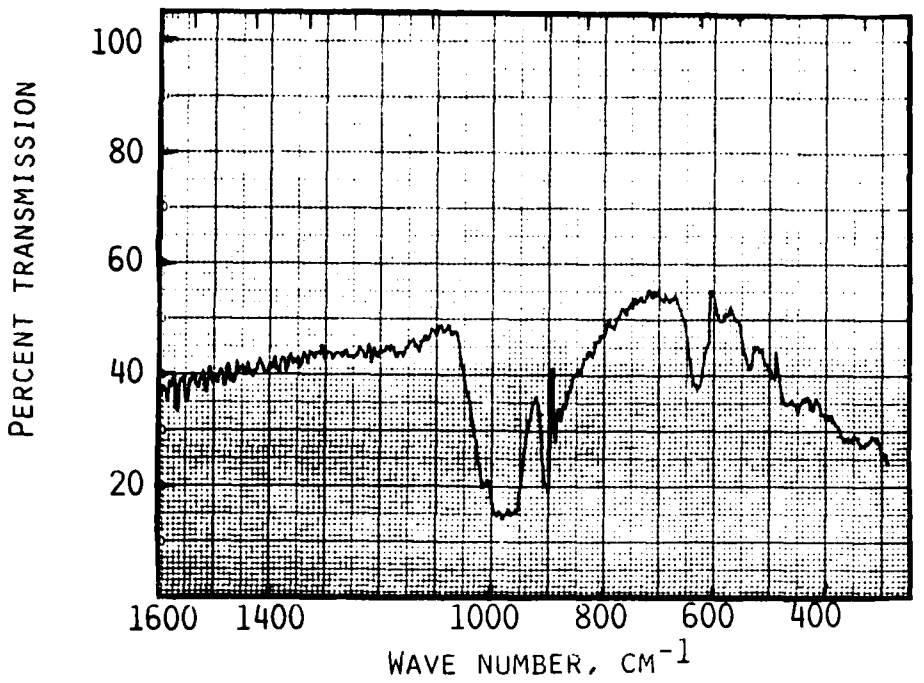

Fig. 39. Infrared spectrum of a burned area of the cathode from Li/SO_2 cell X-23.

flame from the cell lasting 5-10 seconds. Subsequent analysis of the cell remains showed a complete decomposition of the $Li_2S_2O_4$ in the cathode. The CH_3CN had been removed from the cell prior to the explosion thus the reaction clearly was not that between Li and CH_3CN. The reaction probably involved the highly reactive Li which plated onto the cathode during forced overdischarge, as found in cell X-23.

The results from these two cells suggest that the cathodes are in an extremely unstable state after a forced overdischarge at -25°C. Thus it is possible that a Type X cell forced overdischarged under similar conditions may explode if dropped. However, this was not verified.

Four Type Z cells were forced overdischarged at -25°C as described in Table 11. Voltage and temperature profiles of the cells are given in Figs. 40-43. Cells Z-11 and Z-12 forced overdischarged at 300 and 150 mA, respectively, vented with flame. Cells Z-13 and Z-14 both forced overdischarged at 100 mA did not vent.

As found in the room temperature experiments, the capacities of the Type Z cells to 2.0 and 0.0 volts (see Table 11) were less than in the Type X cell. Upon reversal, the potentials of all four cells remained constant at slightly below zero volt. At this potential the most likely reaction is the plating of Li onto the cathode.

Cell Z-13 was warmed to room temperature before it was opened. SO_2 was the only gas present. Unlike the Type X cells there was no plated Li visible on the cathode surface. An infrared spectrum of the cathode showed only $Li_2S_2O_4$. The Al grid of the cathode was fragmented and in areas completely missing. An X-ray diffraction analysis, tabulated in Table 12, showed $Li_2S_2O_4$, small amounts of Al and weak lines that likely correspond to LiAl. There was no evidence of unalloyed Li in the cathode.

Cell Z-14 was opened immediately after the forced overdischarge at -25°C. The analysis of the cell gave identical results to that of cell Z-12, again showing no unalloyed Li on the cathode. No products, except excess Li, were found in the anode compartment of either cell.

Neither cathode displayed any evidence of shock sensitivity as found with the Type X cathodes.

Analyses of the gases released from cells Z-11 and Z-12, confirmed the presence of COS, CS_2, CH_4, C_2H_4, CO_2, H_2S and SO_2 as previously found in the room temperature studies.

The cathodes in both cells were completely fused together. Thus the location where the explosive reaction began could not be identified. Qualitative analyses of the charred cell components confirmed the presence of S, SO_3^{-2}, and SO_4^{-2}.

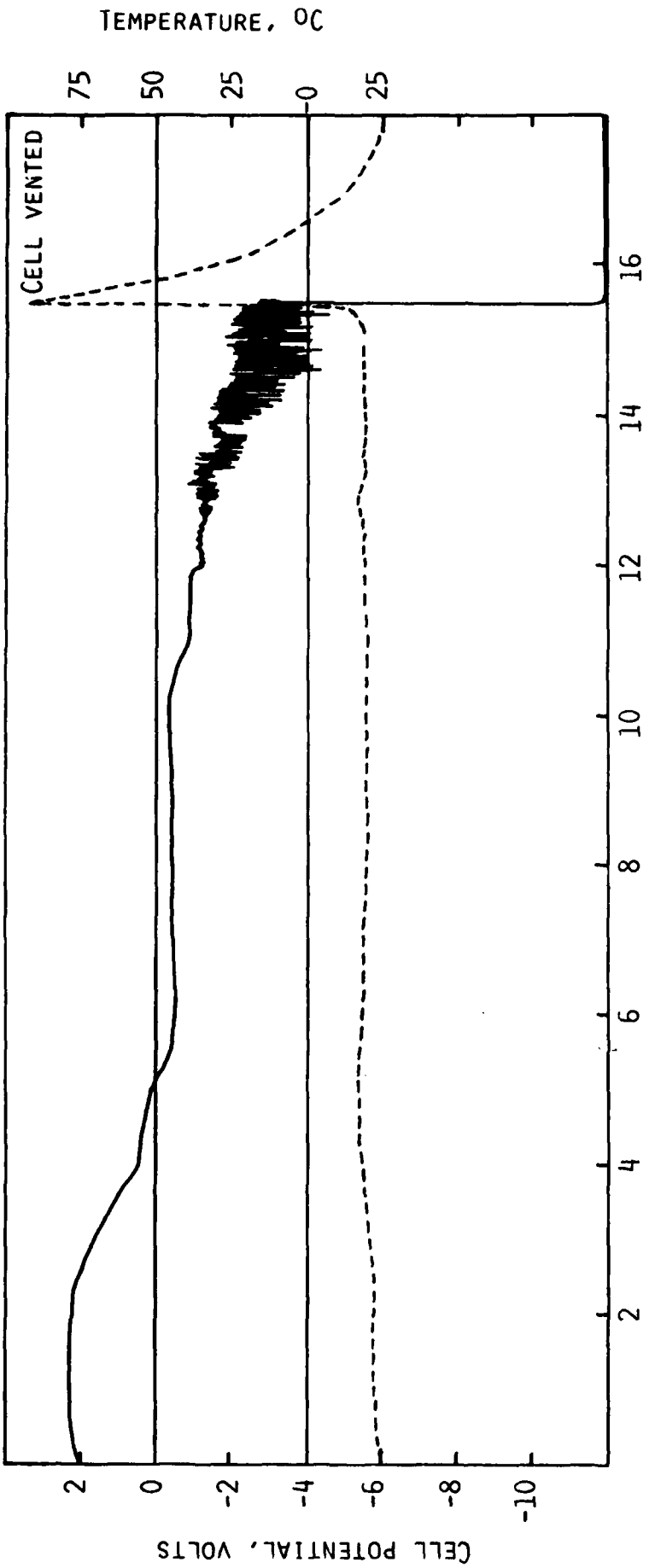

Fig. 40. Voltage (——) and temperature (---) profiles of the low temperature (-25°C) discharge and forced overdischarge of Li/SO_2 cell Z-11 at 300 mA.

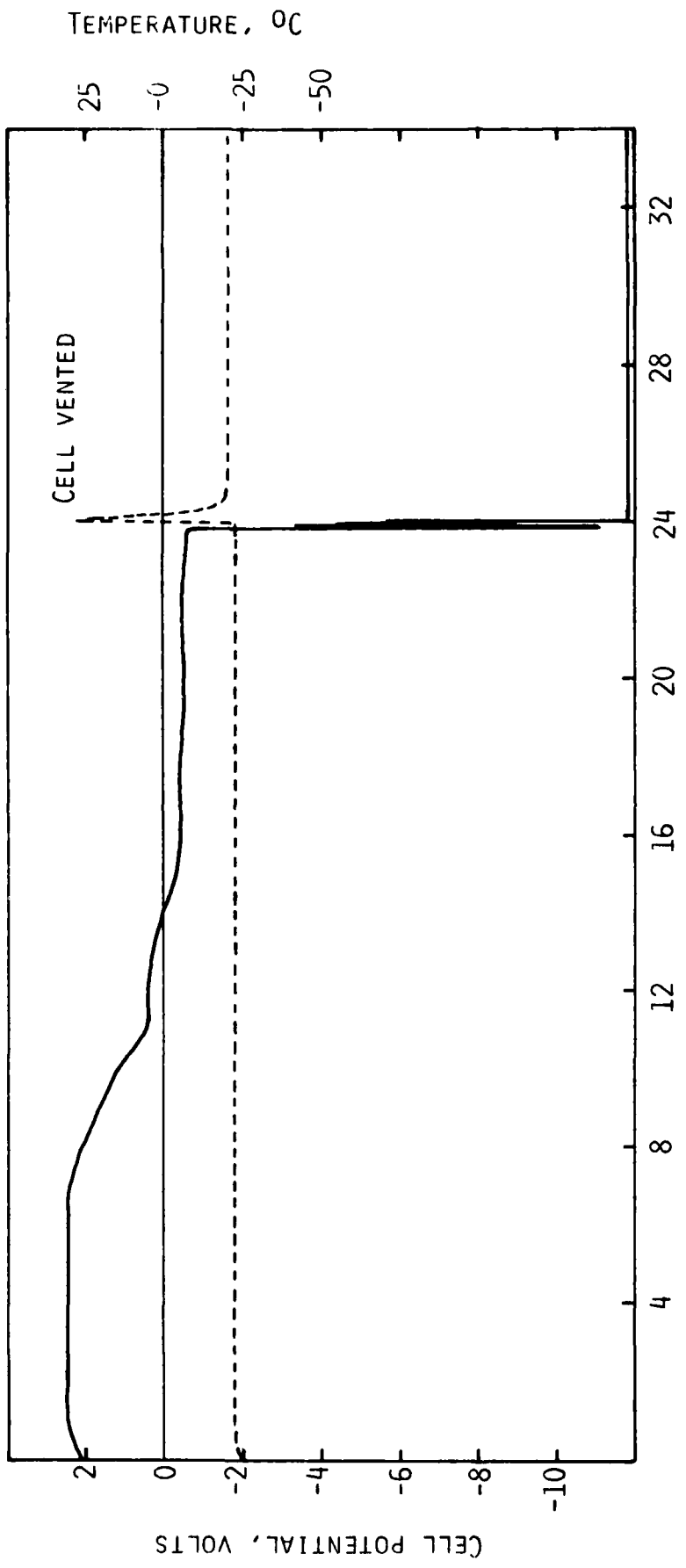

Fig. 41. Voltage (——) and temperature (---) profiles of the low temperature (-25°C) discharge and forced overdischarge of Li/SO_2 cell Z-12 at 150 mA.

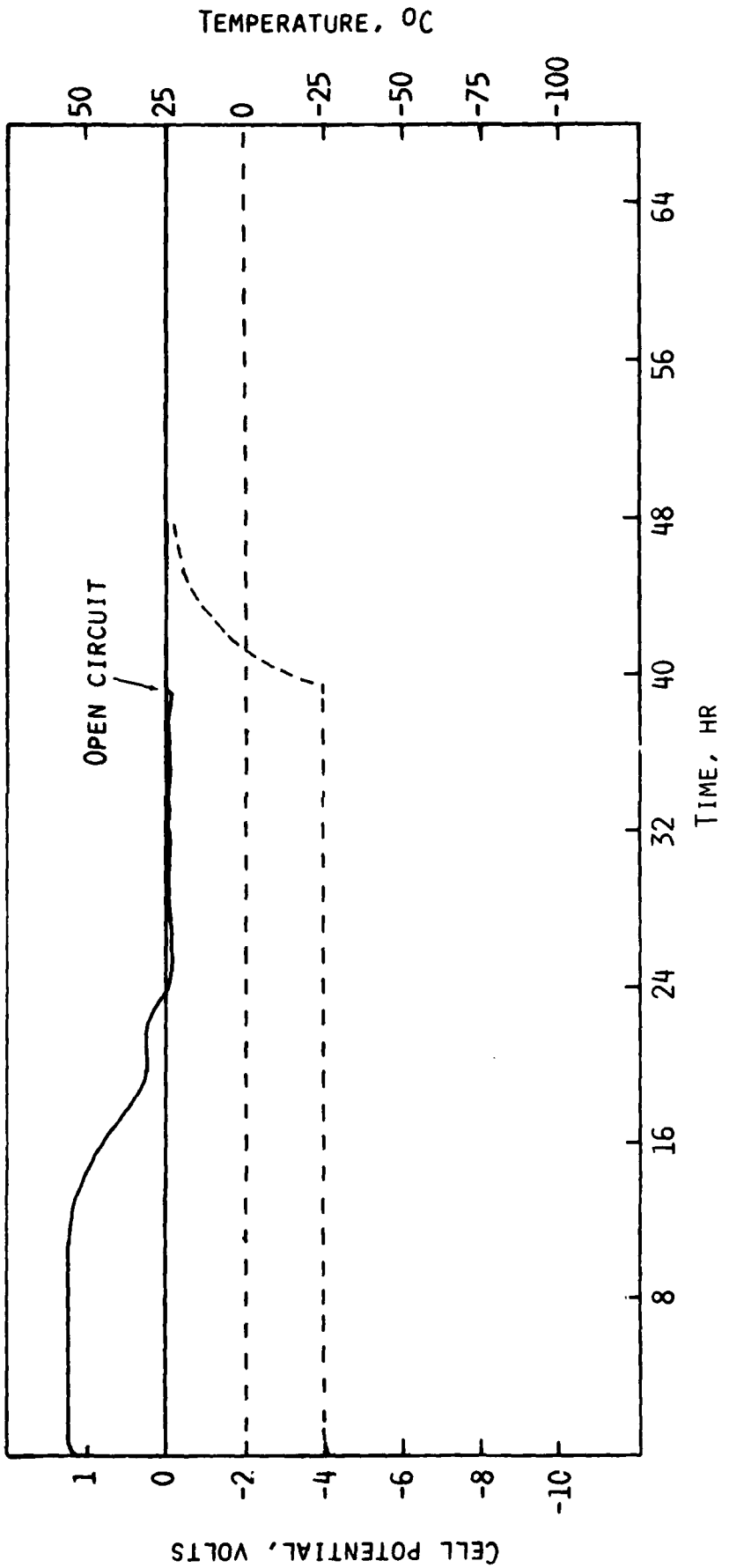

Fig. 42. Voltage (——) and temperature (---) profiles of the low temperature (-25°C) discharge and forced overdischarge of Li/SO_2 cell 2-13 at 100 mA.

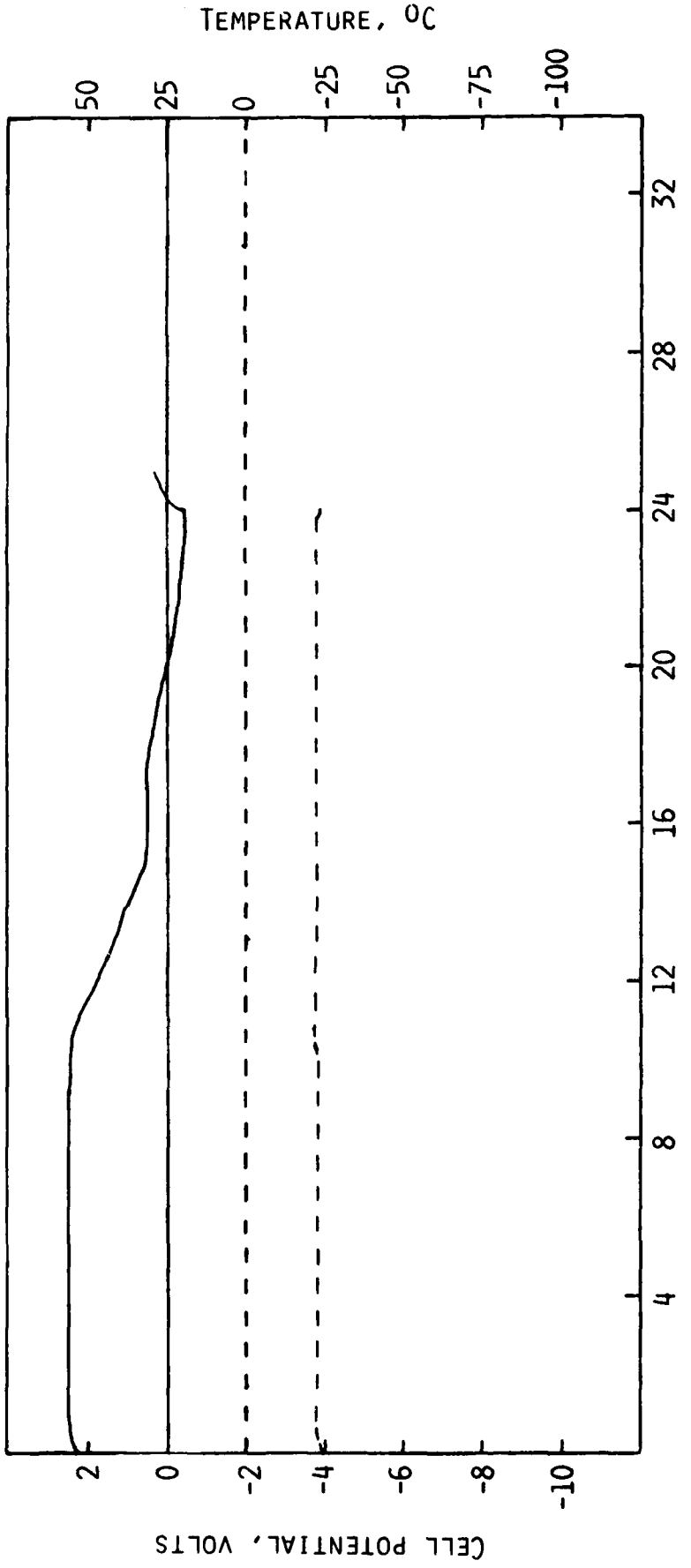

Fig. 43. Voltage (——) and temperature (---) profiles of the low temperature (-25°C) discharge and forced overdischarge of Li/SO_2 cell Z-14 at 100 mA.

TABLE 12

X-RAY[a] DIFFRACTION OF THE CATHODE OF CELL Z-13

Cell Z-13[b]		LiAl		Al	
d, Å	I/I_o	d, Å	I/I_o	d, Å	I/I_o
5.06	20				
4.33	80				
4.07	10				
3.69	100	3.65	75		
3.21	90				
2.93	50				
2.74	15				
2.65	100				
2.53	70				
2.43	10				
2.33	20			2.34	100
2.25	60	2.26	100		
2.01	10			2.02	100
1.91	50	1.92	75		
1.79	5				
1.65	10				
1.61	10				
1.58	10	1.58	60		
1.58	5				
1.46	20	1.46	60	1.47	22
1.41	10				
1.29	30	1.30	100		
1.26	5				
1.22	20	1.22	75	1.22	24

[a]Debye-Scherrer method, CuK_α radiation.

[b]Cell was discharged and forced overdischarged at 100 mA at -25°C.

6.1 Discussion

The low temperature forced overdischarge of both Type X and Type Z cells can result in hazardous cell behavior at relatively low rates.

Cell X-23 and X-24 are the only cells in which unalloyed Li was found on the carbon cathode. In some areas where the Li had plated on the cathode of cell X-23, small localized reactions occurred during forced overdischarge in which the temperature probably exceeded 170°C (the decomposition temperature of $Li_2S_2O_4$).

These reactions on the cathode do not appear to be initiated by the reaction of plated Li and CH_3CN. We believe a likely alternative is the reaction between Li and SO_2 (SO_2 absorbed in the carbon), catalyzed by the carbon surface, i.e., a short circuited cell. The excessive heat from this reaction probably initiates reactions between Li and CH_3CN, SO_2 and CH_4 and the decomposition of $Li_2S_2O_4$.

The fact that no unalloyed Li was found on the cathode of Type Z cell forced overdischarged at 100 mA suggest that the exposed Al grid immediately reacts with any plated Li to form Li/Al alloy. Whether this is beneficial to the cell safety is uncertain.

The reaction in the anode compartment which produces the brown product mixture and CH_4 apparently does not occur at -25°C in either type of cell.

Clearly, additional work is needed in the area of low temperature use of Li/SO_2 cells to evaluate their safe limits of use.

7.0 INVESTIGATION OF THE CHARGING BEHAVIOR OF Li/SO_2 CELLS

The safety aspects of charging the Li/SO_2 cell were briefly investigated with four cells. The experiments are summarized in Table 13.

Cell X-25 was discharged at 100 mA for 16 hours (~50% of the cell capacity) then recharged an equivalent amount. The voltage profile is shown in Fig. 44. The cell displayed no unsafe behavior. Post-mortem examination (2 days after the recharge) of the cell showed SO_2 was the only gas present. The cathode contained no detectable $Li_2S_2O_4$ (see Section 4.1.1). Li was the only product identified in the anode compartment. The analysis of this cell clearly shows that the cathode reaction is reversible.

Cell Z-15 was discharged and recharged under identical conditions. The voltage profile is shown in Fig. 45. The cell was not opened until two days after being charged. Post-mortem analysis of the cell showed only SO_2 in the gas phase. However, unlike cell X-25 the cathode contained $Li_2S_2O_4$. The weight of the cathode indicated the amount of $Li_2S_2O_4$ was equivalent to a discharge of ~2300 mAh - more than the 1600 mAh the cell was initially discharged.

A possible reason why the Type Z cell did not recharge is that a dendritic short developed across the polypropylene separator and carried most of the charge current. Later, when the cell was stored for two days the short allowed the cell to self-discharge, thus producing additional $Li_2S_2O_4$ in the cathode. The non-woven polypropylene separator used in the Type X cell is known to be more resistant to dendritic shorting in secondary Li cells.

Cells X-26 and Z-16 were both forced overdischarged at 100 mA before being recharged as indicated in Table 13. The voltage profiles are shown in Figs. 46 and 47. Neither cell vented.

An analysis of the cells found only CH_4 in gas phase. IR analyses of the cathodes of both cells showed only $Li_2S_2O_4$. The anode compartment of both cells contained the yellow-brown anode product typically found in forced overdischarged cells and very little Li.

Examination of cell X-26 revealed that the electrode had been misaligned during cell manufacture. The inner 3 cm of the cathode (~10% of the length) contained no $Li_2S_2O_4$ (via IR and qualitative tests) and had the flexible texture of a fresh cathode. The capacity to 0V (3100 mAh) was also ~10% lower than obtained from other Type X cells discharged under similar conditions. This indicates that the electrode misalignment existed

TABLE 13

SUMMARY OF THE CHARGING STUDIES OF Li/SO_2 CELLS

Cell	Discharge Current (mA)	Forced-Overdischarge Current (mA)	Charge Current (mA)	Discharge Capacity (mAh) to 2.0V	to 0.0V	Extent of Forced Overdischarge (mAh)	Extent of Charge (mAh)
X-25	100	-	200	1600[a]	-	-	1600
Z-15	100	-	200	1600[a]	-	-	1600
X-26	100	100	100	3290	3100	3800	5500
Z-16	100	100	100	3610	3650	2850	5080

[a]~50% of the normal capacity to 2.0V.

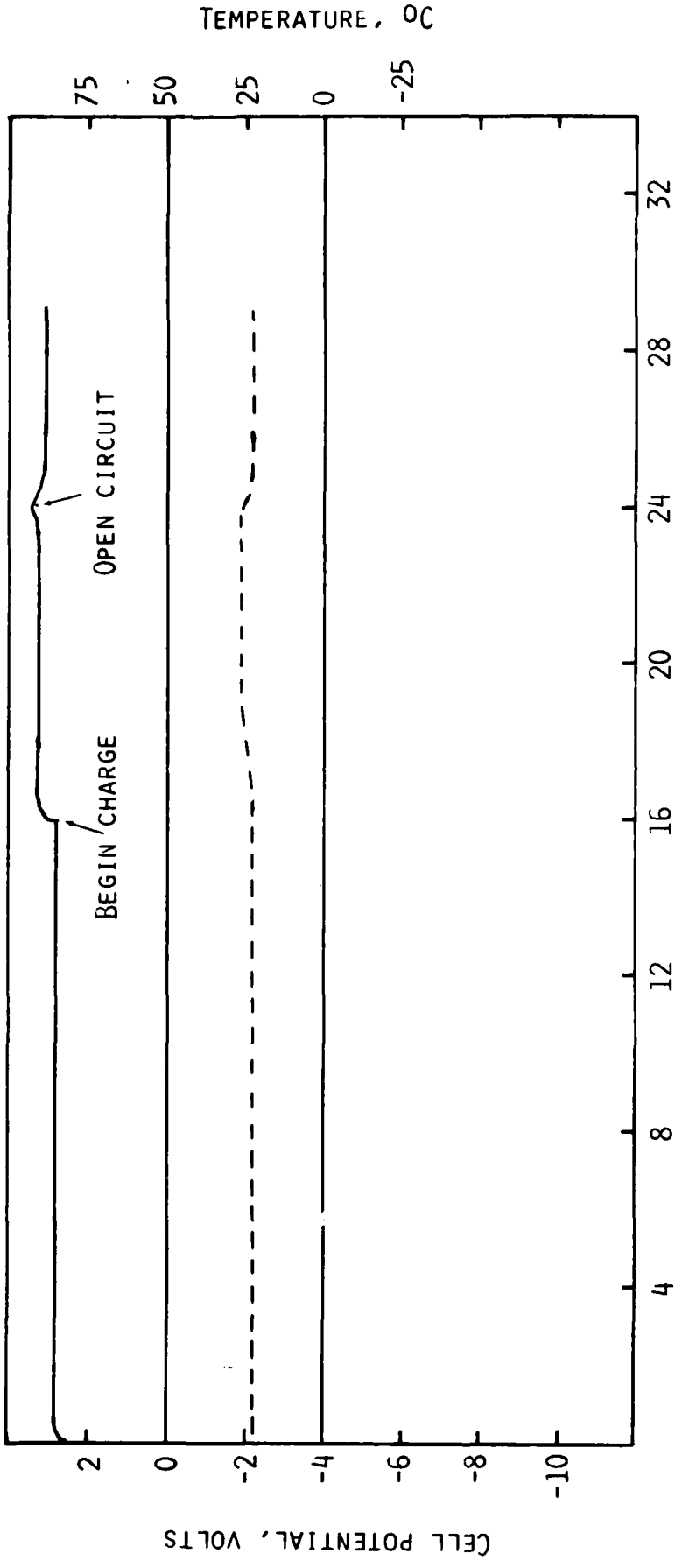

Fig. 44. Voltage (——) and temperature (---) profiles of the discharge (100 mA) and charge (200 mA) of Li/SO_2 cell X-25.

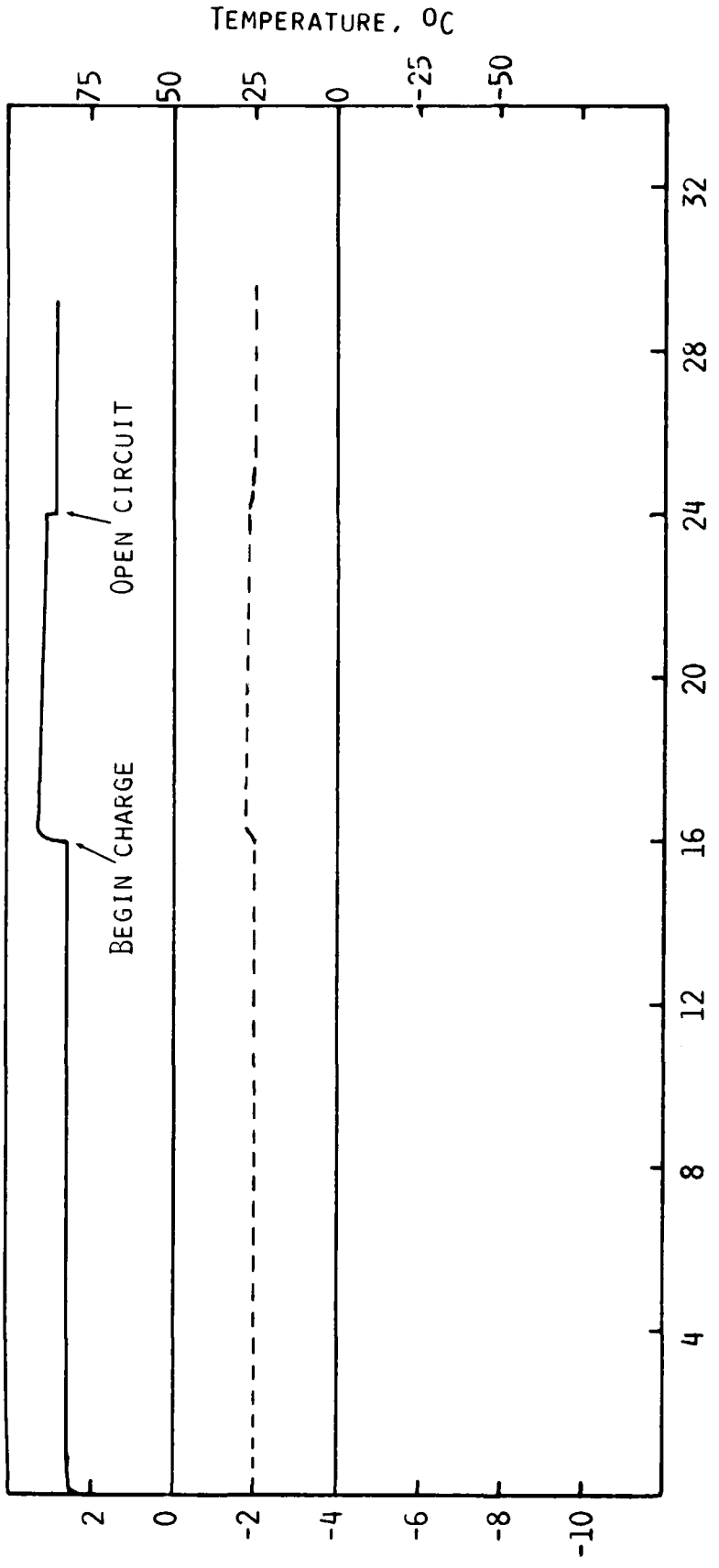

Fig. 45. Voltage (——) and temperature (---) profiles of the discharge (100 mA) and charge (200 mA) of Li/SO_2 cell Z-15.

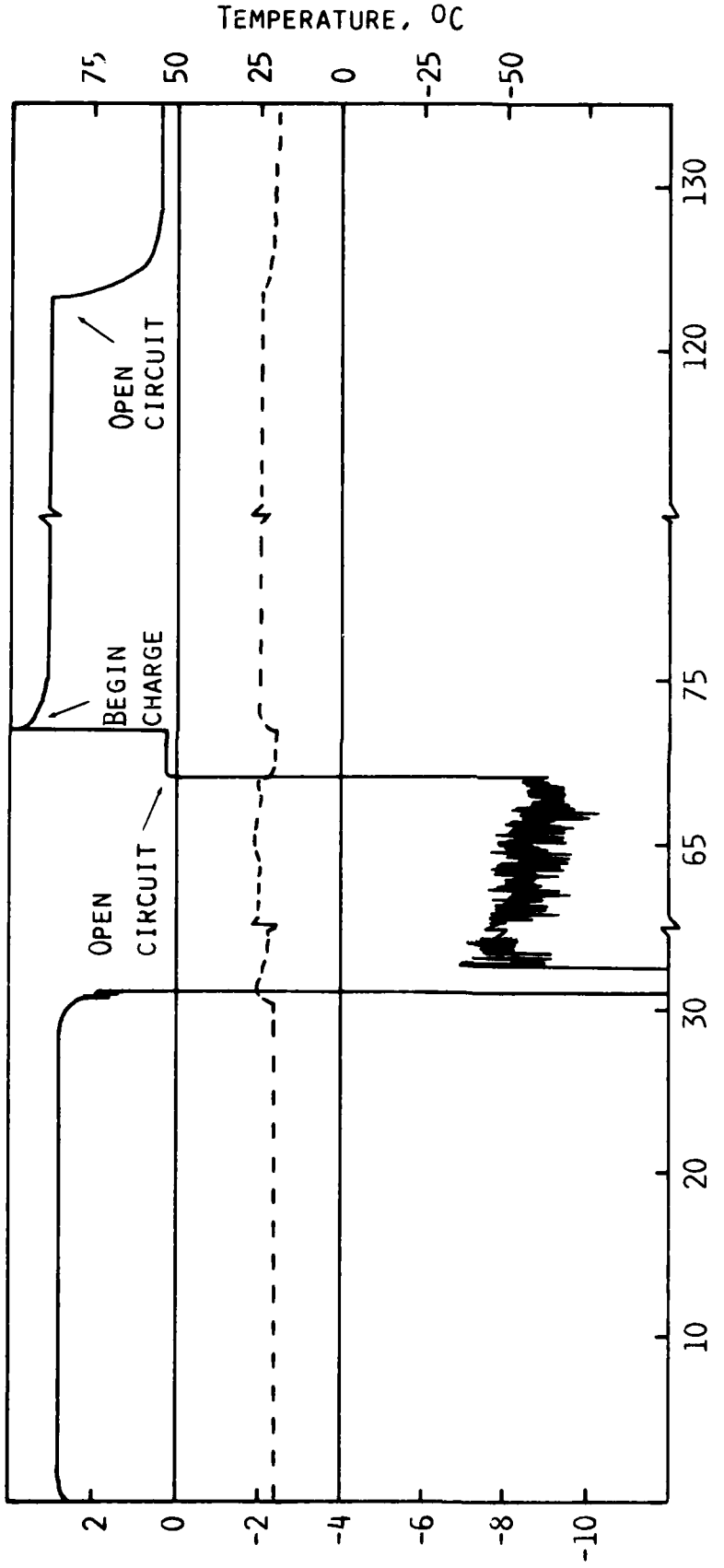

Fig. 46. Voltage (——) and temperature (---) profiles of the discharge, forced overdischarge, and charge of Li/SO_2 cell X-26 at 100 mA.

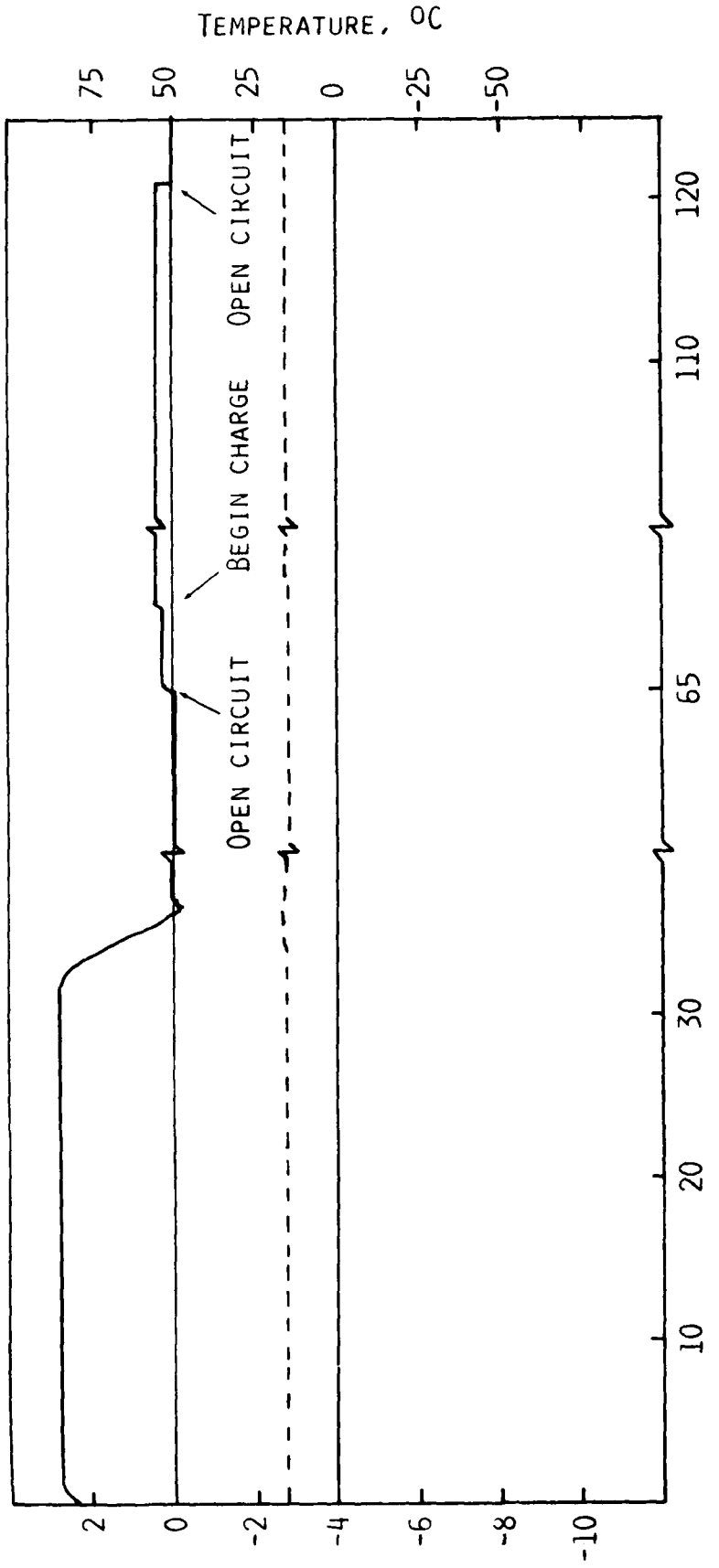

Fig. 47. Voltage (——) and temperature (---) profiles of the discharge, forced over-discharge, and charge of Li/SO_2 cell 2-16 at 100 mA.

in the cell before the test and was not the result of the discharge or charge process. The 3 cm of excess Li was wrapped around the outside of the electrode package and was covered by a black solid. This was not examined further.

If this cell had been used in a series connected battery it could have been forced into reversal even under non abusive discharge conditions. This example shows that the manufacturing procedures are an area that must be considered in the development of safe Li/SO_2 cells.

Neither the Type X nor the Type Z cell could be recharged after forced overdischarge. The exact cause of this is not known at this time.

AD-A118 363 EIC LABS INC NEWTON MA F/G 10/3
INVESTIGATION OF LITHIUM SULFUR DIOXIDE (LI/SO2) BATTERY SAFETY--ETC(U)
APR 82 K M ABRAHAM, M W RUPICH, L PITTS N60921-81-C-0084
UNCLASSIFIED C-656 NSWC-TR-82-148 NL

2 of 2
A-118363

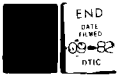

8.0 SUMMARY

A literature and user survey of the safety hazards of Li/SO_2 cells and batteries identified three conditions under which the use of the system can present hazards: room temperature forced overdischarge; low temperature forced overdischarge, particularly with reversal; and, increased vulnerability to abuse (e.g., shorts, high current pulses, overdischarge or incineration) of partially discharged and stored cells.

The chemistry associated with the discharge of the Li/SO_2 cell was investigated in detail. An analytical procedure for the quantitative determination of $Li_2S_2O_4$ in discharged Li/SO_2 cells was developed. Quantitative determinations of $Li_2S_2O_4$ in several discharged cells showed very good agreement with the reaction stoichiometry of

$$2Li + 2SO_2 \rightarrow Li_2S_2O_4 \qquad (9)$$

The formation of $Li_2S_2O_4$ as the principal discharge product in Li/SO_2 cells was further established by infrared, X-ray, and ESCA analyses of discharged cathodes.

The forced overdischarge behavior of two types of commercial C-size Li/SO_2 cells was investigated at 25°C. Type Z cells were found to be resistant to extended forced overdischarge at currents ≤ 300 mA. At currents of ≥ 900 mA, Type Z cells consistently vented during forced overdischarge. Type Z cells did not vent when forced overdischarged at 600 and 800 mA; however, post-test analyses of the cells revealed burned areas within the cells. Resistive heating of the Al cathode tab or areas near to it during forced overdischarge appears to initiate explosive reactions between Li and CH_3CN and/or SO_2 and CH_4. These reactions cause the cell to vent. All cells which vented produced CS_2, CO_2, COS, H_2S, S, CH_4, C_2H_4, C_2H_2, Li_2S, and Li_2SO_3.

Type X cells were found to have good resistance towards extended forced overdischarge. No Type X cells vented when discharged and forced discharged at currents up to 1290 mA.

Post-test analyses of both Type X and Type Z cells, which did not vent during room temperature forced overdischarge, revealed methane in the gas phase and a solid product in the anode compartment. The latter was identified as a mixture of 3,5-diamino-2,4-hexenenitrile, $Li_2S_2O_4$, Li_2SO_3, and other organic compounds. The organic compounds apparently result from reactions of excess Li in the anode compartment and CH_3CN.

The forced overdischarge behavior of both Type X and Type Z cells was also investigated at -25°C. Both types of cells were found to exhibit hazardous behavior under these conditions. The Type Z cells vented during forced overdischarge at currents of $\gtrsim$150 mA. The same products, as were found in cells which vented during room temperature forced overdischarges, were found to form in cells which vented during forced overdischarge at -25°C.

The Type X cells did not vent during forced overdischarge at -25°C. Li was found to plate on the carbon cathode of the Type X cell during forced overdischarge at -25°C. The cathode containing the plated Li is very reactive. Examination of one cell showed that localized, exothermic reactions occurred on the cathode surface during forced overdischarge. The reactions appear to involve plated Li and SO_2 absorbed in the carbon cathode and are likely catalyzed by the carbon surface.

The behavior of Li/SO_2 cells during recharge was briefly investigated. Neither the Type X nor the Type Z cell displayed unsafe behavior when recharged following either a partial discharge or a forced overdischarge. The cathodic reaction was found to be reversible in Type X cells, which were only partially discharged. Type Z cells could not reversibly be recharged because of dendritic shorts across the separator.

9.0 REFERENCES

1. N. Wilburn, Proceedings 25th Power Sources Symposium, 3 (1972).

2. D. L. Warburton, Proceedings 26th Power Sources Symposium, 34 (1974).

3. J. F. McCartney, W. H. Shipman and G. R. Gunderson, Proceedings 27th Power Sources Symposium, 79 (1976).

4. M. Lang, J. R. Backlund and E. C. Weidner, Proceedings 26th Power Sources Symposium, 51 (1974).

5. E. S. Brooks, Proceedings 26th Power Sources Symposium, 31 (1974).

6. H. Taylor, IECEC Conf., Washington, D. C., Sept. 1977, p. 288.

7. P. Bro, R. Holms, N. Marincic and H. Taylor, Power Sources 5, Ed. D. H. Collins, Oriel Press, Brighton, England (1974).

8. P. Bro, H. Y. Kong, C. Schlaikjer and H. Taylor, 10th IECEC, 432 (1975).

9. D. Linden and B. McDonald, J. Power Sources, 5, 35 (1980).

10. A. N. Dey, Thin Solid Films, 43, 131 (1977).

11. H. Taylor and B. McDonald, Proceedings 27th Power Sources Symposium, 66 (1976).

12. H. F. Hunger and J. A. Christopulos, R&D Technical Report ECOM-4292, February 1975.

13. M. W. Rupich and K. M. Abraham, First Quarterly Report, NSWC Contract No. N60921-81-C-0084, May 1981.

14. F. Feigl and V. Anger, Spot Tests in Inorganic Analysis, Elsevier Publishing Co., NY (1972) Ch. 4.

15. The Analytical Chemistry of Sulfur and Its Compounds, J. H. Karchmer, Ed., Wiley Interscience, NY (1970).

16. W. M. Dawson and W. F. Jones, Mikrochim. Acta, 339 (1974).

17. A. N. Dey and R. W. Holmes, J. Electrochem. Soc., 126, 1637 (1979).

18. A. N. Dey, J. Electrochem. Soc., 1000 (1980).

19. A. N. Dey and R. W. Holmes, ERADCOM, DELET-TR-77-0472-F (1979).

20. A. N. Dey, Thin Solid Films, 43, 131 (1977).

21. H. Taylor, W. Bowden, and J. Barrella, Proceedings 28th Power Sources Symposium, 183 (1978).

22. B. F. Becker and H. P. Fritz, Liebigs Ann. Chem., 1015 (1976).

23. W. Kuran, S. Pasynkiewicz, and A. Salek, J. Organomet. Chem., 73, 199 (1974).

24. I. N. Jucknovski, and J. G. Binev, J. Organomet. Chem., 99, 1 (1975).

25. J. J. Helstrom, and A. G. Atwood, Ind. Eng. Chem., Process Des. Dev., 17, 114 (1978).

DISTRIBUTION LIST

Defense Documentation Center
Cameron Station
Alexandria, VA 22314 (12)

Defense Nuclear Agency
Attn: Library
Washington, DC 20301 (2)

Institute for Defense Analyses
R&E Support Division
400 Army-Navy Drive
Arlington, VA 22202 (1)

Naval Material Command
Attn: Code 08T223
Washington, DC 20360 (1)

Office of Naval Research
Attn: G. Neece (Code ONR 413)
800 N. Quincy Street
Arlington, VA 22217 (2)

Naval Research Laboratory
Attn: Dr. Fred Saalfeld
(Code NRL 6100)
4555 Overlook Avenue, SW
Chemistry Division
Washington, DC 20360 (1)

Naval Research Laboratory
Attn: A. Simon (Code NRL 6130)
4555 Overlook Avenue, SW
Chemistry Division
Washington, DC 20360 (1)

Naval Postgraduate School
Attn: Dr. William M. Tolles
(Code 612)
Monterey, CA 93940 (1)

Naval Postgraduate School
Attn: Dr. Oscar Biblarz
Monterey, CA 93940 (1)

Naval Air Systems Command
Attn: Dr. H. Rosenwasser
(Code NAVAIR 301C)
Washington, DC 20361 (1)

Naval Air Systems Command
Attn: E. Nebus
(Code NAVAIR 5332)
Washington, DC 20361 (1)

Naval Electronic Systems Command
Attn: A. H. Sobel
(Code PME 124-31)
Washington, DC 20360 (1)

Naval Sea Systems Command
Attn: F. Romano (Code 63R3)
Washington, DC 20362 (1)

Naval Sea Systems Command
Attn: M. Murphy (Code 63R32)
Washington, DC 20362 (1)

Naval Sea Systems Command
Attn: A. Himy (Code 5433)
Washington, DC 20362 (1)

Naval Sea Systems Command
Attn: E. Daugherty (Code 04H3)
Washington, DC 20362 (1)

Strategic Systems Project Office
Attn: K. N. Boley
(Code NSP 2721)
Department of the Navy
Washington, DC 20360 (1)

Strategic Systems Project Office
Attn: M. Meserole (Code NSP 2722)
Department of the Navy
Washington, DC 20360 (1)

Naval Surface Weapons Center
Attn: W. P. Kilroy (Code R-33)
Silver-Spring, White Oak, MD 20910 (1)

Naval Air Development Center
Attn: J. Segrest (Code 6012)
Warminster, PA 18974 (1)

Naval Air Development Center
Attn: R. Schwartz (Code 30412)
Warminster, PA 18974 (1)

Naval Civil Engineering Laboratory
Attn: Dr. W. S. Haynes (Code L-52)
Port Hueneme, CA 93040 (1)

Naval Civil Engineering Laboratory
Attn: F. Rosell
Port Hueneme, CA 93040 (1)

Naval Intelligence Support Center
Attn: Dr. H. Ruskie (Code 362)
Washington, DC 20390 (1)

Naval Ocean Systems Center
Attn: Code 922
San Diego, CA 92152 (1)

Naval Ocean Systems Center
Attn: Dr. S. Spazk (Code 6343)
San Diego, CA 92152 (1)

Naval Ocean Systems Center
Attn: Dr. S. D. Yamamoto
(Code 513)
San Diego, CA 92152 (1)

US Development & Readiness Command
Attn: J. W. Crellin (Code DRCDE-L)
5001 Eisenhower Avenue
Alexandria, VA 22333 (1)

US Army Electronics Command
Attn: A. J. Legath
(Code DRSEL-TL-P)
Fort Monmouth, NJ 07703 (1)

US Army Electronics Command
Attn: E. Brooks
(Code DRSEL-TL-PD)
Fort Monmouth, NJ 07703 (1)

US Army Electronics Command
Attn: G. DiMasi
Fort Monmouth, NJ 07703 (1)

US Army Electronics Command
Attn: Dr. W. K. Behl
Fort Monmouth, NJ 07703 (1)

Army Material & Mech. Res. Center
Attn: J. J. DeMarco
Watertown, MA 02172 (1)

USA Mobility Equipment R&D Command
Attn: J. Sullivan (Code DRXFB)
Electrochemical Division
Fort Belvoir, VA 22060 (1)

USA Mobility Equipment R&D Command
Attn: Code DRME-EC
Electrochemical Division
Fort Belvoir, VA 22060 (1)

Edgewood Arsenal
Attn: Library
Aberdeen Proving Ground
Aberdeen, MD 21010 (1)

Picatinny Arsenal
Attn: M. Merriman
(Code SARPA-FR-S-P)
U. S. Army
Dover, NJ 07801 (1)

Picatinny Arsenal
Attn: Dr. B. Werbel
(Code SARPA-FR-E-L-C)
U. S. Army
Dover, NJ 07801 (1)

Picatinny Arsenal
Attn: A. E. Magistro (Code SARPA-ND-D-B)
US. Army
Dover, NJ 07801 (1)

Harry Diamond Laboratory
Attn: A. A. Benderly
(Code DRDXO-RDD)
Department of Army Materiel
Chief, Power Supply Branch
2800 Powder Mill Road
Adelphi, MD 20783 (1)

Harry Diamond Laboratory
Attn: W. Kuper
(Code DRDXO-RDD)
Department of Army Materiel
Chief, Power Supply Branch
2800 Power Mill Road
Adelphi, MD 20783 (1)

Harry Diamond Laboratory
Attn: J. T. Nelson
(Code DRKDO-RDD)
Department of Army Materiel
Chief, Power Supply Branch
2800 Powder Mill Road
Adelphi, MD 20783 (1)

Harry Diamond Laboratory
Attn: C. Campanguolo
Department of Army Materiel
Chief, Power Supply Branch
2800 Powder Mill Road
Adelphi, MD 20783 (1)

Deparment of Energy
Attn: L. J. Rogers (Code 2102)
Division of Electric Energy Systems
Washington, DC 20545 (1)

Department of Energy
Attn: Dr. A. Landgrebe
(Code MS E-463)
Energy R&D Agency
Division of Applied Technology
Washington, DC 20545 (1)

Headquarters, Department of Transportation
Attn: R. Potter (Code GEOE-3/61)
U.S. Coast Guard, Ocean Engg. Division
Washington, DC 20590 (1)

NASA Headquarters
Attn: Dr. J. H. Ambrus
(Code RTS-6)
Washington, DC 20546 (1)

NASA Goddard Space Flight Center
Attn: G. Halpert (Code 711)
Greenbelt, MD 20771 (1)

NASA Goddard Space Flight Center
Attn: T. Hennigan (Code 716.2)
Greenbelt, MD 20771 (1)

NASA Lewis Research Center
Attn: J. S. Fordyce
(Code MS 309-1)
21000 Brookpark Road
Cleveland, OH 44135 (1)

NASA Lewis Research Center
Attn: H. J. Schwartz
(Code MS 309-1)
21000 Brookpark Road
Cleveland, OH 44135 (1)

Naval Electronic Systems Command
Attn: T. Sliwa
(Code NAVELEX-01K)
Washington, DC 20360 (1)

Naval Weapons Center
Attn: Dr. E. Royce (Code 38)
China Lake, CA 93555 (1)

Naval Weapons Center
Attn: Dr. A. Fletcher (Code 3852)
China Lake, CA 93555 (1)

Naval Weapons Center
Attn: R. Dettling (Code 4575)
China Lake, CA 93555 (1)

Naval Weapons Support Center
Attn: D. G. Miley (Code 305)
Electrochemical Power Sources
Division
Crane, IN 47522 (1)

Naval Coastal Systems Center
Attn: Library
Panama City, FL 32407 (1)

Naval Underwater Systems Center
Attn: T. Black (Code 3642)
Newport, RI 02840 (1)

Naval Underwater Systems Center
Attn: J. Moden (Code SB332)
Newport, RI 02840 (1)

David W. Taylor Naval Ship R&D Ctr
Attn: A. B. Neild (Code 2723)
Annapolis Laboratory
Annapolis, MD 21402 (1)

David W. Taylor Naval Ship R&D Ctr
Attn: W. J. Levendahl (Code 2703)
Annapolis Laboratory
Annapolis, MD 21402 (1)

David W. Taylor Naval Ship R&D Ctr
Attn: J. Woerner (Code 2724)
Annapolis Laboratory
Annapolis, MD 21402 (1)

David W. Taylor Naval Ship R&D Ctr
Attn: H. R. Urbach (Code 2724)
Annapolis Laboratory
Annapolis, MD 21402 (1)

Scientific Advisor
Attn: Code AX
Commandant of the Marine Corps
Washington, DC 20380 (1)

Air Force of Scientific Research
Attn: R. A. Osteryoung
Directorate of Chemical Science
1400 Wilson Boulevard
Arlington, VA 22209 (1)

Frank J. Seiler Research Lab, AFSC
Attn: Lt. Col. Lowell A. King
(Code FJSRL/NC)
USAF Academy, CO 80840 (1)

Air Force Materials Laboratory
Attn: Major J. K. Erbacher
Wright-Patterson AFB, OH 45433 (1)

Air Force Aero Propulsion Lab
Attn: W. S. Bishop
(Code AFAPL/POE-1)
Wright-Patterson AFB, OH 45433 (1)

Air Force Aero Propulsion Lab
Attn: J. Lander
(Code AFAPL/POE-1)
Wright-Patterson AFB, OH 45433 (1)

Air Force Rocket Propulsion Lab
Attn: Lt. D. Ferguson (Code MKPA)
Edwards Air Force Base, CA 93523 (1)

Headquarters, Air Force Special
Communications Center
Attn: Library
USAFSS
San Antonio, TX 78243 (1)

Office of Chief of R & D
Department of the Army
Attn: Dr. S. J. Magram
Energy Conversion Branch
Room 410, Highland Building
Washington, DC 20315 (1)

US Army Research Office
Attn: B. F. Spielvogel
P. O. Box 12211
Research Triangle Park, NC 27709 (1)

NASA Scientific & Technical
Information Facility
Attn: Library
P. O. Box 33
College Park, MD 20740 (1)

National Bureau of Standards
Metallurgy Division
Inorganic Materials Division
Washington, DC 20234 (2)

Battelle Memorial Institute
Defense Metals & Ceramics
Information Center
505 King Avenue
Columbus, OH 43201 (1)

Bell Laboratories
Attn: Dr. J. J. Auborn
600 Mountain Avenue
Murray Hill, NJ 07974 (1)

Brookhaven National Laboratory
Attn: J. W. Sutherland
Upton, LI, NY 11973 (1)

Brookhaven National Laboratory
Attn: J. J. Egan
Building 815
Upton, NY 11973 (1)

California Institute of Technology
Attn: Library
Jet Propulsion Laboratory
4800 Oak Grove Drive
Pasadena, CA 91103 (1)

Argonne National Laboratory
Attn: H. Shimotake
9700 South Cass Avenue
Argonne, IL 60439 (1)

Argonne National Laboratory
Attn: R. K. Steunenberg
9700 South Cass Avenue
Argonne, IL 60439 (1)

Argonne National Laboratory
Attn: L. Burris
9700 South Cass Avenue
Argonne, IL 60439 (1)

John Hopkins Applied Physics Lab
Attn: Library
Howard County
Johns Hopkins Road
Laurel, MD 20810 (1)

John Hopkins Applied Physics Lab
Attn: R. Rumpf
Howard County
Johns Hopkins Road
Laurel, MD 20810 (1)

Oak Ridge National Laboratory
Attn: K. Braunstein
Oak Ridge, TN 37830 (1)

Sandia Laboratories
Attn: R. D. Wehrle (Code 2522)
Albuquerque, NM 87115 (1)

Sandia Laboratories
Attn: B. H. Van Domelan (Code 2523)
Albuquerque, NM 87115 (1)

Catholic University
Attn: Dr. C. T. Moynihan
(Physics)
Chemical Engineering Department
Washington, DC 20064 (1)

University of Tennessee
Attn: G. Mamantov
Department of Chemistry
Knoxville, TN 37916 (1)

University of Florida
Attn: R. D. Walker
Department of Chemical Engg.
Gainesville, FL 32611 (1)

Applied Research Laboratory
Attn: Library
Penn State University
University Park, PA 16802 (1)

Catalyst Research Corporation
Attn: G. Bowser
1421 Clarkview Road
Baltimore, MD 21209 (1)

Catalyst Research Corporation
Attn: N. Issacs
1421 Clarkview Road
Baltimore, MD 21209 (1)

Catalyst Research Corporation
Attn: F. Tepper
1421 Clarkview Road
Baltimore, MD 21209 (1)

ESB Research Center
Attn: Library
19 W. College Avenue
Yardley, PA 19067 (1)

Old Dominion University
Attn: Dr. Robert Ake
Department of Chemical Science
Norfolk, VA 23508 (1)

Eagle-Picher Industries, Inc.
Attn: D. R. Cottingham
Electronics Division, Couples Dept.
P. O. Box 47
Joplin, MO 64801 (1)

Eagle-Picher Industries, Inc.
Attn: J. Dines
Electronics Division, Couples Dept.
P. O. Box 47
Joplin, MO 64801 (1)

Eagle-Picher Industries, Inc.
Attn: D. L. Smith
Electronics Division, Couples Dept.
P. O. Box 47
Joplin, MO 64801 (1)

Eagle-Picher Industries, Inc.
Attn: J. Wilson
Electronics Division, Couples Dept.
P. O. Box 47
Joplin, MO 64801 (1)

Eagle-Picher Industries, Inc.
Attn: P. E. Grayson
Miami Research Laboratories
200 Ninth Avenue, NE
Miami, OK 74354 (1)

Electrochimia Corporation
2485 Charleston Road
Mountain View, CA 94040 (1)

Eureka Advance Science Division
Attn: D. Ryan
P. O. Box 1547
Bloomington, IL 61701 (1)

Eureka Advance Science Division
Attn: L. Raper
P. O. Box 1547
Bloomington, IL 61701 (1)

Foote Mineral Company
Attn: H. R. Grady
Exton, PA 19341 (1)

General Electric Company
Attn: R. D. Walton
Neutron Devices Department
P. O. Box 11508
St. Petersburg, FL 33733 (1)

General Electric Company
Attn: R. Szwarc
Neutron Devices Department
P. O. Box 11508
St. Petersburg, FL 33733 (1)

Gould, Inc.
Attn: S. S. Nielsen
40 Gould Center
Rolling Meadows, IL 60008 (1)

Gould, Inc.
Attn: G. R. Ault
40 Gould Center
Rolling Meadows, IL 60008 (1)

GTE Laboratory
Attn: *Dr. C. R. Schlaikjer*
40 Sylvan Road
Waltham, MA 02154 (1)

Honeywell, Inc.
Attn: Library
Defense Systems Division
Power Sources Center
104 Rock Road
Horsham, PA 19044 (1)

Honeywell, Inc.
Attn: R. Walk
Defense Systems Division
Power Sources Center
104 Rock Road
Horsham, PA 19044 (1)

Honeywell, Inc.
Attn: W. Ebner
Defense Systems Division
Power Sources Center
104 Rock Road
Horsham, PA 19044 (1)

Honeywell, Inc.
Attn: Dr. P. M. Shah
Defense Systems Division
Power Sources Center
104 Rock Road
Horsham, PA 19044 (1)

Hughes Aircraft Company
Attn: Library
Aerospace Groups
Missile Systems Group
Tucson Engineering Laboratory
Tucson, AZ 87534 (1)

Hughes Aircraft Company
Attn: Dr. L. H. Fentnor
Aerospace Groups
Missile Systems Group
Tucson Engineering Laboratory
Tucson, AZ 85734 (1)

KDI Score, Inc.
Attn: L. A. Stein
200 Wight Avenue
Cockeysville, MD 21030 (1)

KDI Score, Inc.
Attn: F. DeMarco
200 Wight Avenue
Cockeysville, MD 21030 (1)

KDI Score, Inc.
Attn: K. K. Press
200 Wight Avenue
Cockeysville, MD 21030 (1)

Lockheed Missiles & Space Co., Inc.
Attn: Library
Lockheed Palo Alto Research Lab
3251 Hanover Street
Palo Alto, CA 94304 (1)

Duracell International, Inc.
Attn: G. F. Cruze
Battery Division
South Broadway
Tarrytown, NY 10591 (1)

Duracell International, Inc.
Attn: B. McDonald
Battery Division
South Broadway
Tarrytown, NY 10591 (1)

Duracell International, Inc.
Attn: D. Linden
Battery Division
South Broadway
Tarrytown, NY 10591 (1)

Duracell International, Inc.
Attn: Library
Laboratory for Physical Science
Burlington, MA 01803 (1)

Duracell International, Inc.
Attn: Dr. A. N. Dey
Laboratory for Physical Science
Burlington, MA 01803 (1)

Duracell International, Inc.
Attn: Dr. H. Taylor
Laboratory for Physical Science
Burlington, MA 01803 (1)

Power Conversion, Inc.
70 MacQuesten Parkway S
Mount Vernon, NY 10550 (1)

Union Carbide Battery Products Div.
Attn: R. A. Powers
P. O. Box 6116
Cleveland, OH 44101 (1)

Wilson Greatbatch Ltd.
Attn: Library
1000 Wehrle Drive
Clarence, NY 14030 (1)

Yardney Electric Corporation
Attn: Library
82 Mechanic Street
Pawcatuck, CT 02891 (1)

Yardney Electric Corporation
Attn: A. Beachielli
82 Mechanic Street
Pawcatuck, CT 02891 (1)

Callery Chemical Company
Attn: Library
Callery, PA 16024 (1)

Kawecki Berylco Industries, Inc.
Attn: J. E. Eorgan
Boyertown, PA 19512 (1)

Kawecki Berylco Industries, Inc.
Attn: R. C. Miller
Boyertown, PA 19512 (1)

Rockwell International
Attn: Dr. Samuel J. Yosim
Atomics International Division
8900 DeSoto Avenue
Canogo Park, CA 91304 (1)

Union Carbide
Attn: Library
Nuclepore Corporation
7035 Commercial Circle
Pleasanton, CA 94556 (1)

Ventron Corporation
Attn: L. R. Frazier
10 Congress Street
Beverly, MA 01915 (1)

Stanford University
Attn: C. John Wen
Center for Materials Research
Room 249, McCullough Building
Stanford, CA 94305 (1)

EDO Corporation
Attn: E. P. DiGiannantonio
Government Products Division
2001 Jefferson Davis Highway
Arlington, VA 22202 (1)

Perry International, Inc.
Attn: R. A. Webster
117 South 17th Street
Philadelphia, PA 19103 (1)

Ford Aerospace & Comm. Corp.
Attn: M. L. McClanahan
Metallurgical Processes
Advanced Development-Aeronutronic Division
Ford Road
Newport Beach, CA 92663 (1)

Ford Aerospace & Comm. Corp.
Attn: R. A. Harlow
Metallurgical Processes
Advanced Development-Aeronutronic Division
Ford Road
Newport Beach, CA 92663 (1)

Globe Union, Inc.
Attn: Dr. R. A. Rizzo
5757 N. Green Bay Avenue
Milwaukee, WI 53201 (1)

University of Missouri, Rolla
Attn: Dr. J. M. Marchello
210 Parker Hall
Rolla, MO 65401 (1)

RAI Research Corpcration
Attn: Dr. Carl Perini
225 Marcus Boulevard
Hauppauge, NY 11787 (1)

Battery Engineering
Attn: Dr. N. Marincic
80 Oak Street
Newton, MA 02164 (1)

Ray-O-Vac
Attn: R. Foster Udell
101 East Washington Avenue
Madison, WI 53703 (1)

Litton Data Systems Division
Attn: Frank Halula
(Mail Station 64-61)
8000 Woodley Avenue
Van Nuys, CA 91409 (1)

Lawrence Berkeley Laboratory
Attn: F. McLamore
University of California
Berkeley, CA 94720 (1)

TRW Systems
Attn: Ed Moon
Room 2251, Bldg. 0-1
One Space Park
Redondo Beach, CA 90278 (1)

Altus Corporation
Attn: Dr. Adrian E. Zolla
1610 Crane Court
San Jose, CA 95112 (1)

Capt. A. S. Alanis
BME/ENBE
Norton AFB, CA 92409 (1)

Norton Air Force Base
Code AFISC/SES
CA 92409 (1)